

**Mesoporous Catalyst and/or Carrier**

**TUD-1**

**for Sustainable Chemistry**

**Selvedin Telalović**

Cover design by Sedina Telalović

# Mesoporous Catalyst and/or Carrier

TUD-1

## for Sustainable Chemistry

Proefschrift

ter verkrijging van de graad van doctor  
aan de Technische Universiteit Delft,  
op gezag van de Rector Magnificus prof. ir. K. Ch.A.M. Luyben,  
voorzitter van het College voor Promoties,  
in het openbaar te verdedigen

op maandag 7 maart 2011 om 10.00 uur

door

**Selvedin TELALOVIĆ**

scheikundig ingenieur  
geboren te Rotterdam

Dit proefschrift is goedgekeurd door de promotor:

Prof. dr. R. A. Sheldon

Copromotor: Dr. U. Hanefeld

Samenstelling promotiecommissie:

Rector Magnificus	voorzitter
Prof. dr. R. A. Sheldon	Technische Universiteit Delft, promotor
Dr. U. Hanefeld	Technische Universiteit Delft, copromotor
Prof. dr. I. W. C. E. Arends	Technische Universiteit Delft
Prof. dr. E. Bouwman	Universiteit Leiden
Prof. dr. G. Mul	Universiteit Twente
Prof. dr. G. Rothenberg	Universiteit van Amsterdam
Dr. R. Anand	University of Kansas
Prof. dr. ir. H. van Bekkum	Technische Universiteit Delft, reserve lid

The research described in this thesis was supported by NWO (De Nederlandse Organisatie voor Wetenschappelijk Onderzoek) through a Mozaïek fellowship.



ISBN: 978-94-91211-04-1

Copyright © 2010 by Selvedin Telalović

All rights reserved. No part of the material protected by this copyright notice may be reproduced or utilized in any form or by any other means, electronic or mechanical, including photocopying, recording or by any information storage and retrieval system, without written permission from the author.

Printed in the Netherlands

**To my parents**

**Mojim roditeljima**



# Contents

---

<b>Chapter 1</b>	TUD-1: Synthesis and Application of a Versatile Catalyst, Carrier, Material...	<b>1</b>
<b>Chapter 2</b>	Noncovalent Immobilization of Chiral Cyclopropanation Catalysts on Mesoporous TUD-1: Comparison of Liquid-phase and Gas-phase Ion-exchange	<b>37</b>
<b>Chapter 3</b>	Noncovalent Immobilization of Chiral Cyclopropanation Catalysts on Mesoporous TUD-1: Impact of Immobilisation Parameters	<b>57</b>
<b>Chapter 4</b>	On the Synergistic Catalytic Properties of Bimetallic Mesoporous Materials Containing Aluminium and Zirconium: The Prins Cyclisation of Citronellal	<b>83</b>
<b>Chapter 5</b>	Investigation of the Cyanosilylation Catalysed by Metal-Silicious Catalysts	<b>115</b>

Summary	<b>131</b>
Samenvatting	<b>135</b>
List of Publications	<b>139</b>
Acknowledgments	<b>141</b>
Curriculum Vitae	<b>143</b>



# TUD-1: Synthesis and Application of a Versatile Catalyst, Carrier, Material...

1

---

The contents of this chapter have been published in:

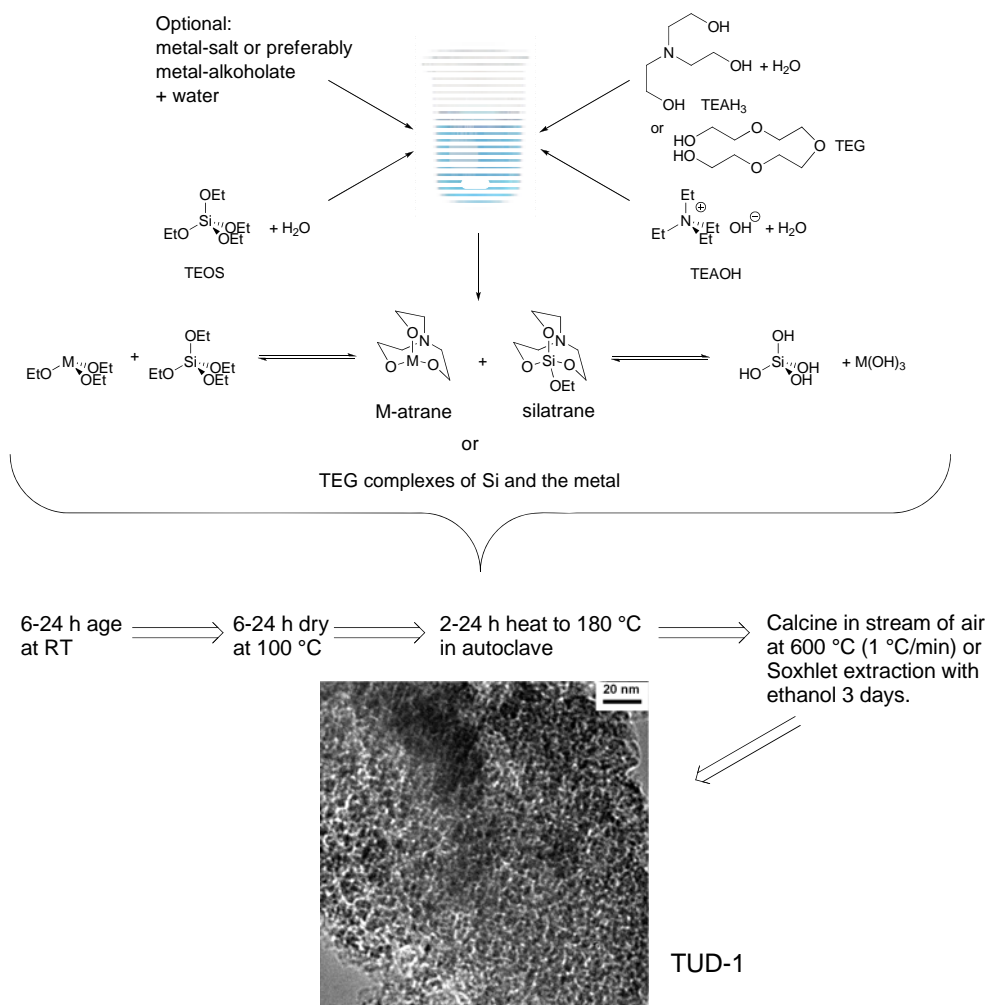
S. Telalović, A. Ramanathan, G. Mul, U. Hanefeld, *J. Mater. Chem.*, **2010**, 20, 642-658.

## 1. Introduction

Mesoporous silicates are versatile materials with many, tuneable properties. Some twenty years ago the first reports on MCM-41 appeared giving the field of these versatile materials a major impulse and since then many differently structured mesoporous silicates have been described.<sup>1</sup> In 2001 TUD-1, a mesoporous silicate first synthesised at the Technische Universiteit Delft, was described by Jansen *et al.*<sup>2</sup> Unlike most other mesoporous materials TUD-1 is straightforward to prepare. It has a sponge-like pore structure, i.e. the pore system is three-dimensional and irregular. This allows for fast diffusion into and out of TUD-1, making the material an ideal starting point for catalyst development. Now, almost a decade after its first description, the catalysis with and chemistry of TUD-1 is well-developed. This chapter aims at bringing together all the different applications of TUD-1 and the underlying syntheses, discussing past achievements and the potential that TUD-1 holds for the future.

## 2. Synthesis and Characterisation of TUD-1

One of the key features of TUD-1 is its straightforward synthesis. It is based on the sol-gel methodology. As silicon source for the siliceous material tetraethyl orthosilicate (TEOS) is the starting material of choice. Unlike in the preparation of many other mesoporous materials no surfactants are used in order to achieve a regular pore structure.<sup>2,3</sup> Instead either triethanolamine (TEAH<sub>3</sub>) or tetraethylene glycol (TEG) is employed to chelate the silicon. At the same time these chelators are crucial to achieve a porous structure. TEAH<sub>3</sub> will form an atrane with silicon, silatrane.<sup>4,5</sup> The initial silatrane can dimerise, trimerise etc. and thus function as a template and as the silicate source at the same time (Scheme 1). The monomers, dimers and oligomers are in equilibrium and they are the source of monomeric orthosilicate which forms the growing structured silicate. Thus the atrane needs to be hydrolysed to release the silicate monomer which then condenses. Recently, chelators were employed for a different synthesis of mesoporous materials. In this “atrane route” TEAH<sub>3</sub> is also utilised for the formation of atranes.<sup>6,7,8,9</sup> However, this occurs in the presence of surfactants to determine the structure of the mesoporous material. In studies on the atrane route it was demonstrated, that before the actual condensation of the metal oxides into



**Scheme 1** The synthesis of mesoporous TUD-1 and M-TUD-1 is straightforward.

mesoporous materials, the atrane is monomeric.<sup>8</sup> Very recently an expansion of the “atrane route” was described in which no surfactant was added. The resulting material denoted UVM-11 essentially is TUD-1.<sup>10</sup> It basically reconfirms the surfactant-free and unique synthesis of TUD-1.

Once TEOS, TEAH<sub>3</sub> and water are mixed a homogeneous solution results. Aging leads to the gel, which is dried at higher temperatures. The resulting solid is thus far not fully condensed nor does it yet have the typical TUD-1 structure.<sup>2,11</sup> It is ground and then

hydrothermally treated in an autoclave leading to further condensation releasing water and alcohols. After the hydrothermal treatment the material has the typical TUD-1 structure (Fig. 1 ). The  $\text{TEAH}_3$  is commonly removed by calcination but can also be extracted (Scheme 1). The resulting material has pore diameters between 5 and 20 nm, surface area between 500 and 1000  $\text{m}^2 \text{g}^{-1}$  and pore volumes of 0.6 to 1.7  $\text{cm}^3 \text{g}^{-1}$ .

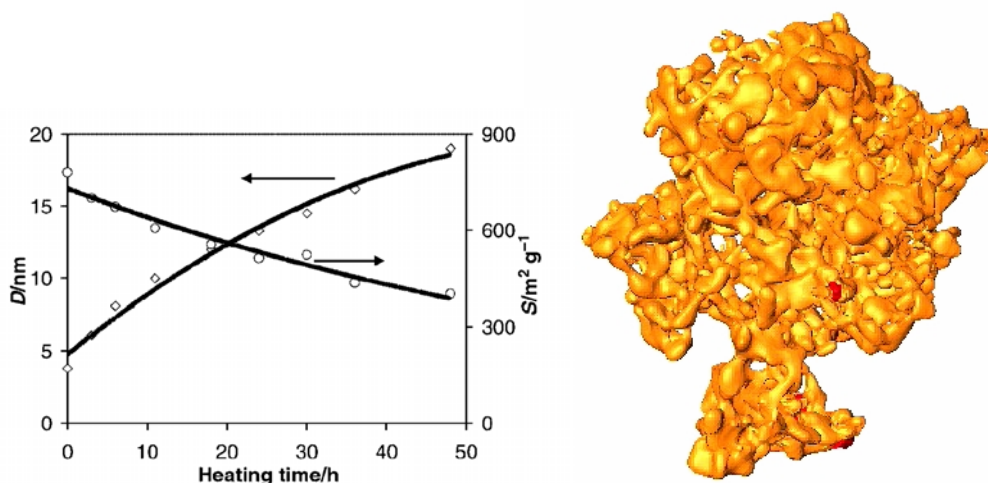


**Figure 1 Left:** Variations of the hydrothermal treatment lead to significant changes in the mesopore diameter (D) and the mesopore surface area (S); allowing fine-tuning of the structure of TUD-1. Reproduced by permission of the Royal Society of Chemistry from ref. 2. **Right:** The huge pore volume of TUD-1 is clearly visible in this 3-D TEM. Reprinted from ref. 24, Copyright (2005) with permission from Elsevier.

Next to the synthesis via the atranes the TEG route to TUD-1 was developed (Scheme 1). In this case the neutral TEG complexes both silicate and other metal oxides. In principle similar results to the atrane approach with  $\text{TEAH}_3$  are obtained. A significant advantage of TEG is that higher metal loadings in silicious TUD-1 can be achieved.

This emphasises that TUD-1 is, from a synthetic point of view a sol-gel; as might be expected from a material prepared via the sol-gel methodology. Its unique characteristics are the mesoporous, three-dimensional, sponge-like structure (Fig. 1 and 2), combined with

high stability and the possibility to incorporate countless metals into the framework. All this is achieved with a very straightforward and environmentally benign synthesis. Thus TUD-1 distinguishes itself from all other mesoporous materials prepared with the aid of a surfactant, while at the same time displaying much higher stability than sol-gels and xerogels.<sup>12</sup> Actually, a typical characteristic of xerogels is their partially collapsed pore structure due to capillary forces during the drying process. This is clearly not the case for TUD-1 (Fig. 1 right).<sup>12,13</sup>

The time of the hydrothermal treatment has a strong influence on the character of TUD-1. Short treatment yields TUD-1 with small pores of approx. 5 nm, while prolonged treatment leads to larger pores. At the same time the surface area drops with extended heating and the wall thickness increases (Fig. 1 left).<sup>2</sup> This synthesis can also be performed with other metal oxides, for instance to produce  $\text{Al}_2\text{O}_3$  with TUD-1 structure.<sup>14,15,16</sup> These processes have been scaled up to ton level and are very robust.<sup>17</sup> Equally the materials are very robust and show long life times in catalytic conversions.<sup>18,19</sup>

The structure of TUD-1 can be further refined by adding tetraethylammonium hydroxide (TEAOH) to the initial reaction mixture.<sup>2</sup> TEAOH induced microporosity into TUD-1 ensuring that a continuous scale of pores, ranging from 20 nm down to less than 1 nm is formed. In most TUD-1 syntheses TEAOH forms part of the reaction mixture, it is however, not an essential part.

The synthesis of siliceous or metal oxide based TUD-1 can be further expanded by adding other metal oxides as salts or preferably as alcoholates, to the reaction mixture.<sup>11,19</sup> In this manner many different metal containing siliceous TUD-1 have been prepared, denoted as M-TUD-1. Just as in the synthesis of purely siliceous TUD-1 the TEOS and the metal alcoholates lead to the formation of atranes if  $\text{TEAH}_3$  is employed, or to TEG complexes if TEG is used (Scheme 1). The atranes ensure that the metal oxide comes available as a single metal species, thus ensuring its isolated incorporation into the silica framework.<sup>8</sup> Metal oxide particles are not formed, since this is prevented by the metal atranes or TEG complexes. Indeed for Si/M ratios of 50 all metal is framework incorporated and isolated and no metal oxide nanoparticles or bulk particles were detected.

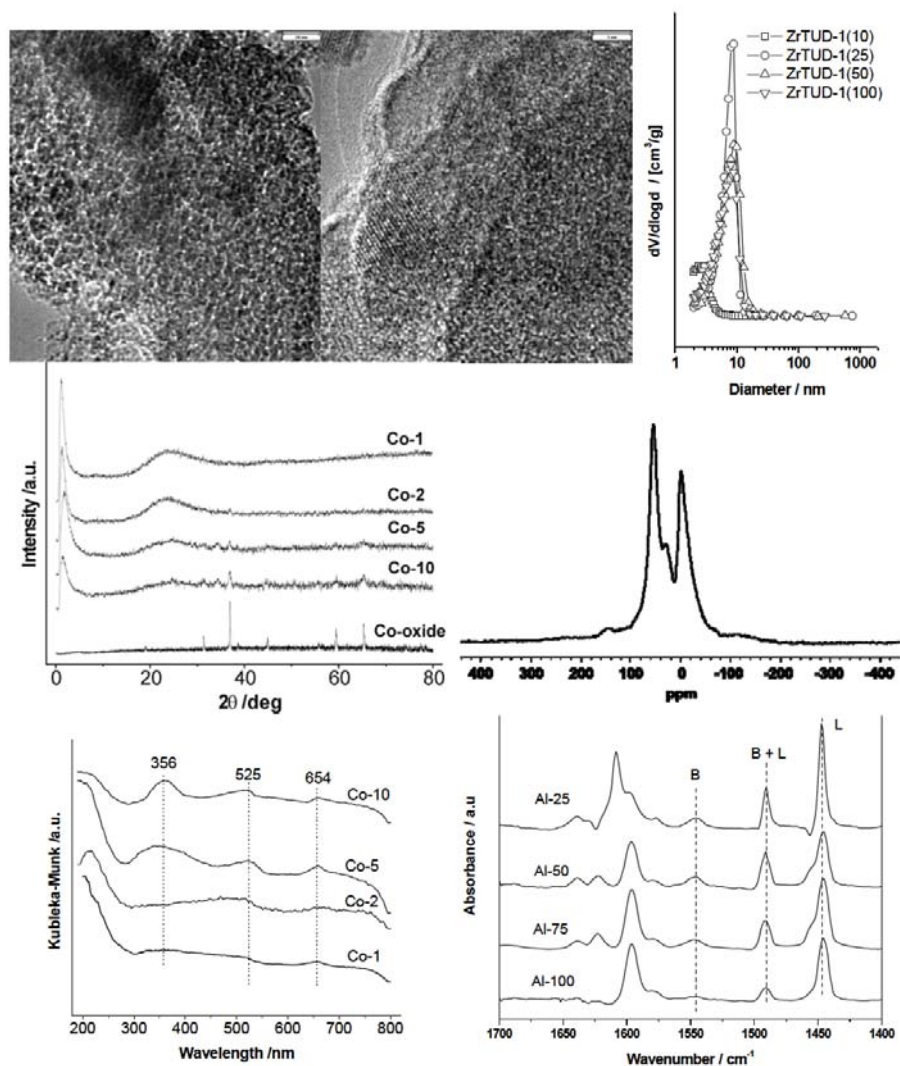


**Figure 2** **Top left:** HR-TEM of Zr-TUD-1 with Si/Zr=25, the bar represents 20 nm, reproduced with permission from ref. 43 Copyright 2008, Wiley-VCH Verlag GmbH&Co. KGaA; **Top middle:** HR-TEM of Zr-TUD-1 with Si/Zr=10, the bar represents 3 nm,  $\text{ZrO}_2$  crystals are visible, reproduced with permission from ref. 43 Copyright 2008, Wiley-VCH Verlag GmbH&Co. KGaA; **Top right:** Pore size distribution of Zr-TUD-1 samples with Si/Zr ratios of 100, 50, 25 and 10 as determined by  $\text{N}_2$  adsorption and desorption isotherms, reproduced with permission from ref. 43 Copyright 2008, Wiley-VCH Verlag GmbH&Co. KGaA; **Middle left:** XRD patterns of Co-TUD-1 samples with Si/Co ratios of 100 (1), 50 (2), 20 (5) and 10 (10) as well as  $\text{Co}_3\text{O}_4$ , reproduced with permission from

ref. 59 Copyright 2006, Wiley-VCH Verlag GmbH&Co. KGaA; **Middle right:** MAS-NMR of  $^{27}\text{Al}$  in Al-TUD-1 with Si/Al = 4, reproduced with permission from ref. 20 Copyright 2004, Wiley-VCH Verlag GmbH&Co. KGaA; **Bottom left:** UV/Vis spectra of Co-TUD-1 samples with Si/Co ratios of 100 (1), 50 (2), 20 (5) and 10 (10), reproduced with permission from ref. 59 Copyright 2006, Wiley-VCH Verlag GmbH&Co. KGaA; **Bottom right:** FT-IR difference spectra of Al-TUD-1 samples with Si/Al ratios of 25, 50, 75 and 100 after pyridine desorption at 200 °C. Reprinted from ref. 35, Copyright (2006) with permission from Elsevier.

For many metals this is also true for ratios as high as 25. If the metal concentration is further increased, metal oxide nanoparticles are observed and with a further increase of the metal concentration, bulk metal oxide particles become part of the structure (Table 1). The appearance of metal particles is combined with a drop in pore volume, indicating that the metal oxide crystals are present in the pores of TUD-1. Another important feature of the M-TUD-1 synthesis is its high predictability. The ratio of Si/M in the synthesis mixture is virtually unchanged in the final M-TUD-1 (Table 1).

If truly high metal concentrations in siliceous TUD-1 need to be achieved,  $\text{TEAH}_3$  has to be replaced by TEG. In the synthesis of Al-TUD-1 with a Si/Al ratio of 4 TEG was used instead of  $\text{TEAH}_3$ . This enabled the synthesis of aluminium rich Al-TUD-1 with more than 40 % of the Al tetrahedrally incorporated, the other Al atoms were incorporated *via* penta-coordination or hexa-coordination. No  $\text{Al}_2\text{O}_3$  particles could be detected.<sup>20,21</sup> This is a special feature of the TUD-1 synthesis and it allows the preparation of M-TUD-1 with low Si/M ratios *via* direct synthesis. In many other materials it is necessary to graft the metal onto the siliceous material in a post synthesis step.<sup>22,23</sup>

The structure of TUD-1 as a three-dimensional mesoporous material was unambiguously demonstrated by 3-D-TEM studies.<sup>24</sup> Fig. 1 (right) depicts the pore volume, *i.e.* the void space in TUD-1. The sponge-like character of TUD-1 with irregular interconnected pores of different diameters is clearly visible. XRD, TEM, IR, UV, XPS, MAS-NMR and  $\text{N}_2$ -sorption studies were employed to confirm these structural features in TUD-1 and all M-TUD-1's.<sup>25</sup> Fig. 2 gives typical examples for all analytical techniques.

**Table 1** Physico-chemical properties of TUD-1 and M-TUD-1.

M-TUD-1	Si/M ratio <sup>a</sup>	S <sub>BET</sub> <sup>b</sup> (m <sup>2</sup> g <sup>-1</sup> )	V <sub>meso</sub> <sup>c</sup> (cm <sup>3</sup> g <sup>-1</sup> )	D <sub>meso</sub> <sup>d</sup> (nm)	Isolated M <sup>e</sup>	Nano-particles M-oxide <sup>e</sup>	Bulk M-oxide <sup>e</sup>	Reference
Si-TUD-1	-	453	0.556	4.9				2, 97
Al <sub>2</sub> O <sub>3</sub> -TUD-1	-	528	0.63	4				14
	-	413	0.58	4.5				14
	-	313	0.61	6				16
	-	619	0.73	4	++	-	-	59
Co-TUD-1	100 (108)	619	0.73	4	++	-	-	59
	50 (47.8)	605	0.65	3.9	+	-	-	59
	20 (18.6)	614	0.69	3.6	+	+	+	59
	10 (9.95)	684	0.58	3.1	+	-	++	59
Ti-TUD-1	1.7 (1.4)	516	0.28	0.2	++	+	-	25
	2.5 (2.3)	570	0.36	3.5	++	+	-	25
	5 (4.6)	741	0.5	3.6	++	+	-	25
	10 (9.7)	764	0.78	3.7	++	+	-	25
	20 (23.8)	633	0.99	7.2	++	+	-	25
	40 (38.8)	555	1.37	13.4	++	+	-	11, 25, 69
	100 (112)	628	1.1	9.1	++	-	-	25, 57
	100 (130)	565	1.54	8.4	++	-	-	25, 76, 77
Cr-TUD-1	20 (18.2)	588	1.1	4.4	+	+	++	25, 76, 77
	10	634	1.14	9.1	+	+	++	25, 76, 77
	100 (96)	634	0.94	8.1	+	-	-	25
V-TUD-1	50 (52)	653	0.98	5.8	+	-	-	25
	20 (19.3)	663	0.91	5.4	+	-	-	25
	10 (10.4)	702	0.51	3.7	+	+	-	25
Fe-TUD-1	100 (113)	568	1.82	15.9	++	-	-	25
	50 (54)	625	1.24	11.5	+	-	-	25
	20 (21)	803	0.70	5.2	+	+	-	25
	10 (10.1)	874	0.45	3.7	+	+	-	25
Fe-Al-TUD-1	25	710	0.57	3.4	+	+	-	68
Mn-TUD-1	10 (8)	626	0.65	4.6	+	+	++	67
	25 (22)	630	0.95	8.8	+	+	+	67
	50 (45)	778	0.99	6.8	++	+	-	67
	100 (89)	818	0.95	5.8	++	-	-	67
Al-TUD-1	3.5	357	0.409	1-40	+	-	-	21
	4	600	1.1	15	+	-	-	20
	4.85	204	0.201	2-4	+	-	-	21
	10 (14)	686	0.6	3.9	+	+	++	35
	25 (26.6)	956	0.95	3.7	+	+	+	35
	50 (51.4)	970	0.99	3.9	++	+	-	35
	75(78)	984	0.88	3.7	++	-	-	35
	100 (106)	880	0.91	3.7	++	-	-	35
Zr-TUD-1	10 (10)	676	0.4	<2	+	+	++	43
	25 (25)	764	1.23	8.8	+	+	+	42, 43
	50 (51)	771	1.2	8.9	++	+	-	43
	100 (102)	753	1.05	8	++	-	-	43
Al-Zr-TUD-1	25 (30)	877	0.70	3.3	+	-	-	47
	25 (28)	686	0.85	4.6	+	-	-	47
	25 (25)	705	0.70	4.2	+	-	-	47
Cu-TUD-1	10 (10.3)	616	0.55	3.7	+	+	++	56
	20 (21.4)	777	0.61	3.4	+	+	+	56
	50 (49.1)	718	0.7	4	++	+	-	56
	100 (105)	762	0.7	3.7	++	-	-	56

<sup>a</sup> Si/M ratio of the synthesis gel and between brackets after calcination. Elemental analysis. <sup>b</sup> Specific surface area.<sup>c</sup> Mesopore volume. <sup>d</sup> Mesopore diameter. <sup>e</sup> (++) abundantly present, (+) weakly or poorly present, (-) absent.



Thus almost ten years after its first synthesis TUD-1 is a material that can easily be synthesised *via* a straightforward and robust synthesis. The properties of TUD-1 can without difficulty be varied and many different properties can be imparted by the judicious choice of the metal added, its amount and the duration of the hydrothermal treatment. The resulting material is particularly stable and its production is scalable for industrial needs.<sup>17,18,26,27</sup> In a recent detailed contribution the large scale synthesis of Al-TUD-1 was described and the environmental and cost advantages of TUD-1 over other mesoporous materials was demonstrated. Starting from low cost silica gel and aluminium hydroxide rather than TEOS and aluminum(III)isopropoxide, significantly reduced costs and the recycling of the complexing agents TEAH<sub>3</sub> and TEG limited costs and reduced the environmental burden of the synthesis of TUD-1. The laboratory synthesis of TUD-1 is already particularly efficient but this industrial preparation of TUD-1 is especially favourable.<sup>27</sup>

Overall, TUD-1 is thus a distinct material with a straightforward, highly reproducible synthesis that allows many modifications and applications, both in the laboratory and in industry.

### 3. Catalysis with TUD-1

Mesoporous materials are such versatile substances as they enable countless new catalytic reactions, expanding the narrow application field of zeolites.<sup>28</sup> TUD-1, with its three-dimensional sponge-like structure is ideal for catalysis, since it facilitates diffusion limitation-free processes, only governed by the activity of the catalyst itself. Indeed, TUD-1, and in particular M-TUD-1, have proven to be very versatile and stable catalysts.

To impart catalytic activity to mesoporous materials it is either possible to utilise the intrinsic acidity or alkaline character of a purely siliceous or Al<sub>2</sub>O<sub>3</sub> based material. The strategy to introduce a metal oxide into the framework of the siliceous, mesoporous material was and is much more successful. Here, another advantage of TUD-1 is revealed. As explained above (Section 2), the incorporation of isolated metal atoms into the TUD-1 framework is straightforward and does not require any post synthesis modification of TUD-

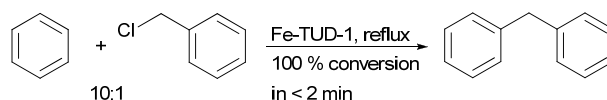
1. Equally the introduction of metal oxide nanoparticles and larger clusters can be achieved during the synthesis. Thus, acidic and redox active TUD-1 catalysts are readily prepared.

### 3.1. Reactions catalysed by acidic M-TUD-1

#### 3.1.1. Fe-TUD-1 as catalyst of Friedel-Crafts alkylations

Friedel-Crafts alkylations are acid-catalysed processes that are applied on a large industrial scale. When the reaction is catalysed by an acid such as  $\text{FeCl}_3$ , this acid is typically hydrolysed at the end of the reaction and not recycled, causing much waste. Replacing these homogeneous catalysts with heterogeneous catalysts is a target. By preparing Fe-TUD-1 with Si/Fe ratio of 10 to 100 both Fe-TUD-1 with only framework incorporated Fe and Fe-TUD-1 with iron oxide nanoparticles distributed throughout the pore system of TUD-1, could be prepared (Table 1).<sup>29,30</sup>

Both types of Fe-TUD-1, with and without nanoparticles, catalysed the benzylation of benzene (Scheme 2); however, the Fe-TUD-1 with high iron content and thus the highest concentration of  $\text{Fe}_2\text{O}_3$  nanoparticles is the most active catalyst. The Fe-TUD-1 catalysts outperformed Ga-TUD-1, Sn-



**Scheme 2** Fe-TUD-1 with Si/Fe=10 is an excellent catalyst for the benzylation of benzene.

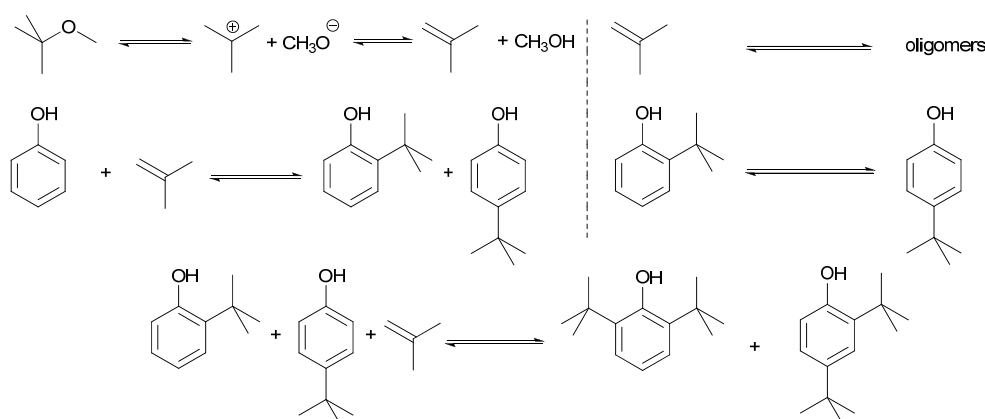
TUD-1, Ti-TUD-1 as well as Fe-HMS, Fe-MCM-41 and Fe-MFI. Hot filtration studies did however; reveal a weakness of the Fe-TUD-1 catalysts. While no activity leached, almost half of the iron was washed out of the material, casting doubt on its recyclability. None the less in the comparison of the catalytic activity (TOF) of different meso- and microporous catalysts such as Fe-MCM-41,<sup>31</sup> Fe-HMS<sup>32</sup> and Fe-MFI<sup>33</sup> with Fe-TUD-1, Fe-TUD-1 showed that irrespective of the Fe loading, it was more active than other Fe-containing micro- or mesoporous materials. This can be attributed again to the 3-dimensional, mesoporous structure which allows higher accessibility of the substrates. This also holds when comparing Fe-TUD-1 with Al-SBA-15.<sup>34</sup>

## 3.1.2. Al-TUD-1 as a versatile catalyst

Al-TUD-1 has been synthesised with many different Si/Al ratios. At low aluminium concentrations TEAH<sub>3</sub> is the chelating reagent of choice, at high aluminium concentrations, however, TEG had to be used as TEAH<sub>3</sub> proved difficult to remove at Si/Al of below 10. Remarkably all aluminium was framework incorporated even at these high aluminium concentrations (Table 1). When the acidity of Al-TUD-1 was studied, it was noted that with increasing Si/Al ratio the total acidity dropped but the acid strength increased – similar to what has been observed in zeolites.

Al-TUD-1's with Si/Al of 3.5 and 4.85 were compared with HY zeolite for the catalytic degradation of high density polyethylene and proved to have higher activity and stability than the zeolite. The mesoporous structure of Al-TUD-1 ensures diffusion limitation-free access to the catalytic site, while this is not the case in the zeolite and equally coking is less of an issue in the wide pores of this material.<sup>21</sup>

The true value of Al-TUD-1 is revealed in the Friedel-Crafts alkylation of phenol.<sup>35</sup> Utilising Methyl *tert*-Butyl Ether (MTBE) or *tert*-Butyl Alcohol (TBA) as alkylating reagent phenol could be alkylated both in the gas phase and in the liquid phase (Scheme 3). The conversion is directly dependant on the ratio of phenol to alkylating



**Scheme 3** The Friedel-Crafts alkylation of phenol with MTBE is an equilibrium reaction with four potential products, *o*- and *p*-*tert*-butylphenol, as well as 2,4- and 2,6-di-*tert*-butylphenol.

reagent, an excess of it leading to 2,4-di-*tert*-butylphenol as main product in the liquid phase, while in the gas phase 4-*tert*-butylphenol always remains the dominant product (Fig. 3). Similar selectivity towards the 2,4-di-*tert*-butylphenol in the liquid phase was recently

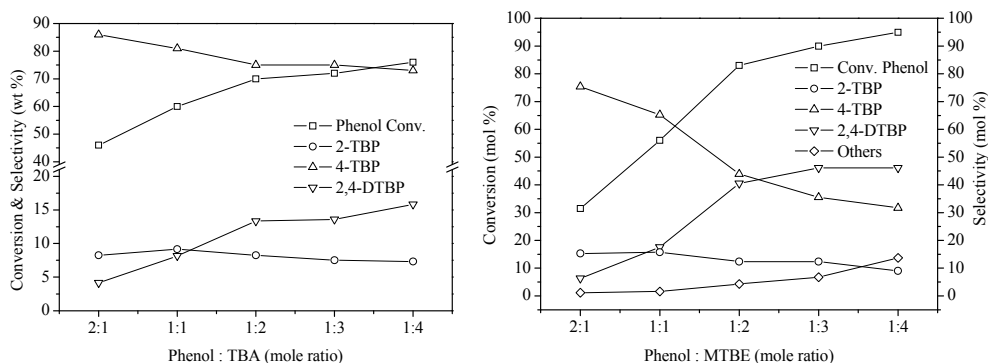


**Figure 3** Effect of phenol to alkylating reagent ratio in Al-TUD-1 Si/Al = 25 catalysed reaction. **Left:** gas phase reaction, TBA alkylating reagent, WHSV of  $1 \text{ h}^{-1}$  at  $175^\circ\text{C}$ . **Right:** Liquid phase reaction, MTBE alkylating reagent,  $150^\circ\text{C}$ , 0.2 g catalyst, 2.0 g reactants, 20 mL cyclohexane, 4 h. Reprinted from ref. 35. Copyright (2006) with permission from Elsevier.

described for a tungsten catalyst. However, the material was not tested in the gas phase.<sup>36</sup> In the gas phase reaction Al-TUD-1 with Si/Al of 25 proved to be the best catalyst, it was stable over a period of 10 h (Fig. 4) and even when the weight hourly space velocity (WHSV) was increased to  $4 \text{ h}^{-1}$  conversions were unaltered at 70 % (Phenol:TBA = 2). This is strong evidence for the high stability and for the diffusion limitation-free character of this catalyst system (Fig. 4) also when comparing with Al-MCM-41, Al-MCM-48 and Al-SBA-15.<sup>37,38,39</sup> Al-MCM-48 and Al-MCM-41 gave 59% and 36% conversion of phenol respectively with 79.8% and 83.3% selectivity towards 4-*tert*-butylphenol ( $175^\circ\text{C}$ ; WHSV =  $4.8 \text{ h}^{-1}$ ; TOS = 1.5 h; TBA:phenol = 2:1).<sup>38</sup> Under similar reaction conditions ( $175^\circ\text{C}$ ; WHSV =  $1 \text{ h}^{-1}$ ; TOS = 2 h; TBA:phenol = 2:1), Al-TUD-1 showed 70% phenol conversion with 77% 4-*tert*-butylphenol selectivity.<sup>35</sup>

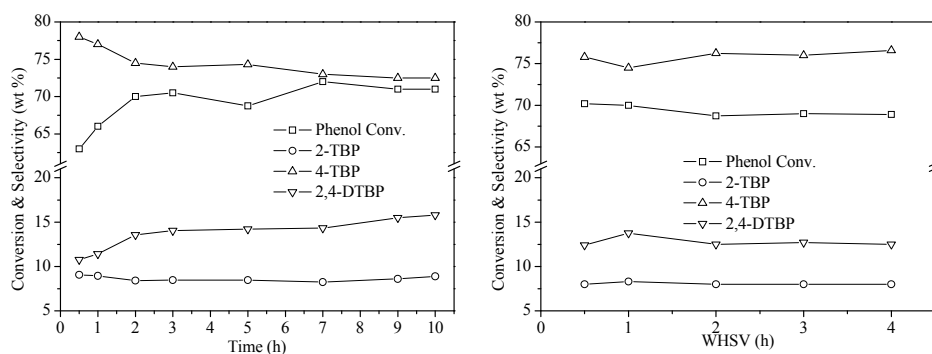
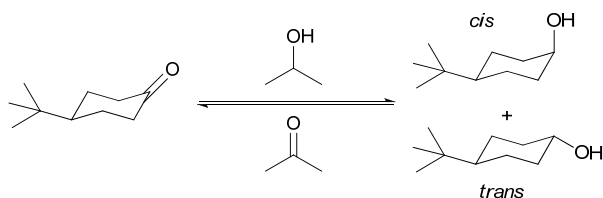


**Figure 4 Left:** Al-TUD-1 with Si/Al=25 is very stable in the gas phase Friedel-Crafts alkylation of phenol with TBA at 175 °C and WHSV of 1 h<sup>-1</sup>. Reprinted from ref. 35. Copyright (2006) with permission from Elsevier. **Right:** Al-TUD-1 with Si/Al=25 is not diffusion limited as is demonstrated by unaltered conversions up to WHSV of 4 h<sup>-1</sup>. Reprinted from ref. 35, Copyright (2006) with permission from Elsevier.

### 3.1.3. Zr-TUD-1 as a Lewis –acidic catalyst

Zirconium in its oxidation state Zr (IV) is a tetrahedrally coordinated metal which is purely Lewis acidic and unlike aluminium or iron, does not impart Brønsted acidity. Consequently the Zr-TUD-1 catalysts that only contain framework incorporated zirconium should be the ideal heterogeneous Lewis acid.<sup>40,41</sup> When tested in the Lewis-acid catalysed Meerwein-Ponndorf-Verley reduction Zr-TUD-1 catalysed the reduction of sterically very demanding steroids such as 5 $\alpha$ -cholestan-3-one to 5 $\alpha$ -cholestan-3-ol, proving that the mesoporous structure enabled the reduction of large molecules.<sup>42</sup> In the reduction of 4-*tert*-butylcyclohexanone (Scheme 4) the solvent dependence of the reaction was demonstrated and



**Scheme 4** The Meerwein-Ponndorf-Verley reduction of 4-*tert*-butylcyclohexanone yields both the *cis* and the *trans* alcohol.

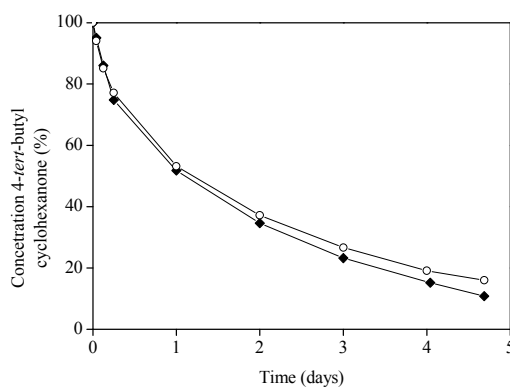
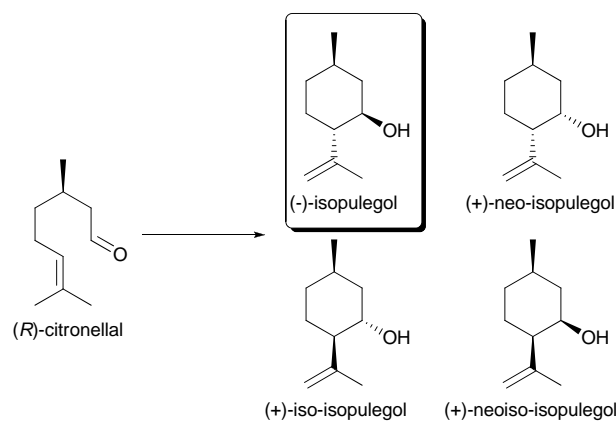


**Figure 5** Recycling of Zr-TUD-1 with Si/Zr=25 in the Meerwein-Ponndorf-Verley reduction of 4-*tert*-butylcyclohexanone; ♦ first run; ○ recycled catalyst. Reprinted from ref. 42, Copyright (2006) with permission from Elsevier.

Zr-TUD-1 could be recycled without loss of activity (Fig. 5).

Zr-TUD-1 displayed great stability in the Prins reaction, as demonstrated in the cyclisation of citronellal to isopulegol (Scheme 5). Even after five cycles virtually no loss



**Scheme 5** The acid catalysed Prins reaction of citronellal is employed industrially for the production of isopulegol. The other stereoisomers of isopulegol occur as minor side products.

of activity was observed and after calcination the initial activity was regained. Furthermore, hot filtration studies proved that no metal leached from the catalyst. When comparing Zr-

TUD-1's with different Si/Zr ratios it was again demonstrated that no diffusion limitation occurs (Fig. 6); the material with the highest Si/Zr has by far the highest TOF.<sup>43</sup>

In a recent further development of the Zr (IV) catalysed Prins reaction, bifunctional catalysts have been described. These allow for the very efficient Prins reaction with for instance Zr-Beta or Ir-Beta and a subsequent reduction in the same pot. Thus a two step one pot synthesis of menthol was created.<sup>44,45,46</sup>

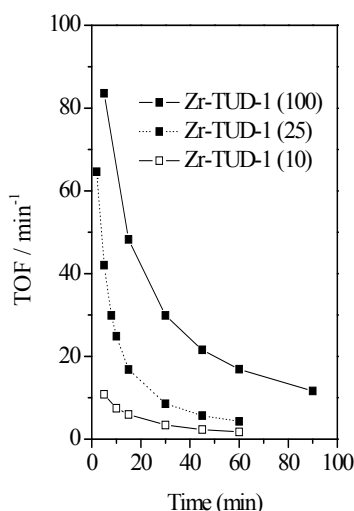


**Figure 6** Prins-reaction of industrial grade citronellal catalysed by Zr-TUD-1 with different Si/Zr ratios (given in brackets). Reproduced with permission from ref. 43 Copyright 2008, Wiley-VCH Verlag GmbH&Co. KGaA.

#### 3.1.4. Is there synergy in bimetallic Al-Zr-TUD-1?

Zr-TUD-1<sup>43</sup> is a purely Lewis acidic material while Al-TUD-1 displays both types of acidity, Lewis and Brønsted.<sup>35</sup> The combination of both metals in one catalyst would thus enable the tuning of the ratio of Lewis acid sites to Brønsted acid sites. This would allow studying the existence of synergy between the two types of acid sites; in particular, since the bimetallic Al-Zr-TUD-1 could be compared with Al-TUD-1 or Zr-TUD-1 with the same overall metal concentration. Thus Al-Zr-TUD-1 with a Si/M ratio of 25 and Al/Zr ratios of 1:3, 2:2 and 3:1 were prepared. Pyridine desorption monitoring by IR spectroscopy

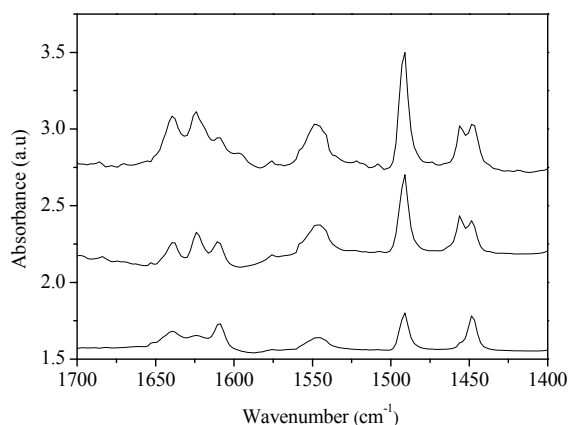


**Figure 7** FT-IR spectra after pyridine desorption at 200 °C. Top: Al-Zr-3:1-TUD-1; Middle: Al-Zr-2:2-TUD-1; Bottom: Al-Zr-1:3-TUD-1. Reproduced by permission of the Royal Society of Chemistry from ref 47.

clearly revealed an altered ratio of Brønsted to Lewis acidity. Brønsted ( $1547\text{ cm}^{-1}$ ) and Lewis acidity (Al:  $1456\text{ cm}^{-1}$ , Zr:  $1448\text{ cm}^{-1}$ ; Fig. 7) could be distinguished and with an increase of Zr the signal for the Lewis acidic site due to Al decreases, as does that for Brønsted acidity. The ratio Brønsted/Lewis acidity decreases from approx. 1.1 for Al/Zr = 3:1 and Al/Zr=2:2 to 0.7 for Al/Zr=1:3. Thus a range of TUD-1 catalysts with either Al or Zr or mixtures thereof was available to study the influence of Brønsted acid sites on Lewis acid sites and *vice versa*.<sup>47</sup> Earlier, theoretical studies on the synergy between Brønsted and Lewis acid sites had indicated that this synergy should exist.<sup>48</sup> Indeed, first experimental evidence for such a synergy had been presented for a Ce-Al-MCM-41.<sup>49</sup>

When Al-Zr-TUD-1 was employed in the Prins reaction (Scheme 5) the synergy between the Brønsted acid sites and the Lewis acid sites becomes obvious. This reaction can actually be catalysed by both Lewis and Brønsted acidic catalysts. Pure Al-TUD-1 and pure Zr-TUD-1 are both relatively weak catalysts, while all Al-Zr-TUD-1 catalysts perform better (Fig. 8). This, although the metal concentration in all five catalysts is the same, clearly proves the existence of synergy between both types of acid sites.<sup>47</sup> A similar study but with heterogeneous inorganic fluorides as catalysts, was published shortly afterwards.<sup>50</sup> Again the Prins reaction of citronellal served as the test reaction, confirming the observations made with TUD-1.



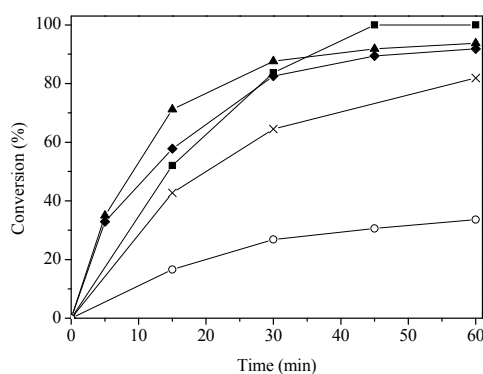


**Figure 8** Prins reaction of citronellal catalysed by Al- and Zr-TUD-1 catalysts with Si/M=25. Reaction conditions: 4 mmol citronellal, 5 g toluene, 80 °C, 50 mg catalyst. (○) Zr-TUD-1 (x) Al-TUD-1 (■)Al-Zr-1:3-TUD-1 (◆)Al-Zr-2:2-TUD-1 and (▲)Al-Zr-3:1-TUD-1. Reproduced by permission of the Royal Society of Chemistry from ref 47.

### 3.1.5. Composites of TUD-1 and zeolites.

The acidity of zeolites is much stronger than that of mesoporous materials. By incorporation of zeolite nanocrystals inside the mesoporous structure of TUD-1, it was aimed to introduce strong acid sites originating from zeolites. At the same time mass transport limitations associated with zeolites should be greatly reduced due to the large pore diameter and the sponge-like pore character of TUD-1, in combination with the small crystallite size of the incorporated zeolite particles.<sup>51,52</sup>

With XRD as well as HR-TEM it was shown that zeolite nanocrystals of 40 nm can be homogeneously dispersed throughout the mesoporous TUD-1 matrix. Integrity of mesostructure is retained to values up to 40 wt% zeolite incorporation. With increased loading of zeolite small aggregates start to emerge, also evidenced by N<sub>2</sub> physisorption.<sup>27,51</sup>

FT-IR spectroscopy using either CO or NH<sub>3</sub> has highlighted the modification of acid sites due to interaction of amorphous TUD-1 and the crystalline zeolite particles. In the sample with 40 wt% of zeolite the highest concentration of partially extra-framework Al-OH groups (Brønsted acid sites with medium acidity) as well as distorted siloxane surface bridges that easily can break up in the presence of adsorbates/reactants have been obtained. At the same time, 40%-Beta-TUD-1, had twice the catalytic activity of pure zeolite Beta in *n*-hexane cracking at 538 °C. The abundant presence of both Brønsted sites with medium

acidity as well as distorted siloxane bridges might have synergistic effect during the cracking reactions in the formation/stabilisation of the carbo-cationic intermediates. When comparing the physical mixture of zeolite Beta and TUD-1 with 40%-Beta-TUD-1 the higher activity of the composite 40%-Beta-TUD-1 illustrates the presence of synergy between the catalytic sites (Fig. 9). An alternative explanation would be the much better dispersion and thus accessibility of the zeolites in the composite material.<sup>51</sup>

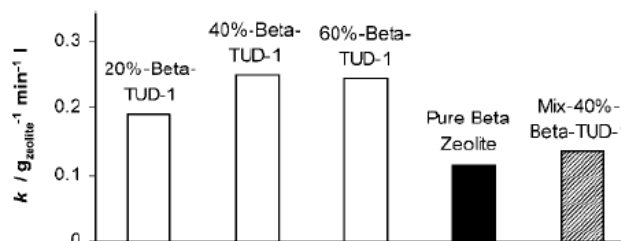
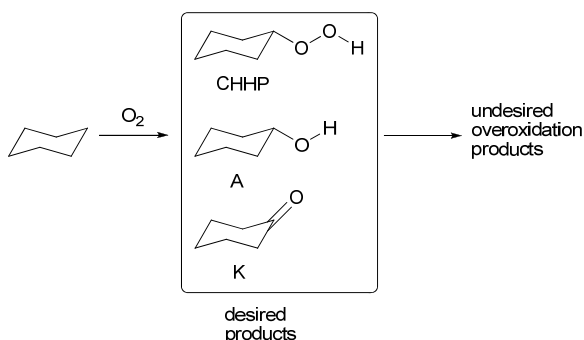


**Figure 9** Composite materials from zeolite Beta and TUD-1 display synergy in the catalytic cracking of *n*-hexane. Reproduced with permission from ref. 51 Copyright 2004, Wiley-VCH Verlag GmbH&Co. KGaA.

### 3.2. Oxidations catalysed by M-TUD-1

#### 3.2.1. Alkane oxidation

M-TUD-1 materials were studied as catalysts for the oxidation of cyclohexane which is of great industrial importance and a major academic challenge (Scheme 6).<sup>53,54,55</sup> As an initial



**Scheme 6** The selective oxidation of unreactive hydrocarbons such as cyclohexane is a veritable challenge since overoxidation of the desired monooxygenated products needs to be avoided.

screening of the catalyst, cyclohexane oxidation with *tert*-butyl hydroperoxide (TBHP) as oxidant revealed that Co-, Cu- and Cr-TUD-1 showed an outstanding performance as they decompose TBHP much faster than other M-TUD-1's and hence effect the conversion of cyclohexane (Fig.10).<sup>56,57,58</sup> However, a plot of conversion of cyclohexane *versus*

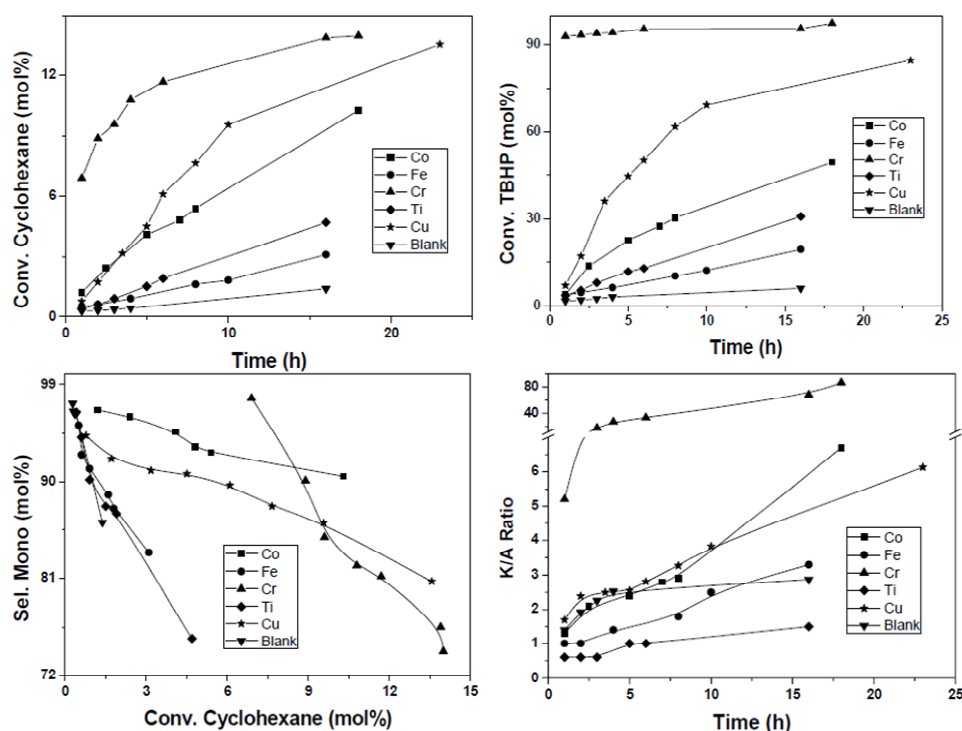


**Figure 10** M-TUD-1 catalysed cyclohexane oxidation with TBHP as sacrificial oxidant.

selectivity for mono-oxygenated products displayed a different trend. Cr-, Ti- and Fe-TUD-1 followed a trend similar to the blank reaction. The selectivity decrease is similar to the blank reaction with respect to conversion. Cu- and Co-TUD-1 showed a very slow decrease even at higher conversion levels of cyclohexane. In particular Co-TUD-1 displayed higher selectivity to mono-oxygenated products for the same cyclohexane conversion as compared to Cu-TUD-1. Cr-TUD-1 produced more cyclohexanone than cyclohexanol, whereas Co-TUD-1 produced initially more of the alcohol, which was then slowly oxidized to the ketone and the K/A ratio improves. Also hot-filtration experiments and the AAS analysis of

the filtrate showed that leaching of Cr (13 %) and Cu (0.5 %) occurred, whereas the reaction is truly heterogeneous with Co-TUD-1 (Fig.11).<sup>58,59</sup>

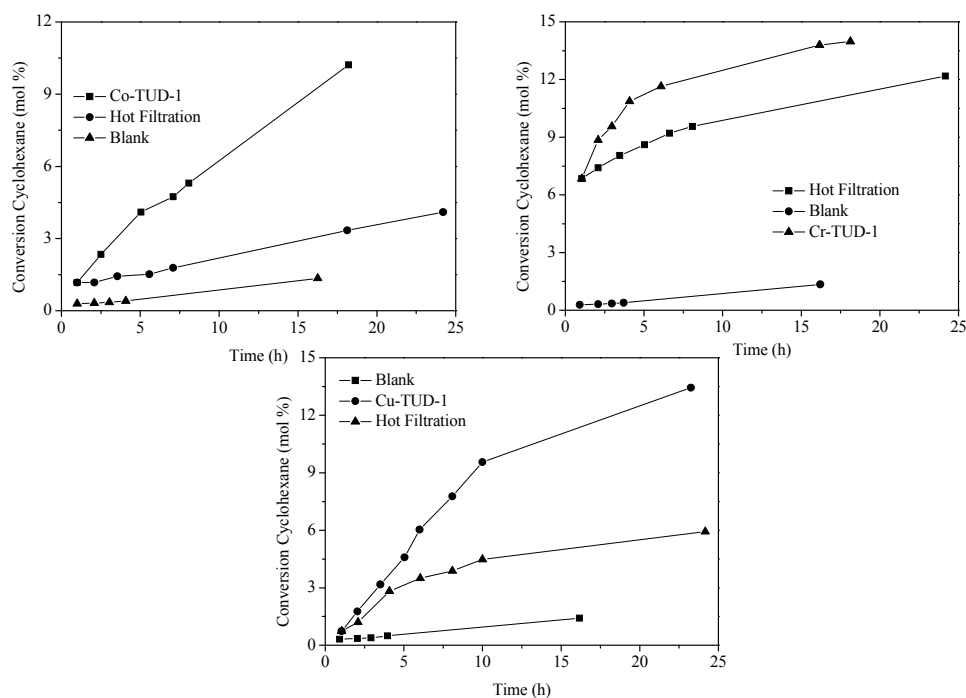


**Figure 11** Hot filtration studies of several M-TUD-1 catalysts reveal that Co-TUD-1 (upper left) is stable and that no cobalt and consequently no activity leaches.

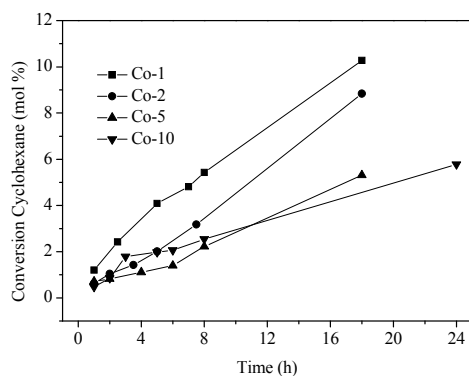


**Figure 12** Co-TUD-1 catalysed oxidation of cyclohexane with TBHP as oxidant. Co-TUD-1 with different Si/Co ratios were employed, Co-1: Si/Co=100, Co-2: Si/Co=50, Co-5: Si/Co=20 and Co-10: Si/Co=10. Reproduced with permission from ref. 59 Copyright 2006, Wiley-VCH Verlag GmbH&Co. KGaA.

Further studies with different loadings of Co (Fig. 12), revealed that Co-TUD-1 (Si/Co=100) with the lowest Co loading, and thus isolated Co atoms (Table 1), displayed the highest activity, directly followed by Co-TUD-1 (Si/Co=50).<sup>59</sup> In addition to the importance of isolated Co species, this result demonstrates that no diffusion limitation occurs in these mesoporous materials. Co-TUD-1 (Si/Co=20) that contains Co<sub>3</sub>O<sub>4</sub> nanoparticles was observed to be less active, most likely due to the reduced accessibility of the Co atoms. However Co-TUD-1 (Si/Co=10) in which bulky Co-oxide clusters are present, showed slightly increased activity, a result in line with the activity of Co<sub>3</sub>O<sub>4</sub> crystals that has been described earlier.<sup>60</sup> The observed improvement of the ketone/alcohol (K/A) ratio was due to mixed Russell termination between cyclohexyl hydroperoxy radicals and *tert*-butyl hydroperoxy radicals.<sup>61</sup> In comparison cyclohexane oxidation catalysed by manganese oxide octahedral molecular sieves showed a turnover number (TON) of 73 in 24 h at 80 °C with *tert*-butyl hydroperoxide as an oxidant and using acetonitrile as solvent,<sup>62</sup> whereas Co-TUD-1 (Si/Co = 100) showed a TON of about 100 in 18 h at 70 °C which was carried out under solvent-less conditions.

Stimulated by these results this study was extended to the aerobic cyclohexane oxidation, simulating the industrial conditions. M-TUD-1's with Si/M ratios of 100 were utilised in the aerobic cyclohexane oxidation (Table 2).<sup>63,64</sup> With TBHP as initiator, the

**Table 2** Aerobic oxidation of cyclohexane over M-TUD-1 (Si/M=100) in the presence of TBHP as radical initiator.<sup>a</sup>

M-TUD-1		Mol%					
		Conv. <sup>b</sup>	K <sup>c</sup>	A <sup>d</sup>	CHHP <sup>e</sup>	S <sub>mono</sub> <sup>f</sup>	K/A
Ti	Si/Ti=100	2.9	33.4	55.5	1.2	90.5	0.6
	Si/Ti=50	2.4	42.4	38.6	87.2	1.1	2.4
	Si/Ti=20	3.4	48.5	33.7	85.6	1.4	3.4
	Si/Ti=10	3.7	54.9	23.7	81.2	2.4	3.7
Cr		3.2	48.2	19.9	6.6	78.3	2.4
Co		3.7	35.4	50.4	3.5	90.9	0.7
Fe		2.7	37.8	49.8	1.6	91.6	0.8
Cu		2.6	42.1	42.8	1.4	88.8	1.0
Mn		2.9	26.6	52.3	3.4	85.5	0.5
Blank		1.3	29.5	25.8	6.5	67.7	1.1

<sup>a</sup> Conditions: Cyclohexane = 175 mmol ; TBHP = 0.05 mmol ; PhCl = 1 g (internal standard) T = 120°C; Catalyst = 0.1 mmol of active metal species. <sup>b</sup> Conversion. <sup>c</sup> Ketone. <sup>d</sup> Alcohol. <sup>e</sup> Cyclohexyl hydroperoxide. <sup>f</sup> Selectivity for mono-oxygenated products.

highest conversions were observed with Co-TUD-1 that also gave the best selectivity toward mono-oxygenated products. Cr-TUD-1 was also very active but displayed low selectivity. Ti-TUD-1 and Mn-TUD-1 showed similar activity, with poor selectivity in the case of Mn-TUD-1. Fe-TUD-1 and Cu-TUD-1 were moderately active and displayed rather high selectivity, Fe-TUD-1 being somewhat more selective. When TBHP was replaced with cyclohexyl hydroperoxide (CHHP), the initiator commonly employed in industry, Ti-TUD-1 lost all its activity, Fe-TUD-1 and also Cu-TUD-1 now displayed low activity, in the case of Cu-TUD-1 coupled with low selectivity (Table 3).<sup>63,64</sup> Co-TUD-1,

**Table 3** Aerobic oxidation of cyclohexane over M-TUD-1 (Si/M = 100) in the presence of CHHP as radical initiator.<sup>a</sup>

M-TUD-1		Mol%					
		Conv. <sup>b</sup>	K <sup>c</sup>	A <sup>d</sup>	CHHP <sup>e</sup>	S <sub>mono</sub> <sup>f</sup>	K/A
Ti		0.5	24.9	43.0	12.7	91.5	0.6
Cr		3.6	64.5	8.3	0.2	75.7	7.7
Co	Si/Co=100	3.8	30.8	56.5	0.5	90.4	0.5
	Si/Co=50	3.8	58.4	31.1	1.1	91.9	1.9
	Si/Co=20	3.0	68.2	20.8	1.0	92.7	3.3
	Si/Co=10	2.1	62.2	23.5	0.9	87.1	2.6
		1.6	53.1	29.4	3.6	90.0	1.8
Fe		2.2	43.5	34.5	2.2	82.9	1.3
Cu		3.1	21.2	36.2	61.8	0.6	3.1
Mn	Si/Mn=100	2.2	21.1	41.9	65.3	0.5	2.2
	Si/Mn=50	2.1	24.2	47.9	74.7	0.5	2.1
	Si/Mn=20	4.0	23.3	49.9	78.6	0.5	4.0
	Si/Mn=10	0.6	49.3	39.0	3.2	93.0	1.2
Blank							

<sup>a</sup> Conditions: Cyclohexane = 175 mmol ; CHHP = 0.05 mmol ; PhCl = 1 g (internal standard) T = 120°C; Catalyst = 0.1 mmol of active metal species. <sup>b</sup> Conversion. <sup>c</sup> Ketone. <sup>d</sup> Alcohol. <sup>e</sup> Cyclohexyl hydroperoxide. <sup>f</sup> Selectivity to mono-oxygenated products.

Cr-TUD-1 and Mn-TUD-1 were the most active catalysts. In addition Co-TUD-1 exhibits very good selectivity making it the catalyst of choice in this row. Extensive studies of Co-TUD-1 with different Si/Co ratios confirmed that Co-TUD-1 with Si/Co=100 is a very stable, active and selective catalyst for the aerobic cyclohexane oxidation. Mn-TUD-1, on the other hand, combines high activity with very low selectivity. The result for Co-TUD-1 is particular remarkable when placed into a general context. Most of the recent cyclohexane oxidation studies were carried out with molecular oxygen with a pressure of about 5-10 bar. In such a catalytic oxidation over metal ion exchanged ZSM-5 catalysts in a solvent-free system, Co-ZSM-5 showed about 10 mol% conversion of cyclohexane and 97% selectivity for KA-oil (a mixture of cyclohexanone and cyclohexanol). However, the leaching of

cobalt from Co-ZSM-5 occurred readily.<sup>65</sup> Equally Ce-MCM-48 did not perform better than Co-TUD-1 in the aerobic oxidation of cyclohexane.<sup>66</sup>

Ti-TUD-1 is a catalyst with excellent selectivity but induces only little conversion of CHHP. The performance is linked to the titanium loading: low loading yields Ti-TUD-1 with isolated titanium species and ensures the highest observed activity for this metal in CHHP decomposition. High titanium loading leads to extra-framework titanium dioxide particles that are effectively inactive towards CHHP decomposition. In contrast, they are very active in the decomposition of TBHP. In the case of the active, but unselective Mn-TUD-1, higher manganese loadings significantly improved selectivity without loss of activity. Manganese oxide clusters at high manganese loading contain more  $\text{Mn}^{3+}$  that improves selectivity.<sup>67</sup>

Comparing all results it is evident, that both metal and Si/M ratio are important parameters for the activity of the M-TUD-1 catalysts in the aerobic cyclohexane oxidation. In particular the fact whether the metal is completely incorporated into the silica framework or is present as metal oxide clusters can greatly influence the activity and selectivity of the catalyst. Consequently, the relative fraction of framework-incorporated and extra-framework metal sites may offer a tool for improving the activity and directing the selectivity of M-TUD-1 catalysts for selective oxidation reactions.

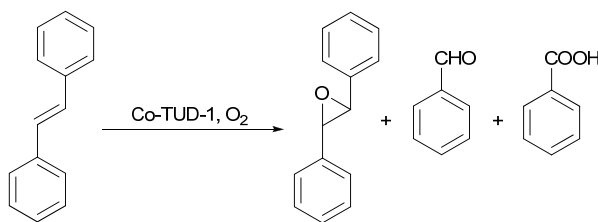
In a completely different line of alkane oxidations Fe-TUD-1 and Fe-Al-TUD-1 were utilised as catalysts for the  $\text{N}_2\text{O}$  mediated oxidation of propane to propene. While both catalysts were less active than Fe- $\text{AlPO}_4$ -5 or Fe-ZSM-5, their stability was significantly better, confirming that TUD-1 is a particularly robust material.<sup>68</sup>

### 3.2.2. Epoxidations of alkenes

Titanium-based catalysts have repeatedly proven their value in the epoxidation of alkenes. To investigate whether the pore structure of TUD-1 offers the expected advantages, *i.e.* a diffusion limitation free catalytic system, Ti-TUD-1 was compared with Ti-MCM-41. In both samples the titanium was framework incorporated. Ti-TUD-1 displayed a five-time higher TOF in the epoxidation of cyclohexene than Ti-MCM-41. Even after boiling Ti-TUD-1 in water the TOF was still more than four-times higher, giving solid evidence for the stability of the catalyst.<sup>11,69</sup>

As explained in section 3.2.1. Ti-TUD-1 catalyses the decomposition of TBHP, the reagent used for the epoxidation of the alkenes. Here this decomposition is an undesired side reaction. In order to reduce this rate, the Ti-TUD-1 was silylated, capping acidic silanol and Ti-OH groups. This approach was indeed successful, and the silylated Ti-TUD-1 displayed higher selectivity in the epoxidation of 1-octene.<sup>70</sup>

Very recently the application of Co-TUD-1 for the epoxidation of stilbene using oxygen was described.<sup>71</sup> At low Co loading when all Co is framework incorporated the highest selectivity for epoxidation combined with excellent TOF was observed. Co-TUD-1 outperformed Co-MCM-41, CoX faujasite zeolite and Co<sub>3</sub>O<sub>4</sub> crystals, it could be recycled for four times without significant loss of activity and no leaching of the active metal was detected (Scheme 7).



**Scheme 7** The selective epoxidation of stilbene is effectively catalysed by Co-TUD-1. High selectivity is observed and little over oxidation occurs.

### 3.3. Photo-catalysis with M-TUD-1

Photo-catalysis is another field where TUD-1 based materials have been successfully employed. Photo-catalysis implies the acceleration of a photon induced reaction by the presence of a catalyst.<sup>72,73,74</sup> The emphasis of the investigations of M-TUD-1 for this type of catalysis was on the enhancement of the level of understanding of selective photo-oxidation of alkanes. The benefit of the TUD-1 based systems as compared to other silica based supports, lies mainly in the formation of well dispersed active phases up to a loading of approximately 5 wt % for group V and group VI elements (Table 1). This is normally difficult to achieve with commercially available silica, or other micro-, or mesoporous materials, and allows to obtain relatively high signals of isolated active catalytic sites and interactions thereof with reacting species in spectroscopic investigations, even in short time



scales and in transient studies. Furthermore, at high loading (10-60 wt %), the synthesis procedure of TUD-1 allows a high level of control of the pore structure and nanoparticle size distribution for some metal oxides (Fig 1), ideal to investigate (nano)particle size effects in photo-catalysis. Three metal oxides dispersed in TUD-1 have been mainly used in the investigation of selective photo-oxidation, *i.e.* Cr-TUD-1, V-TUD-1 and Ti-TUD-1.

### 3.3.1. Cr-TUD-1

Cr-based photo-catalysts were reported in the literature to be highly active in selective photo-oxidation.<sup>75</sup> A TUD-1 catalyst with 10% Cr was used to resolve whether isolated sites are indeed the only active sites, or nanoparticles and crystals contribute (Table 1). Structural information was obtained by testing the performance of the highly loaded catalyst with different wavelengths of activation. By careful analysis of the UV-Vis absorption spectrum of the Cr-TUD-1 catalyst, it was established that the Cr(III) contributions to photo-activity, if any, were to be expected in the wavelength range of 550-650 nm, while Cr(VI) contributions were to be expected at wavelengths in the range of 300-550 nm. By careful evaluation of the performance of the Cr-TUD-1, using IR spectroscopy to analyse the intrinsic surface adsorbed products, a correlation was established between the wavelength of activation and the photo-catalytic performance.<sup>76,77</sup> A clear maximum in the photo-activity was observed at around 460 nm. At this wavelength isolated Cr(VI) oxides in tetrahedral coordination are known to absorb, and therefore this is concluded to be the most active site in the materials. It is remarkable that lower wavelengths of higher energy do not induce higher reactivity. This is the consequence of the quick relaxation of states excited at these smaller wavelengths, leading to the same relatively long lived Cr(VI) triplet state. Together with the absence of a strong selectivity effect of either wavelength or the absence or presence of oxygen in the feed, reaction occurs between the partially relaxed excited chromophore and an adsorbed propane molecule. Cr(III) species did not contribute to photo-activity, light absorbed by these species being wasted, inducing lower quantum efficiencies than observed for the Cr sample with 1 wt %. In conclusion, the study suggests that if a high dispersion of Cr-species can be combined with a high loading, the performance per gram of catalyst can be improved. Indeed TUD-1 catalysts with less Cr, 1-5 wt % (Table 1), show excellent performance in photo-catalytic propane oxidation.<sup>76,77</sup>

### 3.3.2. V-TUD-1

Silica supported vanadium oxides are effective photo-catalysts in selective hydrocarbon oxidation, typically in gas phase applications.<sup>78,79,80</sup> The active vanadia sites are completely dehydrated during reaction and, without promoters, UV radiation is required to photo-activate the catalytic centres.<sup>78,79,80</sup> Hydration results in a shift of the absorption spectrum to the visible, and would in principle generate sites that can be activated by visible light. To further elucidate the structure of the vanadate site during photo-catalysis, and to confirm visible light activity of hydrated sites, vanadia was incorporated in the mesoporous material TUD-1 with a loading of 2 wt % vanadia, assuring that all vanadia is present as isolated sites (Table 1). The performance in the selective photo-oxidation of liquid cyclohexene was investigated using ATR-FT-IR spectroscopy.<sup>81</sup> Under continuous illumination at 458 nm a significant amount of product, *i.e.* cyclohexenone, was identified. This demonstrated for the first time that indeed hydroxylated vanadia centres in TUD-1 can be activated by visible light to induce oxidation reactions. In view of the spectroscopic evidence, the active site was shown to contain at least one hydroxyl group. Using the rapid scan method, a strong perturbation of the vanadyl environment could be observed in the selective oxidation process induced by a 458 nm laser pulse of 480 ms duration. This is proposed to be caused by interaction of the catalytic centre with a cyclohexenyl hydroperoxide intermediate. Molecular rearrangement and dissociation of the peroxide to ketone and water, lead to restoration of the vanadyl site. The use of V-TUD-1 was instrumental to arrive at the conclusions of the study, because of the well defined structure of the active site.<sup>81</sup>

### 3.3.3. Ti-TUD-1

A strategy to influence the photo-catalytic performance of TiO<sub>2</sub>, is to support TiO<sub>2</sub> on inert SiO<sub>2</sub> based materials. One creates isolated molecular Ti sites in tetrahedral coordination, by impregnating mesoporous materials (such as MCM 41<sup>82,83,84</sup> and SBA-15<sup>85,86</sup>) with TiO<sub>2</sub> precursors. In these procedures, besides isolated sites, clustered Ti-sites are often produced if the loading is increased above ~ 1-2 wt %. The relative contribution of these clustered sites and/or nano-particles to the overall photoactivity of TiO<sub>2</sub> supported on SiO<sub>2</sub> based materials, was typically not considered. The studies involving TUD-1 were thus focused on this aspect.<sup>87</sup> By varying the crystallization time (Ti-TUD-1 Si/Ti=2.5; 8 h and Ti-TUD-1

Si/Ti=2.5; 24 h, Table 1) two samples were obtained with well defined different nanoparticle sizes (Fig. 13). The pore structure itself is obscured by the depth of field in the HR-TEM images shown in Figure 13, but the  $\text{TiO}_2$  crystals in the anatase phase can be identified by their electron diffraction fringes. The typical size of these inclusions corresponds well to the pore diameter obtained from the adsorption isotherms.

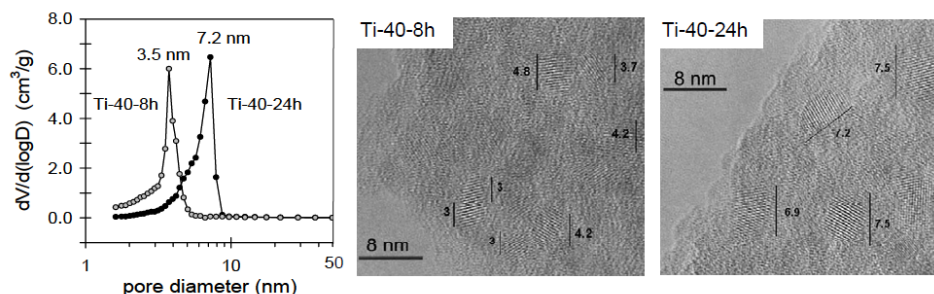


**Figure 13 Left:** Pore size distributions of the Ti-TUD-1 with Si/Ti=2.5 (Ti-40) samples after 8 h and 24 h hydrothermal treatment, as obtained from the isotherms. **Center and right:** transmission electron micrographs of the corresponding samples. The structure of individual pores is not visible, but titania crystallites can be identified by their electron-diffraction fringes. Size estimates are indicated in nm.

To compare the photo-catalytic performance of these materials, the photo-oxidation of propane to acetone (desired), carboxylates (undesired), and water (unavoidable) was analysed with infrared spectroscopy. A narrow width activation of the chromophores (335 nm) was applied, selectively activating the nanoparticles and excluding possible contributions to the reaction of isolated Ti-centres. Without showing all the spectra, the initial reaction rate is greater in sample Ti-TUD-1 Si/Ti=2.5 24 h (7.5 nm particles), yet its activity decreases sharply within the first hour (Fig. 14). For sample Ti-TUD-1 Si/Ti=2.5 8 h (3.5 nm particles) a lower initial rate is observed, by a factor of 4.8, but this rate is maintained over a prolonged period of time. At all stages of product accumulation the selectivity toward acetone of the Ti-TUD-1 Si/Ti=2.5 8 h sample (3.5 nm) is approximately 50% greater than that of Ti-TUD-1 Si/Ti=2.5 24 h (7.5 nm), as shown in Figure 14. These results show that the particles formed at higher loading in mesoporous materials contribute to photo-catalytic activity to a significant extent, while the selectivity

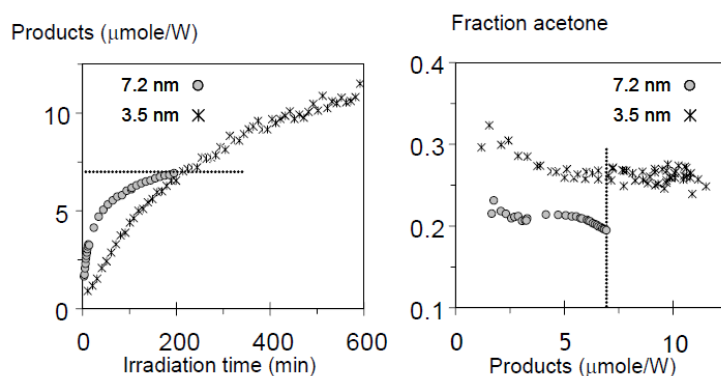


**Figure 14** Left panel: molar sum of adsorbed products (acetone+water+carboxylates) produced as a function of time over two Ti-TUD-1 with Si/Ti=2.5 (Ti-40) samples. The initial slope, or reaction rate, is greater in the large-particle sample. Right panel: molar fraction of acetone as a function of the molar sum of adsorbed products. The 8 h sample, containing smaller TiO<sub>2</sub> crystals, yields a larger fraction of acetone — as is directly evident from the spectra.

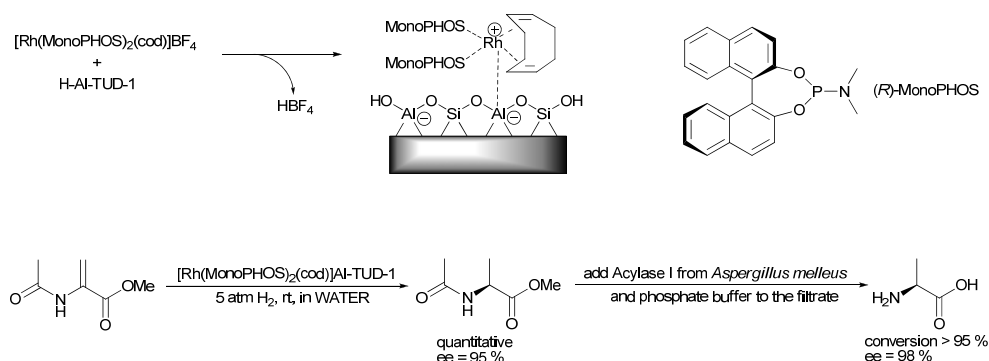
to selective oxidation products seems to be larger, the smaller the particles are. Further studies are underway using these well-defined Ti-TUD-1 materials in combination with fluorescence studies, to better understand the observed differences. Furthermore Ti-TUD-1 will be evaluated in photo-activation of CO<sub>2</sub>.<sup>88,89,90</sup>

#### 4. TUD-1 as catalyst-carrier

In addition to its catalytic activity TUD-1 can also act as a catalyst carrier. Al-TUD-1 with a Si/Al ratio of 4 is a Brønsted acid that can function as an ion exchanger for the ionic immobilisation of transition metal catalysts, a particularly attractive way to immobilise catalysts as the catalyst does not have to be modified.<sup>20,91,92</sup> Due to its three-dimensional, sponge-like pore structure with large mesopores Al-TUD-1 can easily host these catalysts. The immobilised catalysts remain accessible and since they are inside the pore system of Al-TUD-1, they should be compartmentalised and protected against deactivation.

When immobilising catalysts care has to be taken that the catalyst does not lose activity or selectivity. Furthermore the immobilisation method has to be straightforward. This is indeed the case with Al-TUD-1 as carrier. Asymmetric hydrogenation catalysts

based on different rhodium (I) complexes were immobilised *via* ion-exchange. They maintained their activity and selectivity, however some leaching of the metal was observed.<sup>20</sup> When  $[\text{Rh}(\text{MonoPHOS})_2(\text{cod})]\text{BF}_4$  was immobilised on Al-TUD-1 it not only retained activity and selectivity, it could be applied in water (Scheme 8); a solvent



**Scheme 8** Straightforward ion exchange enables the robust immobilisation of rhodium-based enantioselective hydrogenation catalysts. Due to the immobilisation the catalyst can be applied in water, facilitating a cascade of reactions, leading to enantiopure alanine.

otherwise not suitable for this catalyst,<sup>93</sup> adding a significant environmental advantage to this catalyst.<sup>94</sup> Furthermore, it could be recycled several times, demonstrating the versatility of this immobilisation.

The immobilised  $[\text{Rh}(\text{MonoPHOS})_2(\text{cod})]$  was used for the enantioselective reduction of methyl-2-acetamidoacrylate in water. Subsequent filtration and addition of Acylase I allowed the deprotection of the intermediate, yielding enantiopure L-alanine (Scheme 8). Thus Al-TUD-1 as a carrier enables a cascade of two catalytic reactions for the clean and environmentally benign synthesis of chiral amino acids.<sup>95</sup>

To further improve the immobilisation  $\text{Al}_2\text{O}_3$ -TUD-1 was also studied as a carrier. When the catalyst was immobilised in the presence of phosphotungstic acid, a heteropoly acid, it was even better protected against leaching than on Al-TUD-1.<sup>16</sup>

## 5. TUD-1 as material

The applications in chemistry have proven that TUD-1 is a most versatile material. In addition to these more classical utilisations of a mesoporous material, TUD-1 has also been used because of its properties as a material. In medicinal research Gd containing TUD-1 was investigated as a Magnetic Resonance Imaging (MRI) contrast agent. Protic Al-TUD-1 (Si/Al=3.5) was ion exchanged against gadolinium as  $Gd^{3+}$ . The MRI parameters of  $Gd^{3+}$  Al-TUD-1 were tested in the laboratory; however, while its MRI properties were good, the gadolinium leached rapidly.<sup>96</sup> Since gadolinium is highly toxic, this rules out any practical application of  $Gd^{3+}$  Al-TUD-1 as a MRI reagent at the current stage of development.

Due to its large surface area and mesoporous, sponge-like character TUD-1 was tested as a drug delivery system. Siliceous TUD-1 took up 49.5 wt% ibuprofen, thus one third of the loaded TUD-1 was ibuprofen. Importantly the ibuprofen could be released rapidly from the TUD-1. Within 15 min 60% were liberated and after 210 min 96% of the drug had left the carrier. This makes TUD-1 a good candidate as a drug carrier for poorly soluble drugs.<sup>97,98</sup>

## 6. Conclusion and outlook

A decade after its first description TUD-1 is firmly established as a versatile mesoporous material. Its straightforward, scalable and predictable synthesis allows successful preparation of TUD-1 and M-TUD-1 without special knowledge. Its application in catalysis has revealed that M-TUD-1s are highly applicable catalysts even in such demanding reactions as the oxidation of cyclohexane. The high stability of TUD-1 also ensures its application in medicinal research and as carrier of homogeneous catalysts. Additionally, it enabled fundamental insights into the operation of photo-catalysts.

Based on the results achieved within a decade it is obvious that the utilisation of TUD-1 in all its variations is but at the beginning. Indeed, molecularly designed multi-component nanostructures in molecular sieves have a high potential in photo-catalytic conversions using visible light. Novel avenues are the synthesis and evaluation of multi-component nanostructures in TUD-1, creating ideal materials for photo-catalytic studies. Similar to the immobilisation of chemical catalysts, enzymes might be fixated into the pores of TUD-1, or immobilised chemical catalysts might be used in concert with the

catalytic properties of their carrier, achieving cascade reactions. Co-TUD-1 is expected to function as anchor for enzymes with a histidine-tag.<sup>99</sup> These enzymes might then convert the oxidation products prepared with Co-TUD-1 as catalyst. This would enable entirely new routes to esters, diols and chiral alcohols. Equally it might be envisaged that the enzyme immobilised inside the pores of a M-TUD-1 can catalyse the release of a drug from a pro drug and thus help to establish advanced drug delivery systems. As the very different applications in medicinal research demonstrate, it is only imagination that limits the future of TUD-1.

## **Acknowledgments**

I would like to thank NWO (De Nederlandse Organisatie voor Wetenschappelijk Onderzoek) for a Mozaïek fellowship. M. S. Hamdy and O. Berg have significantly contributed to the paragraphs describing the evaluation of the photocatalytic performance of TUD-1 catalysts.

## 7. References

- 1 Y. Wan and D. Zhao, *Chem. Rev.*, **2007**, *107*, 2821-2860.
- 2 J. C. Jansen, Z. Shan, L. Marchese, W. Zhou, N. v. d. Puil and T. Maschmeyer, *Chem. Commun.*, **2001**, 713-714.
- 3 X. S. Zhao, F. Su, Q. Yan, W. Guo, X. Y. Bao, L. Lv and Z. Zhou, *J. Mater. Chem.*, **2006**, *16*, 637-648.
- 4 J. G. Verkade, *Acc. Chem. Res.*, **1993**, *26*, 483-489.
- 5 A. Singh and R. C. Mehrotra, *Coordination Chem. Rev.*, **2004**, *248*, 101-118.
- 6 S. Cabrera, J. El Haskouri, C. Guillem, J. Latorre, A. Beltran-Porter, D. Beltran-Porter, M. Dolores Marcos and P. Amoros, *Solid State Sci.*, **2000**, *2*, 405-420.
- 7 D. Ortiz de Zárate, A. Gómez-Moratalla, C. Guillem, A. Beltrán, J. Latorre, D. Beltrán and P. Amorós, *Eur. J. Inorg. Chem.*, **2006**, 2572-2581.
- 8 J. El Haskouri, S. Cabrera, C. Guillem, J. Latorre, A. Beltran, D. Beltran, M. Dolores Marcos and P. Amoros, *Chem. Mater.*, **2002**, *14*, 5015-5022.
- 9 J. El Haskouri, J. M. Morales, D. Ortiz de Zarate, L. Fernandez, J. Latorre, C. Guillem, A. Beltran, D. Beltran and P. Amoros, *Inorg. Chem.*, **2008**, *47*, 8267-8277.
- 10 D. Ortiz de Zarate, L. Fernandez, A. Beltran, C. Guillem, J. Latorre, D. Beltran and P. Amoros, *Solid State Sci.*, **2008**, *10*, 587-601.
- 11 Z. Shan, E. Gianotti, J. C. Jansen, J. A. Peters, L. Marchese and T. Maschmeyer, *Chem. Eur. J.*, **2001**, *7*, 1437-1443.
- 12 A. C. Pierre, *Biocatal. Biotransform.* **2004**, *22*, 145-170.
- 13 Chapter 5, pages 462-621 in R.K. Iler, *The Chemistry of Silica.*, John Wiley & Sons, New York, Chichester, Bisbane, Toronto, **1979**.
- 14 Z. Shan, J. C. Jansen, W. Zhou and T. Maschmeyer, *Appl. Catal. A: Gen.*, **2003**, *254*, 339-343.
- 15 Z.-X. Zhang, P. Bai, B. Xu and Z.-F. Yan, *J. Porous Mater.*, **2006**, *13*, 245-250.
- 16 C. Simons, U. Hanefeld, I. W. C. E. Arends, T. Maschmeyer and R. A. Sheldon, *J. Catal.* **2006**, *239*, 212-219.
- 17 A. M. Gaffney, TUD-1: A generalized mesoporous catalyst family for industrial applications. Abstr. Papers, 235th ACS National Meeting, New Orleans, LA, United States, April 6-10, **2008**.
- 18 A. Gaffney, TUD-1: Advanced catalytic materials for the refining and petrochemical industry. Abstr. Papers, 236th ACS National Meeting, Philadelphia, PA, United States, August 17-21, **2008**.



- 19 Z. Shan, J. C. Jansen, C. Y. Yeh, P. J. Angevine, T. Maschmeyer and M. S. Hamdy, US **2006/0052234 A1**.
- 20 C. Simons, U. Hanefeld, I. W. C. E. Arends, R. A. Sheldon and T. Maschmeyer, *Chem. Eur. J.*, **2004**, *10*, 5829-5835.
- 21 I. C. Neves, G. Botelho, A. V. Machado, P. Rebelo, S. Ramôa, M. F. R. Pereira, A. Ramanathan and P. Pescarmona, *Polym. Degrad. Stab.*, **2007**, *92*, 1513-1519.
- 22 A. Tuel, *Micropor. Mesopor. Mat.* **1999**, *27*, 151–169.
- 23 Y. Z. Zhu, S. Jaenicke and G.-K. Chuah, *J. Catal.* **2003**, *218*, 396–404.
- 24 K. P. de Jong, A. J. Koster, A. H. Janssen and U. Ziese, *Stud. Surf. Sci. Catal.* **2005**, *157*, 225-242.
- 25 M. S. Hamdy, Ph. D. Thesis, Technische Universiteit Delft, Delft, The Netherlands, **2005**, open access on: <http://www.library.tudelft.nl/ws/search/publications/index.htm>
- 26 C. Aquino and T. Maschmeyer, A New Family of Mesoporous Oxides – Synthesis, Characterisation and Applications of TUD-1. In *Ordered Porous Solids, recent advances and Prospects*, ed. V. Valtchev, S. Mintova and M. Tsapatsis, Elsevier B.V. **2009**, 3-30.
- 27 P. J. Angevine, A. M. Gaffney, Z. Shan and C. Y. Yeh, *Advanced Catalytic Materials for the Refining and Petrochemical Industry: TUD-1*, in ACS Symposium Series, **2009**, 1000, 335-363.
- 28 *Fine Chemicals through Heterogeneous Catalysis*, ed. R. A. Sheldon and H. van Bekkum, Wiley-VCH, Weinheim, **2001**.
- 29 M. S. Hamdy, G. Mul, J. C. Jansen, A. Ebaid, Z. Shan, A. R. Overweg and T. Maschmeyer, *Catal. Today*, **2005**, *100*, 255-260.
- 30 N. N. Tusar, A. Ristic, S. Cecowski, I. Arcon, K. Lazar, H. Amenitsch and V. Kaucic, *Micropor. Mesopor. Mat.*, **2007**, *104*, 289–295.
- 31 J. Cao, N. He, C. Li, J. Dong and Q. Xu, *Stud. Surf. Sci. Catal.* **1998**, *117*, 461-467.
- 32 K. Bachari, J. M. M. Millet, B. Benaichouba, O. Cherifi and F. Figueras, *J. Catal.* **2004**, *221*, 55-61.
- 33 V. R. Choudhary, S. K. Jana and B. P. Kiran, *Catal. Lett.* **1999**, *59*, 217-219.
- 34 A. Vinu, D. P. Sawant, K. Ariga, M. Hartmann and S. B. Halligudi, *Micropor. Mesopor. Mat.* **2005**, *80*, 195–203.
- 35 R. Anand, R. Maheswari and U. Hanefeld, *J. Catal.*, **2006**, *242*, 82-91.
- 36 E. Modrogan, M. H. Valkenberg and W. F. Hoelderich, *J. Catal.* **2009**, *261*, 177–187.
- 37 A. Sakthivel, S. K. Badamali and P. Selvam, *Micropor. Mesopor. Mat.* **2000**, *39*, 457-463.
- 38 P. Selvam and S. E. Dapurkar, *Catal. Today* **2004**, *96*, 135–141.

- 39 A. Vinu, B. M. Devassy, S. B. Halligudi, W. Böhlmann, Martin Hartmann, *Appl. Catal. A: Gen.* **2005**, *281*, 207–213.
- 40 M. Boronat, A. Corma and M. Renz, *J. Phys. Chem. B*, **2006**, *110*, 21168–21174.
- 41 Y. Zhu, G. Chuah and S. Jaenicke, *J. Catal.* **2004**, *227*, 1–10.
- 42 A. Ramanathan, D. Klomp, J. A. Peters and U. Hanefeld, *J. Mol. Catal. A: Gen.*, **2006**, *260*, 62–69.
- 43 A. Ramanathan, M. C. C. Villalobos, C. Kwakernaak, S. Telalovic and U. Hanefeld, *Chem. Eur. J.*, **2008**, *14*, 961–972.
- 44 F. Neatu, S. Coman, V. I. Parvulescu, G. Poncelet, D. De Vos and Pierre Jacobs, *Top. Catal.* **2009**, *52*, 1292–1300.
- 45 Y. Nie, S. Jaenicke and G.-K. Chuah, *Chem. Eur. J.* **2009**, *15*, 1991 – 1999.
- 46 L. Veum and U. Hanefeld, *Chem. Commun.* **2006**, 825–831.
- 47 S. Telalovic, J. F. Ng, R. Maheswari, A. Ramanathan, G. K. Chuah and U. Hanefeld, *Chem. Commun.*, **2008**, 4631–4633.
- 48 S. Li, A. Zheng, Y. Su, H. Zhang, L. Chen, J. Yang, C. Ye and F. Deng, *J. Am. Chem. Soc.* **2007**, *129*, 11161–11171.
- 49 P. Kalita, N. M. Gupta and R. Kumar, *J. Catal.* **2007**, *245*, 338–347.
- 50 S. M. Coman, P. Patil, S. Wuttke and E. Kemnitz, *Chem. Commun.* **2009**, 460–462
- 51 P. Waller, Z. Shan, L. Marchese, G. Tartaglione, W. Zhou, J. C. Jansen and T. Maschmeyer, *Chem. Eur. J.*, **2004**, *10*, 4970–4976.
- 52 Z. Shan, J. C. Jansen, C. Y. Yeh, J. H. Koeqler and T. Maschmeyer, WO 03/045548 A1
- 53 M. T. Musser, Cyclohexanol and Cyclohexanone, in Ullmann's Encyclopedia of Industrial Chemistry, electronic edition, Wiley-VCH Verlag, Weinheim, **2005**.
- 54 I. Hermans, J. Peeters and P. A. Jacobs, *Top. Catal.* **2008**, *48*, 41–48.
- 55 J. A. Labinger, *J. Mol. Catal. A: Chem.*, **2004**, *220*, 27–35.
- 56 M. S. Hamdy, G. Mul, W. Wei, R. Anand, U. Hanefeld, J. C. Jansen and J. A. Moulijn, *Catal. Today*, **2005**, *110*, 264–271.
- 57 R. Anand, M. S. Hamdy, P. Gkourgkoulas, T. Maschmeyer, J. C. Jansen and U. Hanefeld, *Catal. Today*, **2006**, *117*, 279–283.
- 58 R. Anand, M. S. Hamdy, U. Hanefeld and T. Maschmeyer, *Catal. Lett.*, **2004**, *95*, 113–117.
- 59 M. S. Hamdy, A. Ramanathan, T. Maschmeyer, U. Hanefeld and J. C. Jansen, *Chem. Eur. J.*, **2006**, *12*, 1782–1789.
- 60 L. Zhou, J. Xu, H. Miao, F. Wang and X. Li, *Appl. Catal. A: Gen.*, **2005**, *292*, 223–228.
- 61 M. Nowotny, L. N. Pedersen, U. Hanefeld and T. Maschmeyer, *Chem. Eur. J.* **2002**, *8*, 3724–3731.

- 62 R. Kumar, S. Sithambaram and S. L. Suib, *J. Catal.* **2009**, *262*, 304-313.
- 63 A. Ramanathan, M. S. Hamdy, R. Parton, Th. Maschmeyer, J. C. Jansen and U. Hanefeld, *Appl. Catal. A: Gen.*, **2009**, *355*, 78-82.
- 64 R. Anand, M. S. Hamdy, R. Partone, T. Maschmeyer, J. C. Jansen, R. Gläser, F. Kapteijn and U. Hanefeld, *Aust. J. Chem.* **2009**, *62*, 360-365.
- 65 H.-X. Yuan, Q.-H. Xia, H.-J. Zhan, X.-H. Lu and K.-X. Su, *Appl. Catal. A: Gen.* **2006**, *304*, 178-184.
- 66 W. Zhan, G. Lu, Y. Guo, Y. Guo, Y. Wang, Y. Wang, Z. Zhang and X. Liu, *J. Rare Earths* **2008**, *26*, 515-522.
- 67 A. Ramanathan, T. Archipov, R. Maheswari, U. Hanefeld, E. Roduner and R. Gläser, *J. Phys. Chem. C*, **2008**, *112*, 7468-7476.
- 68 W. Wei, J. A. Moulijn and G. Mul, *J. Catal.*, **2009**, *262*, 1-8.
- 69 Z. Shan, J. C. Jansen, L. Marchese and T. Maschmeyer, *Micropor. Mesopor. Mater.*, **2001**, *48*, 181-187.
- 70 M. R. Prasad, M. S. Hamdy, G. Mul, E. Bouwman and E. Drent, *J. Catal.*, **2008**, *260*, 288-294.
- 71 X.-Y. Quek, Q. Tang, S. Hu and Y. Yang, *Appl. Catal. A: Gen.*, **2009**, *361*, 130-136.
- 72 A. Mills and S. LeHunte, *J. Photochem. Photobiol. A-Chem.*, **1997**, *108*, 1-35.
- 73 J. M. Herrmann, *Top. Catal.*, **2005**, *34*, 49-65.
- 74 O. Carp, C. L. Huisman and A. Reller, *Prog. Solid State Chem.*, **2004**, *32*, 33-177.
- 75 H. Yamashita, K. Yoshisawa, M. Ariyuki, S. Higashimoto, M. Che and M. Anpo, *Chem. Commun.*, **2001**, 435-436.
- 76 O. Berg, M. S. Hamdy, T. Maschmeyer, J. A. Moulijn, M. Bonn and G. Mul, *J. Phys. Chem. C*, **2008**, *112*, 5471-5475.
- 77 M. S. Hamdy, O. Berg, J. C. Jansen, T. Maschmeyer, A. Arafat, J. A. Moulijn and G. Mul, *Catal. Today*, **2006**, *117*, 337-342.
- 78 F. Amano, T. Yamaguchi T. and Tanaka, *J. Phys. Chem. B*, **2006**, *110*, 281-288.
- 79 F. Amano, T. Tanaka and T. Funabiki, *Langmuir*, **2004**, *20*, 4236-4240.
- 80 S. Takenaka, T. Tanaka, T. Funabiki and S. Yoshida, *J. Chem. Soc. Faraday Trans.*, **1997**, *93*, 4151-4158.
- 81 G. Mul, W. Wasylenko, M. S. Hamdy and H. Frei, *Phys. Chem. Chem. Phys.*, **2008**, *10*, 3131-3137.
- 82 T. Tanaka, K. Teramura, T. Yamamoto, S. Takenaka, S. Yoshida and T. Funabiki, *J. Photochem. Photobiol. A: Chem.*, **2002**, *148*, 277-281.
- 83 A. Bhattacharyya, S. Kawi and M. B. Ray, *Catal. Today* **2004**, *98*, 431-439.

- 84 R. van Grieken, J. Aguado, M. J. Lopez-Munoz and J. Marugan, *J. Photochem. Photobio. A: Chem.*, **2002**, *148*, 315-322.
- 85 S. Zheng, L. A. Gao, Q.-H. Zhang and J.-K. Guo, *J. Mater. Chem.*, **2000**, *10*, 723-727.
- 86 Z. H. Luan and L. Kevan, *Micropor. Mesopor. Mater.*, **2001**, *44*, 337-344.
- 87 M. S. Hamdy, O. Berg, J. C. Jansen, T. Maschmeyer, J. A. Moulijn and G. Mul, *Chem. Eur. J.*, **2006**, *12*, 620-628.
- 88 J.-S. Hwang, J.-S. Chang, S.-E. Park, K. Ikeue, M. Anpo, *Top. Catal.*, **2005**, *35*, 311-319.
- 89 M. Anpo, H. Yamashita, Y. Ichihashi, Y. Fujii, M. Honda, *J. Phys. Chem. B*, **1997**, *101*, 2632-2636.
- 90 M. Anpo, H. Yamashita, K. Ikeue, Y. Fujii, S. G. Zhang, Y. Ichihashi, D. R. Park, Y. Suzuki, K. Koyano, T. Tatsumi, *Catal. Today*, **1998**, *44*, 327-332.
- 91 J. M. Fraile, J. I. Garcia and J. A. Mayoral, *Chem. Rev.*, **2009**, *109*, 360-417.
- 92 A. F. Trindade, P. M. P. Gois and C. A. M. Afonso, *Chem. Rev.*, **2009**, *109*, 418-514.
- 93 C. Simons, U. Hanefeld, I. W. C. E. Arends, A. J. Minnaard, Thomas Maschmeyer and R. A. Sheldon, *Chem. Commun.*, **2004**, 2830-2831.
- 94 P. Barbaro and F. Liguori, *Chem. Rev.*, **2009**, *109*, 515-529.
- 95 C. Simons, U. Hanefeld, I. W. C. E. Arends, T. Maschmeyer and R. A. Sheldon, *Adv. Synth. Catal.*, **2006**, *348*, 471-475. + **2006**, *348*, 792.
- 96 M. Norek, I. C. Neves and Joop A. Peters, *Inorg. Chem.*, **2007**, *46*, 6190-6196.
- 97 T. Heikkilä, J. Salonen, J. Tuura, M. S. Hamdy, G. Mul, N. Kumar, T. Salmi, D. Yu. Murzin, L. Laitinen, A. M. Kaukonen, J. Hirvonen and V. -P. Lehto, *Int. J. Pharm.*, **2007**, *331*, 133-138.
- 98 T. Heikkilä, J. Salonen, J. Tuura, N. Kumar, T. Salmi, D. Yu. Murzin, M. S. Hamdy, G. Mul, L. Laitinen, A. M. Kaukonen, J. Hirvonen and V.-P. Lehto, *Drug Delivery*, **2007**, *14*, 337-347.
- 99 U. Hanefeld, L. Gardossi and E. Magner, *Chem. Soc. Rev.*, **2009**, *38*, 453-468.

Noncovalent Immobilization of Chiral  
Cyclopropanation Catalysts on  
Mesoporous TUD-1: Comparison of  
Liquid-phase and Gas-phase Ion-  
exchange

2

## 1. Introduction

To date many homogeneous chiral catalysts have been developed. They catalyse essential reactions with excellent yields and selectivities. However, separation from the product and their reuse is often difficult. To overcome these hurdles they can be immobilized.<sup>1</sup>

An important class of chiral compounds are highly strained cyclopropanes found in many natural products.<sup>2</sup> Cyclopropanes bearing simple or complex functionalities are endowed with a large spectrum of biological properties.<sup>3</sup> In addition, the strain associated with the three-membered ring allows cyclopropanes to undergo a variety of synthetically useful ring opening reactions.<sup>3,4</sup>

There are several homogeneous chiral cyclopropanation catalysts based on different transition metals and ligands such as Ir-salen complexes,<sup>5</sup> Co-Porphyrin,<sup>6</sup> Ru-Pybox,<sup>7</sup> Rh<sub>2</sub>(MEPY)<sub>4</sub>,<sup>8</sup> and in particular Cu(I)-bis(oxazoline) complexes.

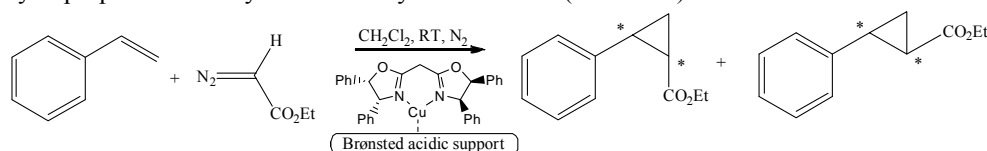
C<sub>2</sub>-symmetric bis-oxazoline ligands, one of the most popular classes of chiral ligands, induce a good level of enantioselectivity and can easily be obtained from a variety of amino acids.<sup>9,10</sup> The bis-oxazoline ligands have been used to chelate different metals and to catalyse a wide range of reactions. The Cu(I)-bis(oxazoline) catalytic system itself has been applied in a variety of reactions, the asymmetric cyclopropanation of olefins being by far the most successful application.<sup>11,12</sup>

Different approaches can be employed to immobilize the Cu(I)-bis(oxazoline) catalytic system.<sup>13</sup> Even though covalent tethering is particularly successful, the steps involved to prepare the covalently bound ligand makes the overall process less attractive. Additionally it inevitably leads to conformational changes of the ligand.

As the Cu(I)-bis(oxazoline) catalytic system is cationic in nature it can be immobilized onto anionic supports through electrostatic interactions. The group of Fraile and García has extensively explored the possibility to immobilize the Cu(I)-bis(oxazoline) catalytic system using non-covalent immobilization. Different parameters involved in this type of immobilization on supports such as clays, nafion and nafion silica nanocomposites were studied.<sup>14</sup> However, the supports used possess low surface area, 280 m<sup>2</sup> g<sup>-1</sup> for clays and around 80 m<sup>2</sup> g<sup>-1</sup> for nafion silica nanocomposite.

Very recently cationic  $[\text{Rh}^{\text{I}}(\text{cod})\{\text{R,R}\text{-MeDuPHOS}\}]\text{BF}_4$ , an asymmetric hydrogenation catalyst, has been successfully immobilized on Brønsted acidic TUD-1.<sup>15</sup> TUD-1 (Technische Universiteit Delft) is a mesoporous material with high surface area and three-dimensional interconnected pore structure.<sup>16</sup> It is prepared using templates like triethanolamine or tetraethylene glycol instead of expensive surfactants. This makes it particularly attractive when comparing it to other mesoporous materials such as MCM-41. The results obtained with immobilized  $\text{Rh}^{\text{I}}$  in the hydrogenation of dimethyl itaconate matched the results found with homogeneous catalyst in terms of yield and enantioselectivities. Only very little leaching of Rh was observed.

Here, we present the immobilization of 2,2'-methylenebis-[(4*R*,5*S*)-4,5-diphenyl-4,5-dihydro-1,3-oxazole] from now on Cu(I)-bis(diphenyl oxazoline) on mesoporous, high surface area supports of TUD-1 structure. The Brønsted acidic supports in question are aluminosilicate Al-TUD-1 and phosphotungstic acid immobilized on mesoporous alumina with TUD-1 structure, PW-TUD- $\text{Al}_2\text{O}_3$ . The catalysts were tested in the benchmark cyclopropanation of styrene with ethyl diazoacetate (Scheme 1).



**Scheme 1** Benchmark cyclopropanation of styrene with ethyl diazoacetate.

## 2. Results and Discussion

### 2.1 Synthesis and characterization of the Brønsted acidic supports

#### 2.1.1 PW-TUD- $\text{Al}_2\text{O}_3$

Amorphous mesoporous alumina, TUD- $\text{Al}_2\text{O}_3$ , was synthesized using tetraethylene glycol as template.<sup>17,19</sup> The XRD measurement (Fig. 1) is characterized by an intensive peak at low angle, an indication of the mesoporous character of the sample. At higher degrees no presence of crystalline alumina,  $\delta$ - or  $\theta$ - $\text{Al}_2\text{O}_3$  was detected. Minor peaks found at 38, 44 and 65  $2\theta$  degrees are due to aluminium from the sample holder.

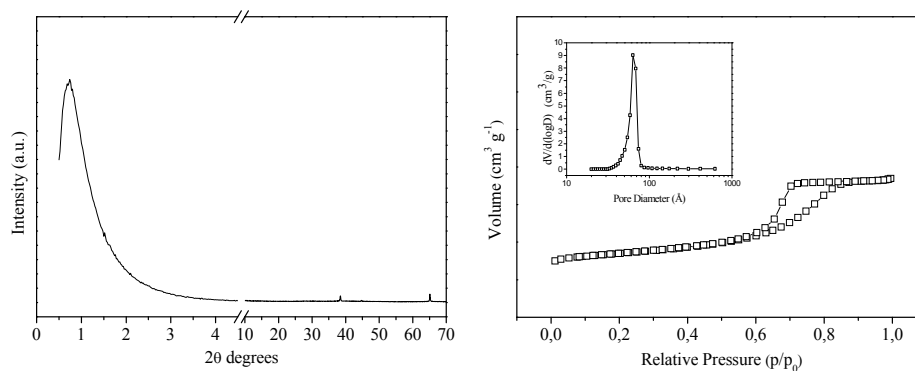


**Figure 1** XRD (left) and N<sub>2</sub> physisorption (right) results of TUD-Al<sub>2</sub>O<sub>3</sub> support. Inset: corresponding pore-size distribution.

The mesoporous character of TUD-Al<sub>2</sub>O<sub>3</sub> was further confirmed by N<sub>2</sub> physisorption measurements. The sample has a type IV hysteresis loop (Fig. 1) characteristic for mesoporous samples with narrow pore size distribution around 6 nm.

The BET surface area of 442 m<sup>2</sup> g<sup>-1</sup> and the pore volume of 0.9 cm<sup>3</sup> g<sup>-1</sup> (Table 1) are in line with previous reports.<sup>17,19</sup>

**Table 1** Data from N<sub>2</sub>-Physisorption measurements for TUD-Al<sub>2</sub>O<sub>3</sub>, Al-TUD-1 and Cu-Al-TUD-1 with different Si/Al ratios.

Support	S <sub>BET</sub> (m <sup>2</sup> g <sup>-1</sup> )	V <sub>meso</sub> (cm <sup>3</sup> g <sup>-1</sup> )	D <sub>meso</sub> (nm)
TUD-Al <sub>2</sub> O <sub>3</sub>	442	0.90	6.2
Al-TUD-1-4	495	1.11	15
Al-TUD-1-25	760	0.75	3
Cu-Al-TUD-1-4	441	1.01	14
Cu-Al-TUD-1-25	267	0.28	3

Dry phosphotungstic acid (PW) was immobilized on dry TUD-Al<sub>2</sub>O<sub>3</sub>, using anhydrous 2-propanol. According to INAA analysis (Table 2) around 0.5 mmol W g<sup>-1</sup><sub>support</sub> was immobilized.



**Table 2** ICP and INAA results for cyclopropanation catalysts immobilized on PW-TUD- $\text{Al}_2\text{O}_3$  using different copper precursors.

Catalyst	Cu (mmol g <sup>-1</sup> )	W (mmol g <sup>-1</sup> )	Cl (mmol g <sup>-1</sup> )	N/Cu
CuOTf-PW-TUD- $\text{Al}_2\text{O}_3$	0.15	0.49	-	-
CuCl-PW-TUD- $\text{Al}_2\text{O}_3$	0.18	0.50	0.18	-
L-CuCl-PW-TUD- $\text{Al}_2\text{O}_3$	0.16	0.49	0.17	2.2
L-CuOTf-PW-TUD- $\text{Al}_2\text{O}_3$	0.15	0.47	-	1.9

<sup>a</sup> In case CuCl was precursor, amount of Cu immobilized on catalyst was determined by INAA in other cases by ICP.

### 2.1.2 Al-TUD-1

Different aluminosilicates Al-TUD-1, with Si/Al ratios of 4 and 25 were prepared. Depending on the Si/Al ratio, different non-surfactant templates are used. Triethanolamine was used for the synthesis of Al-TUD-1 with high Si/Al ratio and tetraethylene glycol for synthesis of Al-TUD-1 with low Si/Al ratio as it is much easier to remove during calcination.<sup>15</sup> For Al-TUD-1 with Si/Al ratio of 4 (Al-TUD-1-4), the peak at low angle centred at around 0.7  $2\theta$  degrees (Fig. 2) confirms its mesoporous nature. A

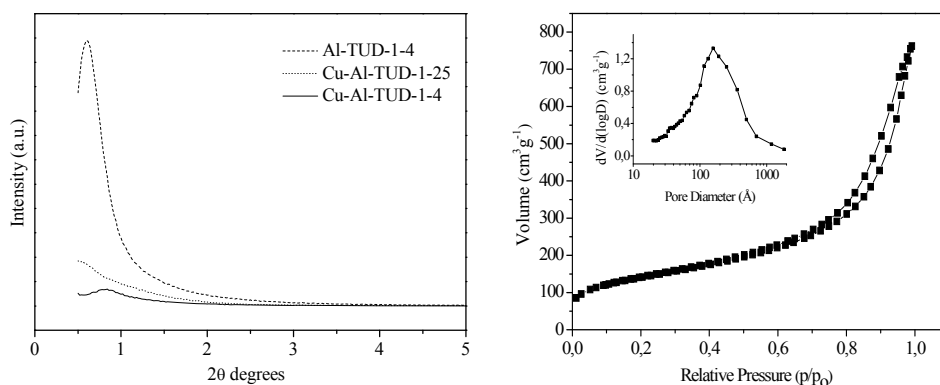


**Figure 2** XRD spectra of Al-TUD-1-4 and Cu-Al-TUD-1 samples (left) and  $\text{N}_2$  sorption isotherms of Al-TUD-1-4 (right). Inset: Corresponding pore-size distribution.

broad peak around 25  $2\theta$  degrees (not shown) is characteristic for mesoporous noncrystalline aluminosilicates.  $\text{N}_2$  sorption isotherm (Fig. 2) shows a typical Type IV isotherm with H1 hysteresis loop characteristic for materials with mesoporous texture. The pore size

distribution for Al-TUD-1-4 with a maximum of 15 nm is however broader than found in TUD-Al<sub>2</sub>O<sub>3</sub>. Aluminosilicate Al-TUD-1-25, has a higher surface area than Al-TUD-1-4, 760 and 495 m<sup>2</sup> g<sup>-1</sup>, respectively (Table 1). In general, aluminosilicates have a higher surface area than mesoporous alumina TUD-Al<sub>2</sub>O<sub>3</sub>.<sup>18,19</sup>

## 2.2 Immobilization of Cu(I)-bis(diphenyl oxazoline) on PW-TUD-Al<sub>2</sub>O<sub>3</sub> and its testing as heterogeneous cyclopropanation catalyst

Encouraged by successful immobilization of chiral hydrogenation catalysts, PW-TUD-Al<sub>2</sub>O<sub>3</sub> was chosen as support for chiral cyclopropanation catalyst. In addition, phosphotungstic acid alone has already successfully been used for immobilization of CuSO<sub>4</sub>.<sup>20</sup>

To have a stable catalyst many aspects have to be taken into account such as ligand and counterion. We used 2,2'-methylenebis-[(4*R*,5*S*)-4,5-diphenyl-4,5-dihydro-1,3-oxazole] (previously abbreviated to Cu(I)-bis(diphenyl oxazoline)) as a ligand as it gives the best results when used in homogeneous cyclopropanation of hexadiene, which is a precursor for synthesis of insecticide pyrethrin.<sup>21</sup> Additionally, this ligand is cheaper than the commonly used 2,2'-isopropylidenebis-[(4*S*)-4-*tert*-butyl-4,5-dihydro-1,3-oxazole].

It is known that the counteranion plays an important role in homogeneous cyclopropanation reactions. In fact, when chloride is used as counterion instead of the weakly coordinating triflate a dramatic decrease in enantioselectivity is observed through a change of geometry of the reaction intermediates and transition structures.<sup>22</sup> In our case if indeed Cu(I)-bis-oxazoline catalytic system has been electrostatically immobilized the choice of the catalytic precursor Cu(I)Cl or Cu(I)OTf should not have a profound influence. In both cases the counterion is assumed to be replaced by the support in this case by PW-TUD-Al<sub>2</sub>O<sub>3</sub> which has been shown to be a suitable counter ion for transition metals.<sup>17</sup>

### 2.2.1 Immobilization of Cu(I) without the ligand on PW-TUD-Al<sub>2</sub>O<sub>3</sub>

The PW-TUD-Al<sub>2</sub>O<sub>3</sub> was used to immobilize Cu(I) in 2-propanol as a protic polar solvent. According to ICP results (Table 2), the amount of copper immobilized on PW-TUD-Al<sub>2</sub>O<sub>3</sub> is rather constant, 150-180 μmol g<sup>-1</sup><sub>support</sub> without or with the ligand. In order to prove that

electrostatic immobilization has taken place, samples were subjected to INAA analysis to analyse for the presence of the counter ion of the catalysts precursors. In samples where CuCl was the precursor (Table 2), the amount of chloride is equal to the amount of copper, implying adsorption of CuCl on PW-TUD-Al<sub>2</sub>O<sub>3</sub> rather than ion-exchange. This finding is regardless of the fact whether the ligand was present or not on PW-TUD-Al<sub>2</sub>O<sub>3</sub>. The ratio of N/Cu in samples containing the ligand varies around 2, proving that all the Cu present on PW-TUD-Al<sub>2</sub>O<sub>3</sub> is complexed by the bis(diphenyl oxazoline) ligand. The integrity of the ligand was demonstrated by FT-IR with the characteristic C=N double bond of the oxazoline ring at 1653 cm<sup>-1</sup> (Figure 3).<sup>14</sup> The ratio of Cu to W found on PW-TUD-Al<sub>2</sub>O<sub>3</sub> is rather constant at around 0.3 for all four samples (Table 2).

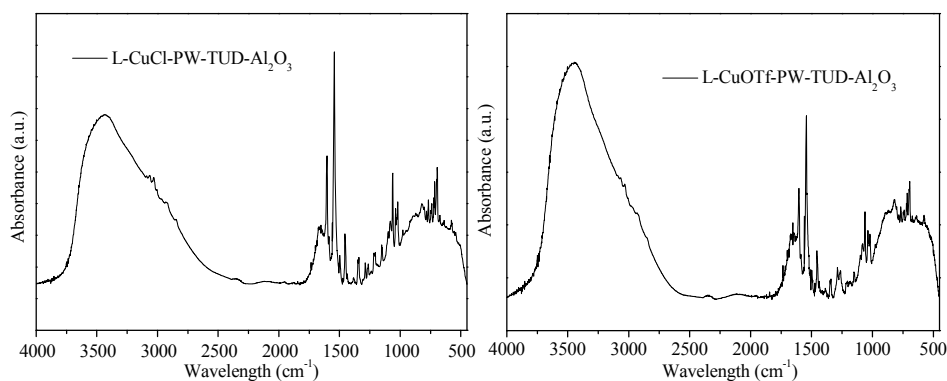


**Figure 3** FT-IR of immobilized CuCl (left) and CuOTf (right) complexed with 2,2'-methylenebis-[(4*R*,5*S*)-4,5-diphenyl-4,5-dihydro-1,3-oxazole] on TUD-Al<sub>2</sub>O<sub>3</sub> bearing phosphotungstic acid.

### 2.2.2 Testing of Cu(I) immobilized on PW-TUD-Al<sub>2</sub>O<sub>3</sub> in heterogeneous cyclopropanation

Both CuCl as well as CuOTf immobilized on PW-TUD-Al<sub>2</sub>O<sub>3</sub> are active in the heterogeneous cyclopropanation of styrene with ethyl diazoacetate (Scheme 1). In both cases leaching is very low, merely 0.22 % (Table 3). However, yields of cyclopropanated styrene obtained are also low, 13 and 35 % for CuCl-PW-TUD-Al<sub>2</sub>O<sub>3</sub> and CuOTf- PW-TUD-Al<sub>2</sub>O<sub>3</sub> respectively. As it has been identified by INAA analysis for immobilized CuCl

**Table 3** Results obtained from heterogeneous cyclopropanation<sup>a</sup> using catalysts immobilized on PW-TUD-Al<sub>2</sub>O<sub>3</sub>, with or without the ligand.

	Homogeneous L-CuOTf	CuCl on PW-TUD-Al <sub>2</sub> O <sub>3</sub>	L-CuCl on PW-TUD-Al <sub>2</sub> O <sub>3</sub>	CuOTf on PW-TUD-Al <sub>2</sub> O <sub>3</sub>	L-CuOTf on PW-TUD-Al <sub>2</sub> O <sub>3</sub>
Yield <sub>GC</sub> (%)	75	13	30	35	25
trans:cis	67:33	54:46	59:41	52:48	59:41
trans ee's	47 <sup>c</sup>	-	28 <sup>c</sup>	-	24 <sup>c</sup>
cis ee's	35 <sup>c</sup>	-	19 <sup>c</sup>	-	13 <sup>c</sup>
Selectivity <sup>b</sup>	98	56	70	55	81
Leaching (%)	-	0.11	21	0.22	11.2

<sup>a</sup> Cyclopropanation reactions were performed in dichloromethane under nitrogen using decane as internal standard with styrene to ethyl diazoacetate molar ratio of 1.25:1 and 1 mol% Cu immobilized relative to ethyl diazoacetate. Main by-products were diethyl maleate and diethyl fumarate. <sup>b</sup> Selectivity determined as (products + by-products)/ethyl diazoacetate. <sup>c</sup> Major cis (1*S*,2*R*), major trans (1*S*, 2*S*).

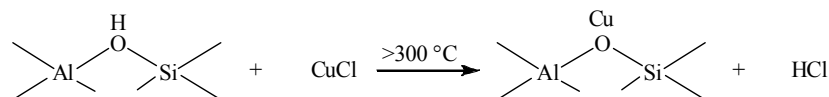
on PW-TUD-Al<sub>2</sub>O<sub>3</sub> adsorption instead of electrostatic immobilization has taken place. Equimolar amount of chloride with respect to Cu have been found. The difference in yield can be explained by the fact that it is generally recognised that presence of a coordinating anion, in our case chloride, leads to a less active catalyst.

### 2.2.3 Cu(I) complexed with a ligand immobilized on PW-TUD-Al<sub>2</sub>O<sub>3</sub>

Upon introduction of the ligand, leaching of Cu immobilized on PW-TUD-Al<sub>2</sub>O<sub>3</sub> considerably increases from 0.11 to 20.9 %, when CuCl is the catalyst precursor (Table 3). The leaching in case of CuCl complexed by ligand is twice as high as can be found for CuOTf. Yields as well as enantioselectivities using these catalysts are comparable, regardless of the catalysts precursor. Due to high leaching these results can therefore be considered to be mostly resulting from the homogeneous catalysed reaction. The strongly chelating bis-oxazoline ligand weakens the interaction of CuCl or CuOTf adsorbed on the support leading to an increase in leaching. Comparable yields can be explained by higher amount of CuCl present in homogeneous phase. Lower leaching of Cu when using CuOTf as catalysts precursor is possibly due to hydrogen bonding between the triflate and hydroxyl groups present on the support as has been previously suggested.<sup>11</sup>

## 2.3 Immobilization of Cu(I)-bis(diphenyl oxazoline) on Al-TUD-1 and its testing as chiral heterogeneous cyclopropanation catalyst

In order to ensure that Cu has been electrostatically immobilized we resorted to solid-gas ion-exchange using Brønsted acidic H-Al-TUD-1 as support (Scheme 2). The



**Scheme 2** Solid-gas ion-exchange of CuCl with Brønsted acid site.

immobilization takes place at high temperatures in order to assure that all of the Cu is immobilized, chloride being removed as HCl gas.<sup>23</sup> This technique cannot be used in the case of PW-TUD-Al<sub>2</sub>O<sub>3</sub> as phosphotungstic acid decomposes at high temperatures.

Introduction of aluminium into the TUD-1 matrix generally creates hexa-, penta- and tetrahedrally coordinated aluminium (III). Only tetrahedrally coordinated aluminium gives Brønsted acid sites (Scheme 2). Al-TUD-1 with a high content of aluminium (Al-TUD-1-4) was treated with aqueous 1 M HCl to remove hexa- and pentacoordinated aluminium.<sup>24</sup> This approach created a support with clearly defined anchoring points, Brønsted acid sites. According to <sup>27</sup>Al NMR measurements (Fig. 4) the number of Brønsted acid sites, tetrahedrally coordinated alumina at around 50 ppm, has been increased from 24

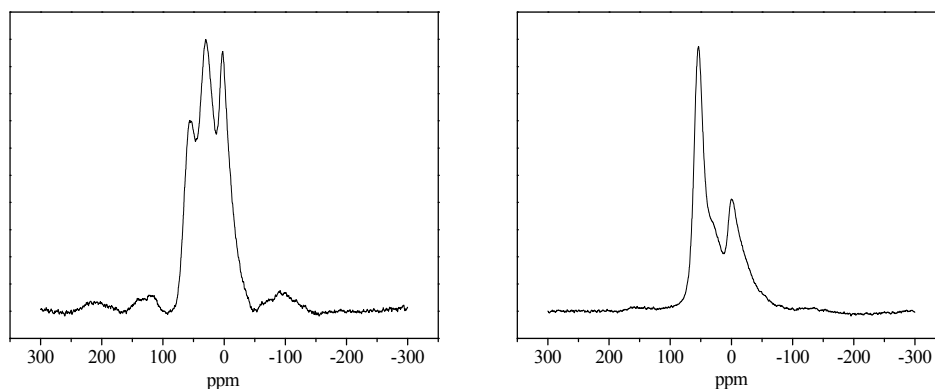


**Figure 4** <sup>27</sup>Al NMR of Al-TUD-1 with Si/Al ratio of 4 before (left ) and after (right) HCl treatment.

to 51 % upon HCl treatment. Al-TUD-1 used for support of hydrogenation catalyst, [Rh<sup>I</sup>(cod){*R,R*-MeDuPHOS}]BF<sub>4</sub>, had only 43 % of aluminium in tetrahedral coordination.<sup>15</sup> In case of Al-TUD-1-25 around 40 % of aluminium is tetrahedrally coordinated.<sup>18</sup>

Supports with Si/Al ratio 25 have strong Brønsted acid sites which ensure greater reactivity with CuCl and at the same time isolated Cu sites can be obtained. Decreasing the Si/Al ratio to 4, the acidity of the Brønsted acid sites is lower but their number is large. This approach increases the chance that CuCl will react with a Brønsted acid site and not with the less acidic silanol groups.

Two different temperatures have been chosen to perform the solid ion-exchange. For Al-TUD-1 with high numbers of Brønsted acid sites, Al-TUD-1-4, a temperature of 550 °C was chosen for a period of 15 h. For the sample with a lower amount of Brønsted acid sites, Al-TUD-1-25, solid ion-exchange was performed at 850 °C for 15 h. Such high temperatures are chosen as mesoporous amorphous aluminosilicates have weaker acid sites than crystalline aluminosilicates such as zeolites. Even using zeolites, CuCl phase was still present when the reaction was performed at sublimation point of CuCl of 300 °C and temperatures above 700 °C are necessary to remove physisorbed CuCl.<sup>23</sup> Combination of strong Brønsted acid sites found in Al-TUD-1-25 and high temperature during solid-gas ion exchange should ensure complete disappearance of the CuCl phase.

### 2.3.1 Solid-gas ion-exchange of CuCl on Al-TUD-1 with different Si/Al ratio

The same amount of copper ( $0.53 \text{ mmol g}^{-1}_{\text{support}}$ ) has been immobilized on Al-TUD-1-4 and on Al-TUD-1-25 even though different amounts of CuCl were used during solid-gas ion-exchange, 59 and 170 mg CuCl  $\text{g}^{-1}_{\text{support}}$  respectively (Table 4). However, the Cu/Al

**Table 4** ICP and INAA results for Al-TUD-1 support and catalysts based on Al-TUD-1.

Support/catalyst	Si/Al	Cu ( $\text{mmol g}^{-1}$ ) <sup>a</sup>	Cl ( $\text{mmol g}^{-1}$ )	N/Cu
Al-TUD-1-4	6	-	-	-
Al-TUD-1-25	24.4	-	-	-
Cu-Al-TUD-1-4	6.7	0.53	0.04	-
Cu-Al-TUD-1-25	22.6	0.53	0.04	-
L-Cu-Al-TUD-1-4	6.7	0.39	-	1.2
L-Cu-Al-TUD-1-25	23.4	0.37	-	0.53

<sup>a</sup> In case CuCl was precursor, amount of Cu immobilized on catalyst was determined by INAA.

ratios obtained are different namely 0.32 for Al-TUD-1-4 and 1 for Al-TUD-1-25. Cu-Al-TUD-1-4 contains therefore residual Brønsted acidic sites. The obtained Cu/Cl ratio on both

supports was equal to 13, even though Al-TUD-1-25 possesses stronger acid sites and the temperature at which solid-gas ion exchange was performed was much higher. In addition the pH value of water through which outlet gasses coming from the solid ion-exchange reaction were led through was at the end of reaction around 2.5. This clearly identifies solid-gas ion-exchange as the method of choice for electrostatic immobilization of Cu (I) on an acidic support without the need to neutralize the Brønsted acid sites beforehand.

However, it should be noted that the surface area was reduced upon solid-gas ion-exchange of CuCl on Al-TUD-1 (Table 1). This is especially the case with Al-TUD-1-25 for which the solid-gas ion-exchange was performed at 850 °C resulting in reduction of surface area from 760 m<sup>2</sup> g<sup>-1</sup> to 267 m<sup>2</sup> g<sup>-1</sup>. Only a minor reduction of surface area was noticed for Al-TUD-1-4, 495 m<sup>2</sup> g<sup>-1</sup> down to 441 m<sup>2</sup> g<sup>-1</sup> (Table 1). High temperature treatment of Al-TUD-1 with CuCl in addition led to a decrease of mesoporous character of both Al-TUD-1 based catalysts identified by reduction in intensity of the peak at low angle (Fig. 2).

### 2.3.2 Introduction of the ligand on solid-gas ion exchanged CuCl on Al-TUD-1

Subsequent introduction of ligand from a CH<sub>2</sub>Cl<sub>2</sub> solution did not lead to complexation of all the Cu sites present as the ratio of N/Cu (theoretically 2.0) was 1.2 for L-Cu-Al-TUD-1-4 and 0.53 for L-Cu-Al-TUD-1-25 (Table 4). This might be due to the irregular pore structure of TUD-1. While Cu can be immobilized in the smaller pores, the ligand cannot reach these cavities. This is especially true for Al-TUD-1-25 whereby solid-gas ion-exchange was performed at 850 °C. Treatment of Cu-Al-TUD-1 catalysts with the ligand led to substantial loss of copper for both catalysts. Integrity of the ligand was once again demonstrated by FT-IR with the characteristic C=N stretch at 1645 cm<sup>-1</sup> (Figure 5).<sup>14</sup> After the introduction of the ligand, the amount of Cu immobilized was reduced by 30 % (Table 4). Most probably weakly immobilized Cu on silanol groups was washed out of the carrier.

Ligand introduction after solid-gas ion-exchange of CuCl on Al-TUD-1 leads to lower leaching in the heterogeneous cyclopropanation reaction than in the case when only bare Cu was present on Al-TUD-1. For Cu-Al-TUD-1-25 leaching was reduced from 5.7 % to just 1 % while for Cu-Al-TUD-1-4 leaching was reduced from 13.25 % to 3.5 % upon ligand introduction (Table 5). Such differences can be explained by the fact that after solid-

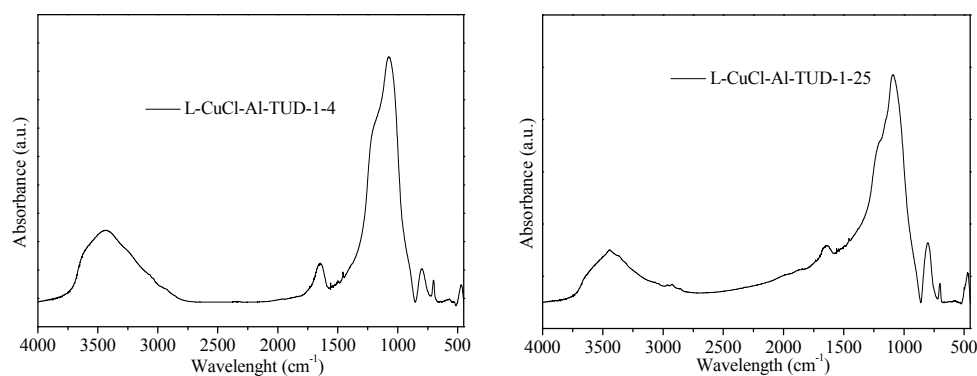


**Figure 5** FT-IR of solid-gas ion-exchanged CuCl on Al-TUD-1-4 (Si/Al=4) (left) and Al-TUD-1-25 (Si/Al=25) (right) complexed with 2,2'-methylenebis-[(4*R*,5*S*)-4,5-diphenyl-4,5-dihydro-1,3-oxazole].

**Table 5** Results obtained from heterogeneous cyclopropanation<sup>a</sup> using catalysts prepared by solid ion-exchange of CuCl on Al-TUD-1, with or without the presence of the ligand.

	L-Cu-Al-TUD-1-4	Cu-Al-TUD-1-4	L-Cu-Al-TUD-1-25	Cu-Al-TUD-1-25
Yield <sub>GC</sub> (%)	33	39	14	35
trans:cis	52:48	60:40	51:49	64:36
trans ee's	19 <sup>c</sup>	-	16 <sup>c</sup>	-
cis ee's	16 <sup>c</sup>	-	3 <sup>c</sup>	-
Selectivity <sup>b</sup>	73	54	33	75
Leaching (%)	3.5	13.25	1	5.7

<sup>a</sup> Cyclopropanation reactions were performed in dichloromethane under nitrogen using decane as internal standard with styrene to ethyl diazoacetate molar ratio of 1.25:1 and 1 mol% Cu immobilized relative to ethyl diazoacetate. Main by-products were diethyl maleate and diethyl fumarate. <sup>b</sup> Selectivity determined as (products + by-products)/ethyl diazoacetate. <sup>c</sup> Major cis (1*S*,2*R*), major trans (1*S*, 2*S*).

gas ion-exchange the catalysts were not washed. Introduction of strongly chelating bis(diphenyl oxazoline) ligand removed loosely bound Cu. The ligand introduction is in fact also the washing step. The difference in leaching between Al-TUD-1 with different Si/Al ratio can be explained by the fact that Al-TUD-1 with Si/Al ratio of 25 possesses stronger Brønsted acid sites. Another explanation is that solid-gas ion-exchange at higher temperatures leads to less accessible Cu sites due to a degraded support. The best results in terms of yield and enantioselectivity are obtained when Al-TUD-1 with a high content of aluminium was used as support, Al-TUD-1-4 (Table 5).

### 3. Conclusion



We have explored the possibility of immobilizing a Cu(I)-bis(diphenyl oxazoline) complex on acidic mesoporous supports of TUD-1 matrix to be used in heterogeneous cyclopropanation of styrene with ethyl diazoacetate. Two different supports have been used, having Brønsted acid sites of different kinds. On PW-TUD-Al<sub>2</sub>O<sub>3</sub> a chiral cyclopropanation catalyst was immobilized whereby all of the copper was complexed by the ligand. However, leaching of the catalyst was substantial, reaching values of 21 % due to the desorption of chiral catalyst. Electrostatic immobilization as chosen immobilization technique was only achieved if solid-gas ion-exchange was used to introduce CuCl onto the aluminosilicate Al-TUD-1. Leaching of copper was much lower and further decreased when Cu-Al-TUD-1 was treated with the ligand; which is an opposite trend compared to PW-TUD-Al<sub>2</sub>O<sub>3</sub>. However a low amount of copper was complexed by ligand on Cu-Al-TUD-1 indicating that copper was partly situated in cavities not accessible to the ligand. Using L-Cu-Al-TUD-1-4, 33 % yield was obtained with 19 and 16 % ee's for trans and cis cyclopropanation products respectively. Summarizing, only the gas-phase ion-exchange led to true ion-exchange and to low leaching of the catalyst.

## 4. Experimental

Introduction of Cu(I) on supports, subsequent manipulations and cyclopropanation reactions catalysed with immobilized Cu(I) were performed under dry nitrogen using Schlenk techniques.

### 4.1 Materials

Dry solvents were purchased from Aldrich except absolute ethanol obtained from J.T. Baker. Styrene was purchased from Merck and distilled before use. All other reagents were purchased from Aldrich, Across or Fluka and used without further purification.

### 4.2 Immobilization of Cu(I)-bis(diphenyl oxazoline) on PW-TUD-Al<sub>2</sub>O<sub>3</sub>

#### 4.2.1 Synthesis of TUD-Al<sub>2</sub>O<sub>3</sub>

TUD-Al<sub>2</sub>O<sub>3</sub> was prepared as previously described.<sup>17</sup> Aluminium isopropoxide (15.32 g, 75 mmol) was added to absolute ethanol (13.82 g, 300 mmol) and anhydrous 2-propanol (13.52 g, 225 mmol) at 45 °C. The solution was stirred for 0.5 h and tetraethylene glycol (14.57 g, 75 mmol) was added. After 3 h of stirring, demineralised water (2.7 g, 150 mmol) dissolved in absolute ethanol (13.82 g, 300 mmol) and anhydrous 2-propanol (13.52 g, 225 mmol) was added dropwise. The resulting mixture was stirred for 0.5 h at room temperature, followed by aging without stirring for 6 h also at room temperature.

The wet gel was dried at 70 °C for 19 h followed by hydrothermal treatment in an autoclave with a Teflon insert at 160 °C for 19 h. Finally the solids were calcined (with 1 °C min<sup>-1</sup> to 550 °C, 4 h at 550 °C and with 1 °C min<sup>-1</sup> to 600 °C, 10 h at 600 °C).

#### 4.2.2 Introduction of Phosphotungstic acid on TUD-Al<sub>2</sub>O<sub>3</sub>

Solid support, TUD-Al<sub>2</sub>O<sub>3</sub> (1.5-1.7 g) was pre-treated at 200 °C under vacuum for 2 h. Phosphotungstic acid hydrate (PW) H<sub>3</sub>PO<sub>4</sub>12WO<sub>3</sub>.xH<sub>2</sub>O (0.26-0.3 g) was dried at 100 °C under vacuum for 12 h. The amount of PW used is based on amounts used for

immobilization of hydrogenation catalyst.<sup>17</sup> To the dried support and PW, anhydrous 2-propanol was added (40 and 20 mL respectively). After 30 min of stirring, the PW solution was filtered through an Acrodisc filter (0.2  $\mu\text{m}$ ) and transferred to a TUD- $\text{Al}_2\text{O}_3$  suspension in anhydrous 2-propanol. The entire mixture was stirred for 30 min.

#### 4.2.3 Immobilization of $\text{CuOTf}$ or $\text{CuCl}$ on PW-TUD- $\text{Al}_2\text{O}_3$

$(\text{CuCF}_3\text{SO}_3)_2 \cdot \text{C}_6\text{H}_5\text{CH}_3$  (0.14 g, 0.54 mmol), or  $\text{CuCl}$  (0.05 g, 0.47 mmol) were used as copper precursors. The amount of copper is based on the aim to immobilize 30  $\mu\text{mol}$  Cu/0.1 g TUD- $\text{Al}_2\text{O}_3$ . The copper precursor was dissolved in 60 mL anhydrous 2-propanol. After stirring for 1 h the copper solution was filtered with an Acrodisc filter (0.2  $\mu\text{m}$ ) and transferred to the suspension of phosphotungstic acid and TUD- $\text{Al}_2\text{O}_3$ . The entire suspension was stirred for 3 h, subsequently filtered and washed with approximately 150 mL anhydrous 2-propanol. Finally a light-green/light-bluish solid was obtained and dried under vacuum at 55  $^\circ\text{C}$  for 2 h.

#### 4.2.4 $\text{CuOTf}$ or $\text{CuCl}$ complexed with ligand on PW-TUD- $\text{Al}_2\text{O}_3$

At first copper precursors were immobilized on PW-TUD- $\text{Al}_2\text{O}_3$  as described above. After the solid was filtered off and washed with anhydrous 2-propanol it was suspended again in 15 mL anhydrous 2-propanol. To the stirred suspended solid, 2,2'-methylenebis-[(4*R*,5*S*)-4,5-diphenyl-4,5-dihydro-1,3-oxazole] dissolved in 30 mL anhydrous 2-propanol was added. The amount of ligand added is based on the amount of copper precursor employed (1:1.1). The entire mixture was stirred for 3 h. Subsequently the solid was filtered off and washed with anhydrous 2-propanol (approximately 5 x 30 mL) and finally dried at 55  $^\circ\text{C}$  for 2 h under vacuum.

### 4.3 Immobilization of Cu(I)-bis(diphenyl oxazoline) on Al-TUD-1

#### 4.3.1 Synthesis of Al-TUD-1 ( $\text{Si}/\text{Al}=4$ )<sup>15</sup>

Aluminium isopropoxide (6.12 g, 0.03 mol) was added to a mixture of absolute ethanol (27.65 g, 0.60 mol) and anhydrous 2-propanol (27.04 g, 0.45 mol) at 45  $^\circ\text{C}$ , followed by

addition of tetraethyl orthosilicate (24.99 g, 0.12 mol) and tetraethylene glycol (29.17 g, 0.15 mol). The entire mixture was stirred for 1 h before dropwise addition of demineralised water (5.41 g, 0.30 mol) dissolved in absolute ethanol (27.65 g, 0.60 mol) and anhydrous 2-propanol (27.04 g, 0.45 mol). After the addition of demineralised water the mixture was stirred for an additional 0.5 h at room temperature followed by aging for 6 h. The resulting wet gel was dried at 70 °C for 21 h and for 2 h at 98 °C. Hydrothermal treatment was performed in an autoclave with Teflon insert at 160 °C for 19 h. Finally the solids were calcined (with 1 °C min<sup>-1</sup> to 550 °C, 4 h at 550 °C, with 1 °C min<sup>-1</sup> to 600 °C, 10 h at 600 °C).

#### 4.3.2 Synthesis of Al-TUD-1 (Si/Al=25)<sup>18</sup>

Al-TUD-1 was synthesized using triethanolamine (TEA) as a template in a one-pot surfactant-free procedure based on the sol-gel technique. Aluminium isopropoxide (2.5 g, 0.01 mol) was dissolved in absolute ethanol (20 g) and anhydrous 2-propanol (20 g). After addition of tetraethyl orthosilicate (63.75 g, 0.31 mol) the mixture was left stirring for a few minutes. TEA (45.69 g, 0.31 mol) dissolved in demineralised water (33.81 g, 3.27 mol) was added followed by addition of tetraethyl ammonium hydroxide (38.62 g, 35 wt %) under vigorous stirring. The clear gel obtained after these steps was then aged at room temperature for 12-24 h and dried at 98 °C for 12-24 h. Hydrothermal treatment was performed in an autoclave with Teflon insert at 180 °C for 4-24 h. Finally the solid was calcined in the presence of air up to 600 °C at a ramp rate of 1 °C min<sup>-1</sup> for 10 h. Full characterization of this material is given in reference 18.

#### 4.3.3 HCl treatment of Al-TUD-1 (Si/Al=4)

To Al-TUD-1 (7.1 g, Si/Al=4) 1 M HCl (71 mL) was added. The resulting mixture was stirred for 0.5 h at 30 °C. Al-TUD-1 was filtered off and extensively washed with demineralised water. Wet solid was dried at 90 °C overnight and subsequently at 60 °C under vacuum for 2 h.

#### 4.3.4 Solid-gas ion-exchange of CuCl on Al-TUD-1

Both HCl treated Al-TUD-1 (1.23 g, Si/Al=4) as well as Al-TUD-1 (2.11 g, Si/Al = 25) were dried at 200 °C for 2 h under vacuum. CuCl (72.76 mg and 358 mg, respectively) were dried at 100 °C for 2 h under vacuum. Al-TUD-1 and CuCl were mixed together and placed in a quartz reactor equipped with a P1 filter under N<sub>2</sub> flow (2.0 % or 20 mL min<sup>-1</sup>) at 550 °C for 15 h with a ramp rate of 5 °C min<sup>-1</sup> and 850 °C for 15 h with ramp rate of 5 °C min<sup>-1</sup> respectively. The outlet gasses were directed through a water trap (120 mL, pH = 6.38). After the reaction the pH of the water had dropped to 2.50.

#### 4.3.5 Introduction of the ligand to Al-TUD-1 ion-exchanged with CuCl

To Cu-Al-TUD-1-4 and Cu-Al-TUD-1-25 10 mL dry CH<sub>2</sub>Cl<sub>2</sub> was added. The equimolar amount of ligand needed was based on amount of immobilized Cu determined by ICP or INAA. Ligand used, 2,2'-methylenebis-[(4*R*,5*S*)-4,5-diphenyl-4,5-dihydro-1,3-oxazole] was dissolved in 10 mL dry CH<sub>2</sub>Cl<sub>2</sub>. The entire mixture was stirred for 24 h, filtered and washed with dry CH<sub>2</sub>Cl<sub>2</sub> (30 mL in total). Finally the solid was dried at 50 °C for 2 h under vacuum.

#### 4.4 Sample characterization

X-ray powder diffraction patterns were recorded by using CuK<sub>α</sub> radiation on a Philips PW 1840 diffractometer equipped with a graphite monochromator. N<sub>2</sub> physisorption studies were measured on a Quantachrome Autosorb at 77 K. IR spectra were recorded from KBr discs using a Perkin Elmer Spectrum One FT-IR spectrometer. For samples where CuCl was precursor, tungsten, copper as well as chloride amount present on solid supports were measured by instrumental neutron activation analysis (INAA), which was performed at “Het Reactor Instituut Delft” (RID). The “Hoger Onderwijs Reactor” nuclear reactor, with neutronflux of 10<sup>17</sup> neutrons s<sup>-1</sup> cm<sup>-2</sup>, was used as a source of neutrons, and the gammaspectrometer was equipped with a germanium semiconductor as detector. Cu amount immobilized on solids where CuOTf was precursor was measured by ICP-OES technique using Perkin Elmer Optima 300dv. Cu leaching was determined by analysing the reaction filtrates with graphite AAS on a Perkin Elmer AAnalyst 200.

### 4.5 Heterogeneous Cyclopropanation reaction

To weighted amount of Cu immobilized (1 % relative to ethyl diazoacetate, 20  $\mu\text{mol}$ ) dry  $\text{CH}_2\text{Cl}_2$  (6 mL) was added. Followed by addition of styrene (0.26 g, 2.5 mmol) and decane (0.36 g, 2.5 mmol) used as internal standard. Reactions were started by addition of purified ethyldiazoacetate (0.23 g, 2 mmol) dissolved in 5 mL dry  $\text{CH}_2\text{Cl}_2$  using a syringe pump ( $1.2 \text{ mL h}^{-1}$ ). The reaction was left to stir overnight at room temperature.

The yield of the reaction was determined by Varian Star 3400 CX equipped with CP Wax 52 CB column with dimension of 50 m x 0.53 mm (ID) and film thickness of 2  $\mu\text{m}$ . GC Injector was programmed, 70  $^{\circ}\text{C}$  (hold time 1 min) to 250  $^{\circ}\text{C}$  (hold time 4 min) with a rate of 40  $^{\circ}\text{C min}^{-1}$ . GC detector (FID) was set at 250  $^{\circ}\text{C}$ . He was used as carrier gas. The temperature programme of the column was 70  $^{\circ}\text{C}$  (hold time 2 min), ramp 10  $^{\circ}\text{C min}^{-1}$  to 240  $^{\circ}\text{C}$  (hold time 7 min), in total 26 min. Trans/cis ratio and ee values were determined using Shimadzu GC 17A equipped with a Chirasil Dex CB column with dimensions 25 m x 0.32 mm (ID) and film thickness of 0.25  $\mu\text{m}$ . Samples were analysed at 131  $^{\circ}\text{C}$  (isotherm), during 13 min. He was used as carrier gas, the split injector (30/100) was set at 220  $^{\circ}\text{C}$ , and GC detector (FID) at 200  $^{\circ}\text{C}$ .

## 5. References

- 1 (a) A. F. Trindade, P. M. P. Gois, C. A. M. Afonso, *Chem. Rev.*, **2009**, *109*, 418-514.  
 (b) J. M. Fraile, J. I. García, J. A. Mayoral, *Chem. Rev.*, **2009**, *109*, 360-417.  
 (c) L. Veum, U. Hanefeld, *Chem. Commun.*, **2006**, 825-831.
- 2 (a) R. Faust, *Angew. Chem. Int. Ed.*, **2001**, *40*, 2251.  
 (b) H. Lebel, J-F. Marcoux, C. Molinaro, A. B. Charette, *Chem. Rev.*, **2003**, *103*, 977-1050.
- 3 H. Pellissier, *Tetrahedron* **2007**, *64*, 7041-7095.
- 4 M. Yu, B. L. Pagenkopf, *Tetrahedron* **2005**, *61*, 321-347.
- 5 S. Kanchiku, H. Souematsu, K. Matsumoto, T. Uchida, T. Katsuki, *Angew. Chem. Int. Ed.*, **2007**, *46*, 3889-3891.
- 6 M. P. Doyle, *Angew. Chem. Int. Ed.*, **2009**, *48*, 850-852.
- 7 G. Maas, *Chem. Soc. Rev.*, **2004**, *33*, 183-190.
- 8 M.P. Doyle, W.R. Winchester, J.A.A. Hoorn, V. Lynch, S.H.Simonsen, R. Gosh, *J. Am. Chem. Soc.*, **1993**, *115*, 9968-9978.
- 9 G. Desimoni, G. Faita, K. A. Jørgensen, *Chem. Rev.*, **2006**, *106*, 3561-3651.
- 10 A. K. Gosh, P. Mathivanan, J. Cappiello, *Tetrahedron Asym.*, **1998**, *9*, 1-45.
- 11 P. O'Leary, N. P. Krosveld, K. P. De Jong, G. van Koten, R. J. M. Klein Gebbink, *Tetrahedron Lett.*, **2004**, *45*, 3177-3180.
- 12 A. V. Bedekar, E. B. Koroleva, P. G. Andersson, *J. Org. Chem.*, **1997**, *62*, 2518-2526.
- 13 (a) P. McMorn, G. J. Hutchings, *Chem. Soc. Rev.*, **2004**, *33*, 108-122.  
 (b) D. Rechavi, M. Lemaire, *Chem. Rev.*, **2002**, *102*, 3467-3494.
- 14 (a) J. M. Fraile, J. I. García, C. I. Herrerías, J. A. Mayoral, E. Pires, *Chem. Soc. Rev.*, **2009**, *38*, 695-706.  
 (b) J. M. Fraile, J. I. García, J. A. Mayoral, *Coord. Chem. Rev.*, **2008**, *252*, 624-646.  
 (c) J. I. García, B. López-Sánchez, J. A. Mayoral, E. Pires, I. Villalba, *J. Catal.*, **2008**, *258*, 378-385.  
 (d) J. M. Fraile, J. I. García, C. I. Herrerías, J. A. Mayoral, M. A. Harmer, *J. Catal.*, **2004**, *221*, 532-540.  
 (e) J. M. Fraile, J. I. García, J. A. Mayoral, M. Roldán, *Org. Lett.*, **2007**, *9*, 731-733.  
 (f) J. M. Fraile, J. I. García, M. A. Harmer, C. I. Herrerías, J. A. Mayoral, *J. Mol. Catal. A: Chem.*, **2001**, *165*, 211-218.  
 (g) J. M. Fraile, J. I. García, M. A. Harmer, C. I. Herrerías, J. A. Mayoral, O. Raiser, H. Werner, *J. Mater. Chem.*, **2002**, *12*, 3290-3295.

- (h) A. Cornejo, J. M. Fraile, J. I. García, M. J. Gil, C. I. Herrerías, G. Legarreta, V. Martínez-Merino, J. A. Mayoral, *J. Mol. Catal. A: Chem.*, **2003**, *196*, 101-108.
- (i) A. I. Fernández, J. M. Fraile, J. I. García, C. I. Herrerías, J. A. Mayoral, L. Salvatella, *Catal. Commun.*, **2001**, *2*, 165-170.
- (j) P. J. Alonso, J. M. Fraile, J. García, J. I. García, J. I. Martínez, J. A. Mayoral, M. C. Sánchez, *Langmuir*, **2000**, *16*, 5607-5612.
- (k) J. M. Fraile, J. I. García, J. A. Mayoral, T. Tarnai, M. A. Harmer, *J. Catal.*, **1999**, *186*, 214-221.
- (l) J. M. Fraile, J. I. García, J. A. Mayoral, T. Tarnai, *Tetrahedron: Asymmetry* **1998**, *9*, 3997-4008.
- (m) J. M. Fraile, J. I. García, J. A. Mayoral, T. Tarnai, *Tetrahedron: Asymmetry* **1997**, *8*, 2089-2092.
- 15 C. Simons, U. Hanefeld, I.W.C.E. Arends, R.A. Sheldon, Th. Maschmeyer, *Chem. Eur. J.*, **2004**, *10*, 5829-5835.
- 16 (a) J. C. Jansen, Z. Shan, L. Marchese, W. Zhou, N. van der Puil, T. Maschmeyer, *Chem. Commun.*, **2001**, *8*, 713 – 714.
- (b) S. Telalović, A. Ramanathan, G. Mul, U. Hanefeld, *J. Mater. Chem.*, **2010**, *20*, 642-658.
- 17 C. Simons, U. Hanefeld, I. W. C. E. Arends, T. Maschmeyer, R. A. Sheldon, *J. Catal.*, **2006**, *239*, 212-219.
- 18 R. Anand, R. Maheswari, U. Hanefeld, *J. Catal.*, **2006**, *242*, 82-91.
- 19 Z. Shan, J. C. Jansen, W. Zhou, T. Maschmeyer, *Appl. Catal. A: Gen.*, **2003**, *254*, 339-343.
- 20 J. S. Yadav, B. V. Subba Reddy, K. V. Purinama, K. Nagaiah, N. Lingaiah, *J. Mol. Catal. A: Chem.*, **2008**, *285*, 36-40.
- 21 (a) R. E. Lowenthal, S. Masamune, *Tetrahedron Lett.*, **1991**, *32*, 7373-7376.
- (b) R. E. Lowenthal, A. Abuko, S. Masamune, *Tetrahedron Lett.*, **1990**, *31*, 6005-6008.
- 22 (a) J. M. Fraile, J. I. García, J. A. Mayoral, T. Tarnai, *J. Mol. Catal. A: Chem.*, **1999**, *144*, 85-89.
- (b) J. M. Fraile, J. I. García, M. J. Gil, V. Martínez-Merino, J. A. Mayoral, L. Salvatella, *Chem. Eur. J.*, **2004**, *10*, 758-765.
- 23 Z. Li, K. Xie, R. C. T. Slade, *Appl. Catal. A: Gen.*, **2001**, *209*, 107-115.
- 24 J. P. Marques, I. Gener, P. Ayrault, J. M. Lopes, F. R. Ribeiro, M. Guisnet, *Chem. Commun.*, **2004**, 2290-2291.



Noncovalent Immobilization of Chiral  
Cyclopropanation Catalysts on  
Mesoporous TUD-1: Impact of  
Immobilisation Parameters

3

## 1. Introduction

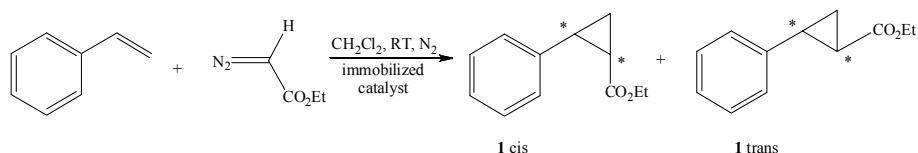
Mesoporous molecular sieves are already well established as catalysts by framework incorporation of different transition metals or as carriers for covalent or non-covalent immobilisation of chiral catalysts.<sup>1,2</sup> The most prominent examples of mesoporous molecular sieves are MCM-41 (Mobile Crystalline Material) and SBA-15 (Santa Barbara Amorphous material).<sup>3</sup> More recently TUD-1 (Technische Universiteit Delft) was described, with several advantages: tuneable pore size (5-50 nm) and surface area (500-1000 m<sup>2</sup>/g), three-dimensional structure leading to less mass-transfer limitations as experienced in two-dimensional MCM-41.<sup>4,5</sup> In addition the material is much more stable. Its synthesis requires templates which are less expensive than the surfactants employed in the synthesis of MCM-41 or the triblock polymers for the synthesis of SBA-15. The synthesis of TUD-1 is very flexible and even allows use of environmentally benign silica gel instead of commonly employed tetraethyl orthosilicate (TEOS).<sup>6</sup>

Using tetraethylene glycol as a template, aluminium has been incorporated into the siliceous TUD-1 structure.<sup>7</sup> Thus synthesized Brønsted acidic catalysts, Al-TUD-1 have been successfully used as carriers for chiral hydrogenation catalysts through non-covalent immobilisation.<sup>8</sup> In the hydrogenation of methyl 2-acetamidoacrylate, [Rh<sup>I</sup>(cod)((*R*)-MonoPhos)<sub>2</sub>]BF<sub>4</sub> immobilised on Al-TUD-1 proved to be stable and reusable, retaining its activity and enantioselectivity with only minor leaching of Rh.

Based on the above mentioned benefits of carriers based on TUD-1, our aim was to immobilise a chiral catalyst for C-C bond formation. In particular, a chiral cyclopropanation catalyst based on cationic Cu (I)-bis(oxazoline). This catalytic complex has earlier been heterogenized by the group of Fraile and Garcia and applied in cyclopropanation reactions. However, their supports of interest had low surface area, 280 m<sup>2</sup> g<sup>-1</sup> for clays, and around 80 m<sup>2</sup> g<sup>-1</sup> for nafion silica nanocomposite.<sup>9</sup>

Following the successful immobilisation of an asymmetric hydrogenation catalyst, here we report the immobilisation of Cu (I)-bis(oxazoline) on TUD-1, a mesoporous material with high surface area. The support in question is amorphous aluminosilicate Al-TUD-1, a Brønsted acidic support. Different parameters influencing successful immobilisation of the

chiral catalyst will be explored: the influence of the polarity of the solvent used during immobilisation on the amount of immobilised catalyst and its leaching during reaction; the support itself, the amount of tetrahedrally coordinated alumina into the TUD-1 and the presence of different cations on the support,  $H^+$  and  $Na^+$ . For this, protonic aluminosilicate (H-Al-TUD-1) was compared with sodium aluminosilicate (Na-Al-TUD-1). Finally the choice of catalyst to be immobilised, Cu (I)-bis(oxazoline) compared with the Ru (II)-Pybox cyclopropanation catalyst was studied. The immobilised catalysts were tested in the benchmark cyclopropanation of styrene with ethyl diazoacetate (Scheme 1).



**Scheme 1** Benchmark cyclopropanation of styrene with ethyl diazoacetate

## 2. Results and Discussion

### 2.1 Synthesis of the supports

#### 2.1.1 H-Al-TUD-1

Amorphous aluminosilicate Al-TUD-1, with a low Si/Al ratio of 4 (Al-TUD-1-4) was synthesized in order to ensure high ion-exchange capability. The template used is tetraethylene glycol, usually utilized in the synthesis of TUD-1 based materials with low Si/Al ratios.<sup>7,8</sup> The mesoporous character of Al-TUD-1 was determined by XRD as well as by  $N_2$  physisorption measurements. The sample possesses a peak at low angles, situated at 0.5 2 $\theta$  degrees, characteristic for mesoporous materials (Fig. 1). At higher degrees no presence of crystalline alumina,  $\delta$ - or  $\theta$ - $Al_2O_3$  was detected. Minor peaks found at 38, 44 and 65 2 $\theta$  degrees are due to aluminium from the sample holder. The mesoporous character was further confirmed by  $N_2$  physisorption measurements (Fig. 1) characterized by a type IV isotherm with a type *HI* hysteresis loop characteristic for mesoporous samples with a

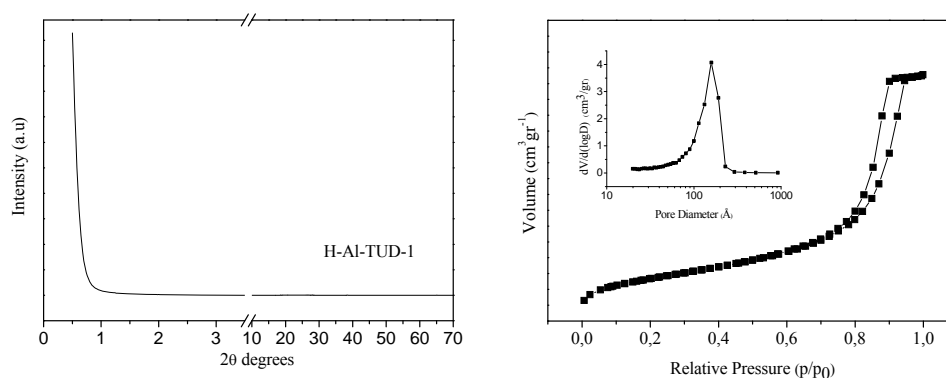


**Figure 1** XRD (left), N<sub>2</sub> sorption isotherms (right) and pore size distribution (inset) of H-Al-TUD-1 with Si/Al ratio of 4.

pore size distribution around 16 nm, pore volume of 1.2 cm<sup>3</sup> g<sup>-1</sup> and surface area around 485 m<sup>2</sup> g<sup>-1</sup> (Table 1).

**Table 1** Data from N<sub>2</sub>-Physisorption measurements for H-Al-TUD-1 and Na-Al-TUD-1 samples.

Carrier	$S_{\text{BET}}$ (m <sup>2</sup> g <sup>-1</sup> )	$V_{\text{meso}}$ (cm <sup>3</sup> g <sup>-1</sup> )	$D_{\text{meso}}$ (nm)	Tetrahedral Aluminium (%)	Si/Al	Na/Al
H-Al-TUD-1	485	1.20	16	28	5.4	-
H-Al-TUD-1 <sup>a</sup>	600	1.1	15	43	4	-
Na-Al-TUD-1.4	255	0.8	9.15	>95	4.2	1.4
Na-Al-TUD-0.7	384	0.35	2.88	>95	3.6	0.7

<sup>a</sup> Literature ref. 8.

Introduction of aluminium into the TUD-1 matrix generally creates hexa-, penta- and tetrahedrally coordinated aluminium. According to <sup>27</sup>Al-NMR measurements the amount of tetrahedrally coordinated aluminium is 28 % (Table 1, Fig. 2). Tetrahedrally coordinated aluminium is responsible for Brønsted acidity needed for anchoring of a chiral cyclopropanation catalyst via liquid-phase ion-exchange (Scheme 2).

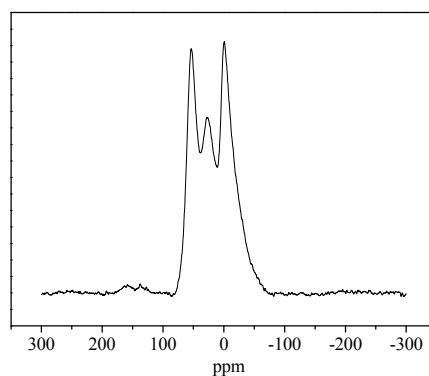
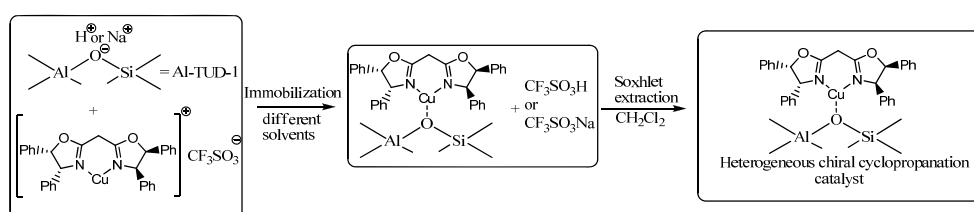


**Figure 2**  $^{27}\text{Al}$ -NMR of H-Al-TUD-1 (Si/Al=4) (signal at 50 ppm is assigned to tetraordinated aluminium, at 27 ppm pentacoordinated and at 3 ppm hexacoordinated aluminium).



**Scheme 2** Immobilisation of Cu(I)-bis(oxazoline) on Brønsted acidic site of Al-TUD-1 (Si/Al-4).

### 2.1.2 Na-Al-TUD-1

As discussed above Al-TUD-1 possesses different alumina sites which act as anchoring sites for the cyclopropanation catalyst and/or have side effects on the cyclopropanation reaction. Hexacoordinate aluminium, often recognized as extraframework species, can affect adsorption and catalytic properties.<sup>10</sup> In order to have well defined anchoring sites a support containing solely tetrahedrally coordinated aluminium was synthesized, while maintaining the Si/Al ratio of 4.

It is generally known that when aluminosilicates are synthesized in the presence of  $\text{Na}^+$  aluminium becomes mainly tetrahedrally incorporated.<sup>11</sup> For mesoporous MCM-41 structural aluminium is thermally less stable than, for example, in zeolite Y, because the MCM-41 structure lacks strict crystallographic order at the atomic level and very small  $\text{H}^+$

cations cannot satisfy the framework charge balance as efficiently as  $\text{Na}^+$  cations.<sup>12</sup> In the synthesis of Al-MCM-41 sodium aluminate was employed as source of Al. This ensured a high degree of structural order and all of the aluminium was in tetrahedral position.<sup>13,14,15</sup> However our strategy to use either triethanolamine or tetraethylene glycol as a template with sodium aluminate in the TUD-1 synthesis, led to the synthesis of greyish material with a low surface area. We turned our attention to NaOH to introduce  $\text{Na}^+$  instead of protons as charge balance for the tetrahedral coordination of trivalent aluminium. In the synthesis of mesoporous MCM-41, NaOH has been recognised to have a positive influence on tetrahedral incorporation of aluminium.<sup>16</sup> It was reported that, when applying NaOH it became possible to synthesize MCM-41 with Si/Al ratio close to the Loewenstein limit (Si/Al ratio of 1) with all aluminium in tetrahedral position.<sup>17</sup>

Two different samples of Na-Al-TUD-1 were successfully synthesized applying NaOH during the synthesis. Triethanolamine rather than tetraethylene glycol was employed as complexing reagent and aluminium isopropoxide as source of aluminium. The mesoporous character was demonstrated by XRD and  $\text{N}_2$  physisorption measurements. XRD measurements revealed that both samples synthesized displayed a peak at low angles characteristic for mesoporous samples (0.8 2 $\theta$  degrees; Fig. 3). Minor peaks found at 38, 44 and 65 2 $\theta$  degrees are due to aluminium from the sample holder.

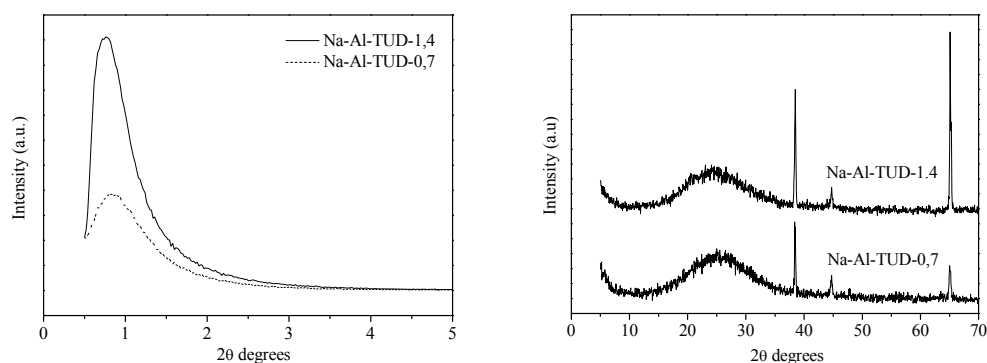


**Figure 3** XRD of different Na-Al-TUD-1 with Si/Al ratio of 4. Left figure ( Low angle XRD), Right figure (High angle XRD).

The Type IV isotherms obtained from  $\text{N}_2$  physisorption measurements further confirmed the mesoporosity of the materials characteristic for these materials (Fig. 4). Their

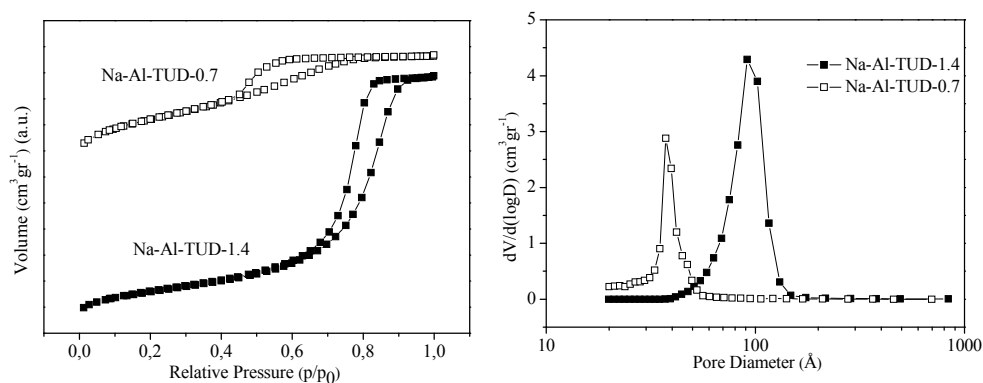


**Figure 4**  $N_2$  sorption isotherms (left) and pore size distribution (right) of Na-Al-TUD-1 supports.

hysteresis loops are however, different. For the sample having the higher amount of Na (Na-Al-TUD-1.4) the adsorption and desorption branches are almost vertical and nearly parallel belonging to *H1* hysteresis loop characteristic for uniform, near-cylindrical pores. In contrast Na-Al-TUD-0.7 displays a *H4* hysteresis loop where the desorption branch is much steeper than the adsorption branch due to non-uniform pores.

The Na-Al-TUD-1 samples have a Si/Al ratio of around 4 (Table 1). For the sample with high amount of sodium, Na-Al-TUD-1.4, the surface area is lower ( $255 \text{ m}^2 \text{ g}^{-1}$ ) than that of Na-Al-TUD-0.7 with surface area of  $384 \text{ m}^2 \text{ g}^{-1}$ . In contrast the pore volume as well as the pore size are larger for the sample containing the larger amount of sodium.<sup>27</sup> Al NMR measurements of both samples Na-Al-TUD-1 clearly show that these materials contain only tetrahedrally incorporated aluminium (Fig. 5).

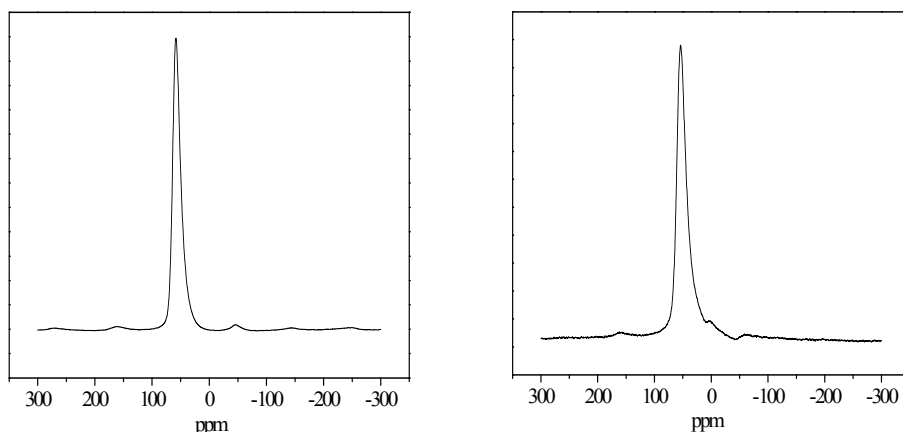


**Figure 5**  $^{27}\text{Al}$ -NMR of Na-Al-TUD-1.4 (left) and Na-Al-TUD-0.7 (right).

## 2.2 Immobilisation of cyclopropanation catalysts

As Rhodium based chiral hydrogenation catalysts were successfully immobilised on Brønsted acidic H-Al-TUD-1 we were interested in parameters governing successful immobilisation of the Cu (I)-bis(oxazoline) catalyst on the same support. To probe the performance of heterogeneous catalysts we chose the cyclopropanation of styrene with ethyl diazoacetate as benchmark (Scheme 1). Cu (I) complexed with 2,2'-methylenebis-[(4*R*,5*S*)-4,5-diphenyl-4,5-dihydro-1,3-oxazole] (from now on called bis(diphenyl oxazoline)) was immobilised. The commonly used 2,2'-isopropylidenebis-[(4*S*)-4-*tert*-butyl-4,5-dihydro-1,3-oxazole] (from now on called bis(*tert*-butyl oxazoline)) was not chosen since it is known that it leaches due to steric hindrance.<sup>9</sup> Secondly, bis(diphenyl oxazoline) ligand gives the best results when used in homogeneous cyclopropanation of 2,5-dimethyl-2,4-hexadiene, which is a precursor for the synthesis of the pyrethrin insecticides.<sup>18</sup> A schematic representation of the immobilisation procedure is given in Scheme 2 on page 61.

### 2.2.1 Influence of the solvent used during immobilisation

To date different solvents have been used during immobilisation of chiral catalysts. For the immobilisation of chiral Rh diphosphine complexes both dichloromethane and methanol



are applied.<sup>8,19</sup> In addition there are two different non-covalent immobilisation techniques that can be utilised: adsorption and ion-exchange. Adsorption being the weaker of the two methods. Nonetheless this method has already been applied for the immobilisation of different Cu (I)-bis(oxazolines) on commercially available chromatography grade silica.<sup>20</sup> The heterogeneous catalyst was tested in the Diels-Alder reaction and depending on the ligand used it could be successfully reused. The immobilisation of the catalyst was based on hydrogen bonds between the triflate anion and silanol groups present on silica. The solvent used during immobilisation was weakly polar dichloromethane. For ion-exchange in solution to take place a much more polar solvent has to be used. To distinguish between different non-covalent immobilisation techniques we employed solvents with different polarity during immobilisation. The polarity of different solvents tested was expressed by a normalised empirical parameter  $E_T^N$ . The empirical parameter is obtained from spectroscopic measurements and provides complex and very accurate characterisation of solvent polarity. Values of  $E_T^N$  range from 0.000 for tetramethylsilane to 1.000 for water.<sup>21,22</sup> The anhydrous solvents of choice sorted by increasing  $E_T^N$  were: dichloromethane (0.309), nitroethane (0.398), acetonitrile (0.46) and methanol (0.762).

The polarity of the solvent used during immobilisation had a profound influence on the amount of copper immobilised, the level of complexation of immobilised Cu (I) by the ligand as well as the leaching of Cu (I) during catalysis of the cyclopropanation reaction (Fig. 6). The larger the  $E_T^N$  of a solvent the lower the amount of copper immobilised and

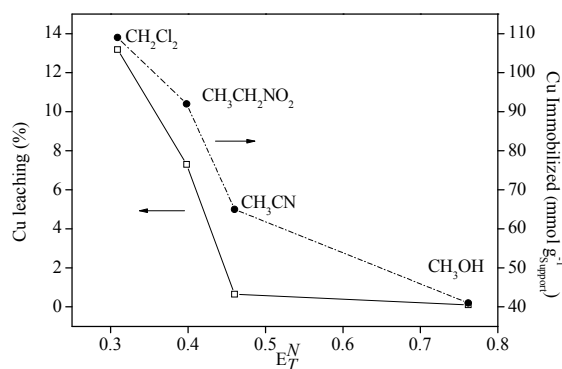


**Figure 6:** Influence of the polarity of solvent used during immobilisation on the amount of Cu immobilised and the loss of Cu during the cyclopropanation reaction.

the lower is the leaching during catalysis. When applying a less polar solvent, the Cu immobilised is much better complexed by the bis(oxazoline) ligand. With the most polar and protic solvent, methanol, the Cu/N ratio is below 2 while it is above 2 for all other solvents (first four rows in Table 2). The integrity of the ligand was demonstrated by FT-IR with the characteristic C=N double bond of the oxazoline ring at  $1653\text{ cm}^{-1}$  (Fig. 7).<sup>9</sup>

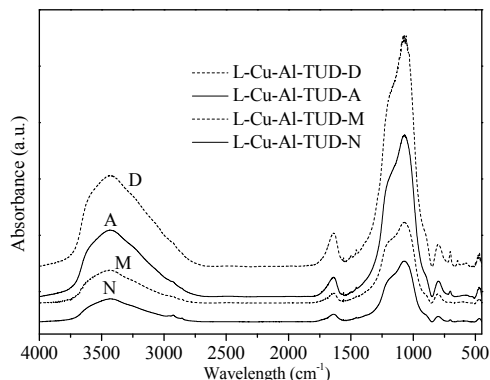


**Figure 7:** FT-IR analysis of immobilized Cu(I)-bis(diphenyl oxazoline) ligand on Al-TUD-1 (Si/Al=4) using different solvents during immobilization: (M) methanol (A) acetonitrile, (N) nitromethane and (D) dichloromethane.

**Table 2** ICP and HCN results for different immobilised catalysts on H-Al-TUD-1 and Na-Al-TUD-1 carriers were methanol was used as solvent of choice during immobilization, unless otherwise indicated.

Catalysts	Si/Al	Cu ( $\mu\text{mol g}^{-1}$ )	N/Cu	Ru ( $\mu\text{mol g}^{-1}$ )	N/Ru
L-Cu-Al-TUD-M <sup>a</sup>	5,3	40.91	1.75	-	-
L-Cu-Al-TUD-A <sup>a</sup>	5,1	65.54	2.61	-	-
L-Cu-Al-TUD-N <sup>a</sup>	4,9	91.90	2.17	-	-
L-Cu-Al-TUD-D <sup>a</sup>	5,9	109.37	2.48	-	-
L-Cu-Al-TUD-1.4 <sup>b</sup>	5,0	115.66	0.62	-	-
L-Cu-Al-TUD-0.7 <sup>b</sup>	5,9	129.04	0.74	-	-
L-Cu-Al-TUD- <i>t</i> <sup>c</sup>	3,6	-	0.55	-	-
L-Ru-Al-TUD-1 <sup>d</sup>	5,7	-	-	59.26	3.37

<sup>a</sup> (M) stands for Methanol, (A) stands for acetonitrile, (N) stands for nitromethane and (D) stands for dichloromethane used during immobilization. <sup>b</sup> Cu-bis(diphenyl oxazoline) catalysts immobilized on Na-Al-TUD-1 support with different Na/Al ratios, 1.4 and 0.7. <sup>c</sup> (*t*) stands for bis(*tert*-butyl oxazoline) ligand or 2,2'-isopropylidenebis [(4*S*)-4-*tert*-butyl-4,5-dihydro-1,3-oxazole] used instead of bis(diphenyl oxazoline) ligand or 2,2'-methylenebis [(4*R*,5*S*)-4,5-diphenyl-4,5-dihydro-1,3-oxazole] found in other catalysts with Cu as metal of choice. <sup>d</sup> Ru(II)-Pybox or Ru(II)-2,6-Bis[(4*R*)-(+)-isopropyl-2-oxazolin-2-yl] pyridine immobilized on H-Al-TUD-1.

When tested in the cyclopropanation reaction of styrene (using in all cases dichloromethane as the solvent) the influence of the solvent used during immobilisation becomes even more

evident. Utilising dichloromethane as least polar solvent, even though the highest amount of Cu was immobilised per g of carrier, 13% leaching was observed and therefore we considered the reaction to be largely homogeneously catalysed (Table 3).

**Table 3** Results obtained from heterogeneous cyclopropanation<sup>a</sup> using catalysts immobilized on H-Al-TUD-1, different solvents were employed during immobilization.

	Homogeneous reaction	L-Cu-Al-TUD-M	L-Cu-Al-TUD-A	L-Cu-Al-TUD-N	L-Cu-Al-TUD-D
Yield <sub>GC</sub> (%)	75	23	48	64	61
trans:cis	67:33	48:52	49:51	55:45	59:41
trans ee's <sup>b</sup>	47	2	8	23	34
cis ee's <sup>b</sup>	35	4	2	11	19
Leaching (%)	-	<0.11	0.65	7,3	13.18

<sup>a</sup> Cyclopropanation reactions were performed in dichloromethane under nitrogen using decane as internal standard with styrene to ethyl diazoacetate molar ratio of 1.25:1 and 1 mol % Cu immobilised relative to ethyl diazoacetate. Main byproducts were diethyl maleate and diethyl fumarate. <sup>b</sup> Major trans (1*S*, 2*S*), major cis (1*S*, 2*R*).

While in the Diels-Alder reaction adsorbed Cu (I)-bis(oxazoline) could be re-used with retention of its activity in the cyclopropanation, this is not the case,<sup>20</sup> clearly adsorption of Cu (I)-bis(oxazoline) on the support using weakly polar solvents during immobilisation is not sufficiently strong. Catalysts-support interactions are too weak for this catalyst to be applied in cyclopropanation. Employing polar solvents leaching could be greatly reduced to 0.65 % in case of acetonitrile and even below detection limit of < 0.11% when methanol was used during immobilisation. However, the yields were quite low (48% and 23% respectively), moreover the reaction lacked enantioselectivity (Table 3).

As the polarity of the solvent can have an influence on the adsorption or ion-exchange of the chiral catalysts they were subjected to solid <sup>13</sup>C NMR to detect the presence of the triflate anion. The chemical shift of <sup>13</sup>C due to CF<sub>3</sub>SO<sub>3</sub><sup>-</sup> was reported at 120.52 ppm.<sup>23</sup> To our surprise on none of the CuOTf catalysts immobilised on H-Al-TUD-1 triflate could be detected. Possible explanation could be low amount of catalyst and therefore triflate being immobilised, hampering detection. Indeed, it had earlier been reported that there are cases where the <sup>13</sup>C resonance due to CF<sub>3</sub>SO<sub>3</sub><sup>-</sup> was not visible.<sup>24</sup>

Clearly methanol as most polar solvent among the solvents tested for immobilisation of Cu (I)-bis(diphenyl oxazoline) on H-Al-TUD-1 is the most favourable medium.

### 2.2.2 Influence of the support

To achieve high activity and selectivity it is important to synthesize heterogeneous catalysts with well defined catalytic sites.<sup>25</sup> H-Al-TUD-1 possesses, in addition to Brønsted acid sites, also pentacoordinated aluminium sites and Lewis acid sites due to extraframework aluminium generally ascribed to hexacoordinated aluminium. For these reasons we synthesized a support containing exclusively tetrahedrally coordinated aluminium, namely Na-Al-TUD-1.

Having identified methanol as the solvent of choice for ion-exchange to take place, we used it during immobilisation of Cu (I)-bis(diphenyl oxazoline) on Na-Al-TUD-1. The amount of Cu (I) immobilised was higher in case of Na-Al-TUD-1 than in case of H-Al-TUD-1 as support. An almost threefold increase of Cu (I) immobilised was obtained (Table 2, entries 1, 5, 6). Due to the successful increase of percentage tetrahedrally coordinated aluminium, the TUD-1 structure now has a higher ion-exchange capability. However, the Cu/N ratio as indication of the presence of the ligand was very low, below 1 for Cu (I)-bis(diphenyl oxazoline) immobilised on both samples of Na-Al-TUD-1 (Table 2, entries 5 and 6). The smaller pore size of the sodium based Al-TUD-1 support could be an explanation for this observation. The presence of the ligand on the Na-Al-TUD-1 samples was demonstrated by FT-IR with the characteristic C=N double bond of the oxazoline ring at  $1653\text{ cm}^{-1}$  (Fig. 8).<sup>9</sup>

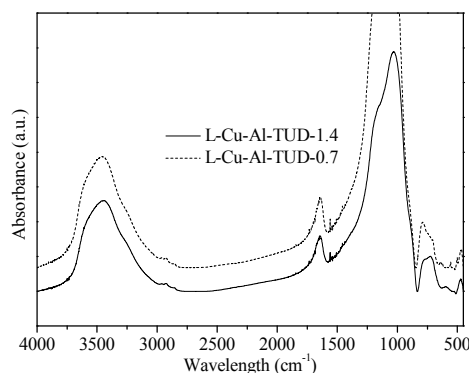


**Figure 8:** FT-IR analysis of immobilized Cu(I)-bis(diphenyl oxazoline) on Na-Al-TUD-1 with different Al/Na ratios ( 1,4 and 0.7) using methanol during immobilization.

When tested in the cyclopropanation reaction one striking difference when compared to H-Al-TUD-1 as support is the high leaching when using Na-Al-TUD-1's as carriers (Table 4). There is also a clear difference between the two synthesized

**Table 4** Comparison between cyclopropanation catalysts immobilised on H-Al-TUD-1 and Na-Al-TUD-1 using methanol during immobilisation.<sup>a</sup>

	L-Cu-Al-TUD-1.4	L-Cu-Al-TUD-0.7	L-Cu-Al-TUD-M
Yield <sub>GC</sub> (%)	31	53	23
trans:cis	54:46	49:51	48:52
trans ee's <sup>b</sup>	2	5	2
cis ee's <sup>b</sup>	3	6	4
Leaching (%)	22	4	<0.11

<sup>a</sup>Cyclopropanation reactions were performed in dichloromethane under nitrogen using decane as internal standard with styrene to ethyl diazoacetate molar ratio of 1.25:1 and 1 mol % Cu immobilised relative to ethyl diazoacetate. Main byproducts were diethyl maleate and diethyl fumarate. <sup>b</sup> Major trans (1*S*, 2*S*), major cis (1*S*, 2*R*).

Na-Al-TUD-1; Cu-Al-TUD-1.4 displaying very high leaching (22% compared to 4% for Cu-Al-TUD-0.7) (Table 4). The difference between the two supports, besides the Na/Al ratio is the use of tetraethylammonium hydroxide (TEAOH) in the synthesis. In the synthesis of TUD-1 TEAOH is generally used in order to introduce micro porosity. TEAOH was used only during the synthesis of Na-Al-TUD-0.7. With smaller non-uniform pores, micro porosity and larger surface area, Na-Al-TUD-0.7 is much better suited than Na-Al-TUD-1.4 with large uniform pores and high degree of order (Fig. 3 and 4).

Based on these results, clearly H-Al-TUD-1 is a more suitable support for Cu (I)-bis(oxazoline) catalytic system than Na-Al-TUD-1 is. This despite the presence of different catalytic sites (penta- and hexacoordinated aluminium) that could interfere with the reaction.

### 2.2.3 Choice of the ligand

Methanol as the best solvent to be used during immobilisation and H-Al-TUD-1 as the support of choice to achieve low leaching, we looked at the possibility to increase the enantioselectivity of our catalyst. For that reason we used this time the commonly used bis(*tert*-butyl oxazoline) as a ligand. With the improved immobilisation techniques it was expected that the disadvantage of leaching due to sterical hindrance would be overcome.

However, the level of complexation of Cu was much lower than in case when bis(diphenyl oxazoline) was used as ligand (Table 2, entries 1 and 7). The integrity of the ligand was demonstrated by FT-IR with the characteristic C=N double bond of the oxazoline ring at  $1653\text{ cm}^{-1}$  (Fig. 9).<sup>9</sup> The yield of the cyclopropanation reaction was improved; however no

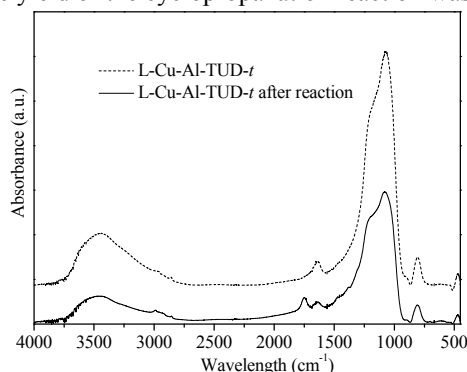


**Figure 9:** FT-IR analysis of immobilized Cu(I)-bis(*tert*-butyl oxazoline) on Al-TUD-1 using methanol during immobilization, before and after the cyclopropanation reaction.

increase in enantioselectivity was observed (Table 5). At the same time we notice a minor increase in leaching from below detection limit ( $< 0.11\%$ ) to  $0.50\%$  (Table 5). The leaching could be attributed to the steric interaction of the bulky *tert*-butyl groups with the support.

**Table 5** Comparison between different heterogeneous catalysts bearing different bis(oxazoline) ligands immobilised on H-Al-TUD-1.<sup>a</sup>

	Homogeneous	L-Cu-Al-TUD-M	L-Cu-Al-TUD- <i>t</i>
Yield <sub>GC</sub> (%)	77	23	45
trans:cis	73:27	48:52	46:53
trans ee's <sup>b</sup>	99	2	2
cis ee's <sup>b</sup>	97	4	2
Leaching (%)		<0.11	0.5

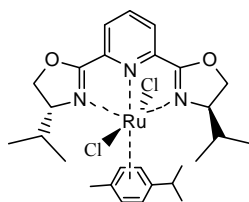
<sup>a</sup> Cyclopropanation reactions were performed in dichloromethane under nitrogen using decane as internal standard with styrene to ethyl diazoacetate molar ratio of 1.25:1 and 1 mol % Cu immobilised relative to ethyl diazoacetate. Main byproducts were diethyl maleate and diethyl fumarate. <sup>b</sup> Major trans (1*S*, 2*S*), major cis (1*S*, 2*R*).

The catalyst was subjected to hot filtration studies. The leached copper proved not to be active. In the reuse of the catalyst, after overnight stirring in the second run the reaction was still not finished. Upon closer investigation of the spent catalysts by FT-IR, an additional peak appeared at  $1750\text{ cm}^{-1}$ , that can be attributed either to the cyclopropane esters ( $\text{COOR}$ ,  $1726\text{ cm}^{-1}$ )<sup>26</sup>, diethyl maleate ( $\text{COOR}$ ,  $1730\text{ cm}^{-1}$ ) or diethyl fumarate ( $\text{COOR}$ ,  $1720\text{ cm}^{-1}$ ) (Fig. 9).<sup>27</sup> In the second run, the leaching has also increased to 1 %. The increase of the leaching of the catalyst could be explained by the side products formed, diethyl maleate and diethyl fumarate. Therefore the impact of different substrates and products on leaching of the catalyst was tested, namely:  $\text{CH}_2\text{Cl}_2$ , styrene, diethyl fumarate and diethyl maleate (see experimental part 4.4). The catalyst was immobilised using  $\text{CH}_2\text{Cl}_2$  as a solvent. It proved that all of the substrates used contribute to the leaching of the catalyst in the following order:  $\text{CH}_2\text{Cl}_2 < \text{styrene} < \text{diethyl fumarate} < \text{diethyl maleate}$ . Leaching caused by traces of diethyl maleate and diethyl fumarate dissolved in  $\text{CH}_2\text{Cl}_2$  proved to be the highest. Based on these findings the reaction conditions should be adjusted such as to avoid formation of diethyl maleate and diethyl fumarate as much as possible.

#### 2.2.4 Comparison of Cu (I)-bis(oxazoline) with Ru (II)-Pybox immobilised on H-Al-TUD-1

Even though leaching was reduced below detection limits, yields as enantioselectivities were moderate in case of cationic Cu (I)-bisoxazoline catalysts. For that reason we looked for a different cationic asymmetric cyclopropanation catalyst based on transition metals other than Cu (I). As chiral hydrogenation catalyst a Rh complex immobilised on H-Al-TUD-1 was successful,<sup>8</sup> however this and similar catalysts are not suitable for cyclopropanation.

Therefore we turned to the very versatile Ru (II)-Pybox (Scheme 3), a



**Scheme 3:** Ru(II)-2,6-Bis[(4*R*)-(+)-isopropyl-2-oxazolin-2-yl] pyridine or Ru(II)-Pybox.

cyclopropanation catalyst more robust than Cu (I)-bis(oxazoline). The Ru (II)-pybox system does not require anhydrous conditions. Using methanol during immobilisation of Ru (II)-pybox on H-Al-TUD-1 60  $\mu\text{mol Ru g}^{-1}_{\text{support}}$  was immobilised. All of the Ru was complexed by the Pybox ligand (N/Ru ratio, Table 2, entry 8). The precursor used for the immobilisation  $[\text{RuCl}_2(\text{p-cymene})]_2$ , allowed us to test whether liquid ion-exchange has taken place or adsorption based on the presence of Cl anions. INAA analysis revealed around 70  $\mu\text{mol Cl g}^{-1}_{\text{support}}$ . An amount similar to the amount of Ru immobilised thus implying adsorption of the catalyst. A striking result given that the most polar solvent was used during immobilisation of the catalyst and that HCl is very soluble in MeOH and  $\text{CH}_2\text{Cl}_2$ . In the homogeneously catalysed reaction this catalyst leads to a yield of 73 % with a trans : cis ratio of 91:9 and corresponding enantioselectivities of 89 and 79 % respectively. When immobilised, the results obtained in the cyclopropanation reaction were less favourable (Table 6). Compared to non-detectable leaching in case of immobilised Cu (I)-bis(diphenyl oxazoline) some leaching of Ru (II) was observed, 2.82 %. Nevertheless a considerable increase in enantioselectivity was obtained in case of immobilised Ru (II)-Pybox compared to immobilised Cu (I)-bisoxazoline.

**Table 6** Results obtained with Ru (II)-Pybox in heterogeneous and homogeneous reaction.<sup>a</sup>

	Homogeneous reaction <sup>a</sup>	L-Ru-Al-TUD-1
Yield <sub>GC</sub> (%)	73	47
trans : cis	91:9	62:38
trans ee's <sup>b</sup>	89	32
cis ee's <sup>b</sup>	79	15
Leaching (%)	-	2.82

<sup>a</sup> Cyclopropanation reactions were performed in dichloromethane under nitrogen using decane as internal standard with styrene to ethyl diazoacetate molar ratio of 1.25:1 and 1 mol % Cu immobilised relative to ethyl diazoacetate. Main byproducts were diethyl maleate and diethyl fumarate. <sup>b</sup> Major trans (1*S*, 2*S*), major cis (1*S*, 2*R*).

Hot filtration studies revealed that the leached catalyst was mildly active. An increase of 3 % in yield was observed during overnight stirring of the filtrated reaction mixture. In the second run of the catalyst, the reaction was not completed (16 h) and a yield of only 6 % was obtained. In the FT-IR studies (Fig. 10) of the used and virtually inactive catalyst the same ester bands were observed as for immobilised Cu (I)-bis(oxazoline)



catalyst (Fig. 9). This indicates that again the reaction products might have an unfavourable influence on the catalyst.

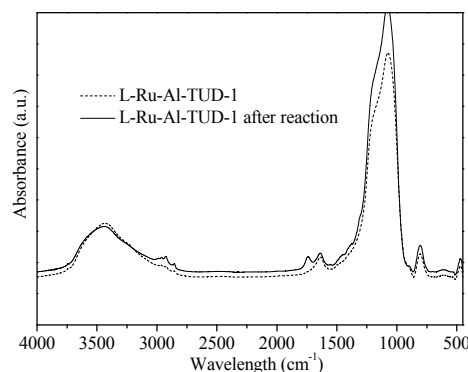


**Figure 10:** FT-IR analysis of immobilized R(II)-Pybox on Al-TUD-1 using methanol during immobilization, before and after the cyclopropanation reaction.

### 3. Conclusion

The Brønsted acidic support of TUD-1 structure, H-Al-TUD-1 and its Na-form Na-Al-TUD-1 have been explored as supports for the immobilisation of chiral cyclopropanation catalysts applying non-covalent techniques, adsorption and liquid ion-exchange. Heterogeneous catalysts were tested for the cyclopropanation of styrene with ethyl diazoacetate as benchmark (Scheme 1). Different parameters have been studied to achieve the best results in terms of yield, enantioselectivity and leaching of the metal. Solvents with different polarities were used during immobilisation of Cu (I)-bis(diphenyl oxazoline) on H-Al-TUD-1 to distinguish between adsorption and ion-exchange. Out of the solvents used (dichloromethane, nitroethane, acetonitrile and methanol) the most polar solvent, methanol, yielded the only immobilised catalyst with no detectable leaching. However, activity and selectivity of the catalyst were significantly reduced.

To increase the performance of the heterogeneous catalyst a closer look was taken at the support itself. To have well defined catalytic sites Na-Al-TUD-1 was synthesized whereby all of aluminium was tetrahedrally coordinated according to  $^{27}\text{Al}$  NMR. Utilizing Na-Al-TUD-1 as support of Cu (I)-bis(diphenyl oxazoline) yields as well as enantioselectivities in the cyclopropanation were increased. Unfortunately a leaching of 4

% was measured. Since it had been established that H-Al-TUD-1 was an excellent carrier for other transition metals we decided to immobilise also a chiral cyclopropanation catalysts based on a transition metal other than Cu (I). For cationic Ru (II)-Pybox, H-Al-TUD-1 possessing both Brønsted acid sites as well as Lewis acid sites proved to be a suitable carrier, too. An active and enantioselective immobilised catalyst was obtained. However it did display some leaching and was less active than the homogeneous catalyst. Overall, Brønsted acidic H-Al-TUD-1 is suitable for immobilisation of chiral C-C bond forming catalysts provided that all involved parameters are carefully taken into account.

## 4. Experimental

Introduction of Cu (I) on supports, subsequent manipulations and cyclopropanation reactions catalysed with immobilised Cu (I) were performed under dry nitrogen using Schlenk techniques.

### 4.1 Materials

Dry solvents were purchased from Aldrich except absolute ethanol which was obtained from J.T. Baker. Styrene was purchased from Merck and distilled before use. Ethyl diazoacetate was purified as follows: dissolved in diethyl ether, it was washed several times with 10 wt% Na<sub>2</sub>CO<sub>3</sub> solution and dried over anhydrous MgSO<sub>4</sub>. Subsequently diethyl ether was removed at reduced pressure at room temperature. All other reagents were purchased from Aldrich, Across or Fluka.

### 4.2 Synthesis of supports

#### 4.2.1 Al-TUD-1 (Si/Al=4)<sup>8</sup>

Aluminium isopropoxide (6.12 g, 0.03 mol) was added to a mixture of absolute ethanol (27.65 g, 0.60 mol) and anhydrous 2-propanol (27.04 g, 0.45 mol) at 45 °C followed by addition of tetraethyl orthosilicate (24.99 g, 0.12 mol) and tetraethylene glycol (29.17 g, 0.15 mol). The entire mixture was stirred for 1 h before dropwise addition of demineralised water (5.41 g, 0.30 mol) dissolved in absolute ethanol (27.65 g, 0.60 mol) and anhydrous 2-propanol (27.04 g, 0.45 mol).

After the addition of demineralised water the mixture was stirred for an additional 0.5 h at room temperature followed by aging for 6 h. The resulting wet gel was dried at 70 °C for 21 h and 2 h at 98 °C. Hydrothermal treatment was performed in an autoclave with Teflon insert at 160 °C for 19 h. Finally the solid was calcined in air (with 1 °C min<sup>-1</sup> to 550 °C, 4 h at 550 °C, with 1 °C min<sup>-1</sup> to 600 °C, 10 h at 600 °C).

#### 4.2.2 Na-Al-TUD-1 (Si/Al=4)

Two Na-Al-TUD-1's were prepared with different Na/Al ratios. Samples were denoted as Na-Al-TUD-1.4 and Na-Al-TUD-0.7. The last number standing for the final Na/Al ratio determined by ICP. The synthesis of Na-Al-TUD-1.4 was as follows. To aluminium isopropoxide (4.24 g, 0.21 mol) anhydrous 2-propanol was added. The entire mixture was stirred for 2 h, then tetraethyl orthosilicate (17.30 g, 0.08 mol) was added as silica source followed by dropwise addition of solution of triethanolamine (12.50 g, 0.08 mol) and demineralised water (5.03 g, 0.28 mol). Finally, to the clear mixture NaOH (0.97 g, 0.02 mol) dissolved in demineralised water (11.46 g, 0.64 mol) was added dropwise under vigorous stirring. The obtained molar composition was 1 SiO<sub>2</sub> : 0.25 Al<sub>2</sub>O<sub>3</sub> : 1 TEA : 0.29 NaOH : 11 H<sub>2</sub>O.

The synthesis of Na-Al-TUD-0.7 was slightly adjusted. Before the final addition of NaOH dissolved in water tetraethylammonium hydroxide (TEAOH, 35 wt % in H<sub>2</sub>O, 4.37 g, 0.01 mol) was added. The molar composition was 1 SiO<sub>2</sub> : 0.25 Al<sub>2</sub>O<sub>3</sub> : 1 TEA : 0.175 NaOH : 0.125 TEAOH : 11 H<sub>2</sub>O.

The obtained gels were left to stir for 0.5 h and poured into a porcelain bowl to age overnight. After drying the gels at room temperature they were dried at 98 °C for 21 h followed by hydrothermal treatment at 180 °C for 21 h in an autoclave equipped with Teflon inserts. Finally solids were calcined in air at 600 °C for 10 h with a ramp rate of 1 °C min<sup>-1</sup>.

### 4.3 Immobilisation of chiral cyclopropanation catalysts

#### 4.3.1 Immobilisation of Cu (I)-bis(oxazolin)

The amount of Cu to be immobilised was based on results from <sup>27</sup>Al-NMR of H-Al-TUD-1. With calculated amount of tetrahedrally coordinated aluminium (0.56 mmol g<sup>-1</sup><sub>H-Al-TUD-1</sub>) and a ratio of tetrahedral coordinated alumina to copper equals 2.6, 214 µmol Cu g<sup>-1</sup><sub>H-Al-TUD-1</sub> was immobilised. In case of Na-Al-TUD-1's, whereby according to <sup>27</sup>Al-NMR almost all Al is tetrahedrally coordinated, 212 µmol Cu/g Na-Al-TUD-1.4 was immobilised (ratio Al/Cu = 11.48). In case of Na-Al-TUD-0.7, 207 µmol Cu/g Na-Al-TUD-0.7 was immobilised (ratio Al/Cu = 14).

Supports, Al-TUD-1 or Na-Al-TUD-1, were first dried at 200 °C under vacuum for 2 h. Separately, in 30 mL dry CH<sub>2</sub>Cl<sub>2</sub> (Cu(I)CF<sub>3</sub>SO<sub>3</sub>)<sub>2</sub>\*C<sub>6</sub>H<sub>5</sub>CH<sub>3</sub> was complexed by a

bisoxazoline ligand, namely 2,2'-methylenebis-[(4*R*,5*S*)-4,5-diphenyl-4,5-dihydro-1,3-oxazole] (from now on called bis(diphenyl oxazoline)) or 2,2'-isopropylidenebis-[(4*S*)-4-*tert*-butyl-4,5-dihydro-1,3-oxazole] (from now on called bis(*tert*-butyl oxazoline)). After removal of CH<sub>2</sub>Cl<sub>2</sub> under vacuum conditions, Cu (I) complexed by bis(oxazoline) ligand was redissolved in 30 mL anhydrous solvent, either methanol (M), acetonitrile (A), nitroethane (N) or dichloromethane (D). The same amount of appropriate anhydrous solvent was added to dried Al-TUD-1 or Na-Al-TUD-1. Complexed Cu (I) dissolved in 30 mL anhydrous solvent was added to the suspension of Al-TUD-1 or Na-Al-TUD-1 via a syringe equipped with a PTFE 0.2 µm Rotilabo®-Spritzenfilter. The entire mixture was stirred for 24 h at room temperature or at 50 °C when methanol was used as solvent.

After stirring, the solid was filtered and thoroughly washed with dry CH<sub>2</sub>Cl<sub>2</sub> until a colourless fraction was collected, usually 3 times 30 mL dry CH<sub>2</sub>Cl<sub>2</sub> were used. The solid was subsequently Soxhlet extracted overnight using again dry CH<sub>2</sub>Cl<sub>2</sub>. Finally the solid was dried under vacuum at 50 °C for 2 h. The presence and integrity of the ligand was subsequently confirmed by FT-IR.

All the catalysts were first denoted by L for ligand then by the metal immobilised followed by notation for aluminosilicate, Al-TUD-1 and at the end indicating specific condition. According to solvent used during immobilisation, catalysts are denoted as L-Cu-Al-TUD-M, A, N or D. In case Na-Al-TUD-1 was used as support only methanol was used as solvent. When bis(*tert*-butyl oxazoline) was used as ligand notation *t* was used at the end.

#### 4.3.2 Immobilisation of Ru (II)-Pybox

The same procedure as above was followed for immobilisation of the Ru (II)-Pybox catalyst using methanol during immobilisation. 1.8 g dry Al-TUD-1 was employed in order to eventually immobilise 20 µmol Ru/ 100 mg carrier (ratio Al<sub>tetrahedral</sub>/Ru = 1.7). [RuCl<sub>2</sub>(p-cymene)]<sub>2</sub> (365 µmol, 112 mg) was complexed by 2,6-Bis[(4*R*)-(+)-isopropyl-2-oxazolin-2-yl] pyridine (Pybox-ip) (370 µmol, 121 mg) in 30 mL anhydrous CH<sub>2</sub>Cl<sub>2</sub>. The heterogeneous catalyst obtained was denoted as L-Ru-Al-TUD-1.

#### 4.4 Influence of different substrates of the cyclopropanation reaction on the leaching of catalyst

Cu (I)-bis(diphenyl oxazoline) immobilised on Al-TUD-1 (0.10 g) following the above procedure ( $\text{CH}_2\text{Cl}_2$  was used during immobilisation) was stirred either with  $\text{CH}_2\text{Cl}_2$  (3 mL), styrene (3 mL), diethylmaleate (5  $\mu\text{L}$  dissolved in 3 mL  $\text{CH}_2\text{Cl}_2$ ) or diethylfumarate (5  $\mu\text{L}$  dissolved in 3 mL  $\text{CH}_2\text{Cl}_2$ ) overnight. Subsequently the catalyst was removed with a syringe equipped with a PTFE 0.2  $\mu\text{m}$  Rotilabo<sup>®</sup>-Spritzenfilter. Copper leaching into the filtrate was determined by ICP-OES analysis.

#### 4.5 Homogeneous cyclopropanation

In 15 mL dry  $\text{CH}_2\text{Cl}_2$  ( $\text{Cu(I)CF}_3\text{SO}_3)_2 \cdot \text{C}_6\text{H}_5\text{CH}_3$  was complexed by a bis(diphenyl oxazoline) ligand. Complexed Cu (I) was filtered with a PTFE 0.2  $\mu\text{m}$  Rotilabo<sup>®</sup>-Spritzenfilter. Decane (5 mmol, 0.71 g) was added followed by freshly distilled styrene (40 mmol, 4.17 g, 4.60 mL). Ethyl diazoacetate (4 mmol, 0.46 g) was dissolved in 5 mL dry  $\text{CH}_2\text{Cl}_2$  and added via a syringe pump at speed of 0.36 mL  $\text{h}^{-1}$ . The reaction was left to stir overnight.  $\text{CH}_2\text{Cl}_2$  was removed by evaporation and the crude mixture was purified using silica column chromatography. Eluent was Petroleum ether : Ethyl acetate = 90:10.

#### 4.6 Heterogeneous Cyclopropanation reaction

To weighted amount of Cu immobilised (1% Cu relative to ethyl diazoacetate, 20  $\mu\text{mol}$ ) dry  $\text{CH}_2\text{Cl}_2$  (6 mL) was added. This was followed by addition of styrene (0.26 g, 2.50 mmol) and decane (0.36 g, 2.50 mmol) as internal standard. The reaction was started by addition of ethyl diazoacetate (0.23 g, 2 mmol) dissolved in 5 mL dry  $\text{CH}_2\text{Cl}_2$  using a syringe pump (1.20 mL  $\text{h}^{-1}$ ). The reaction was left to stir overnight.

#### 4.7 Hot filtration studies

After the addition of ethyl diazoacetate by syringe pump ( $1.20 \text{ mL h}^{-1}$ ), the catalyst was filtered off and the solution left to stir overnight. The samples were taken immediately after filtration and after overnight stirring.

#### 4.8 The reuse of the catalyst

The catalyst was filtered off, washed with dry  $\text{CH}_2\text{Cl}_2$  ( $3 \times 15 \text{ mL}$ ) before it was reused in second run following the above procedure.

#### 4.9 GC Analysis

The conversion of the reaction was determined by Varian Star 3400 CX equipped with CP Wax 52 CB column with dimension of  $50 \text{ m} \times 0.53 \text{ mm}$  (ID) and film thickness of  $2 \mu\text{m}$ . GC Injector was programmed,  $70^\circ\text{C}$  (hold time 1 min) to  $250^\circ\text{C}$  (hold time 4 min) with a rate of  $40^\circ\text{C min}^{-1}$ . GC detector (FID) was set at  $250^\circ\text{C}$ . He was used as carrier gas. The temperature programme of the column was  $70^\circ\text{C}$  (hold time 2 min), ramp  $10^\circ\text{C min}^{-1}$  to  $240^\circ\text{C}$  (hold time 7 min), in total 26 min. Retention times: decane 4.4 min, styrene 8.7 min, diethylfumarate 14.4 min, diethylmaleate 15.8 min, **1** cis (Scheme 1) 19.8 and **1** trans (Scheme 1) 20.4 min. Trans/cis ratio and ee values were determined using a Shimadzu GC 17A equipped with Chirasil Dex CB column with dimensions of  $25 \text{ m} \times 0.32 \text{ mm}$  (ID) and film thickness of  $0.25 \mu\text{m}$ , samples were analysed at  $131^\circ\text{C}$  (isotherm), during 13 min. He was used as carrier gas, total flow  $166 \text{ mL min}^{-1}$ , pressure 155 kPa, column flow  $5.18 \text{ mL min}^{-1}$ , split injector (30/100) was set at  $220^\circ\text{C}$ , and GC detector (FID) at  $200^\circ\text{C}$ . Retention times: **1** cis (1*S*, 2*R*) 4.5 min, **1** cis (1*R*, 2*S*) 4.8 min, **1** trans (1*R*, 1*R*) 5.1 min, **1** trans (1*S*, 2*S*) 5.3 min.

#### 4.10 Sample characterization

X-ray powder diffraction patterns were recorded using  $\text{Cu}_{K\alpha}$  radiation on a Philips PW 1840 diffractometer equipped with a graphite monochromator.  $\text{N}_2$  physisorption was measured on a Quantachrome Autosorb at 77 K. IR spectra were recorded as KBr discs using a PerkinElmer Spectrum One FT-IR spectrometer. Aluminium, silicon, copper and ruthenium amounts present on solid samples were determined by the ICP-OES technique

using a Perkin Elmer Optima 3000dv. Chloride amounts present on solid supports were measured by instrumental neutron activation analysis (INAA), which was performed at “Het Reactor Instituut Delft” (RID). The “Hoger Onderwijs Reactor” nuclear reactor, with a neutronflux of  $10^{17}$  neutrons  $\text{s}^{-1}\text{cm}^{-2}$ , was used as a source of neutrons, and the gamma spectrometer was equipped with a germanium semiconductor as detector. Cu and Ru leaching was determined by analysing the reaction filtrates with graphite AAS on a Perkin Elmer AAnalyst 200. Solid state  $^{27}\text{Al}$  NMR MAS spectra were recorded on a Bruker Avance 400 spectrometer operating at 100 MHz.



## 5. References

- 1 C. E. Song, S. Lee, *Chem. Rev.*, **2002**, *102*, 3495-3524.
- 2 J. M. Fraile, J. I. García, J. A. Mayoral, *Chem. Rev.*, **2009**, *109*, 360–417.
- 3 Y. Wan, D. Zhao, *Chem. Rev.*, **2007**, *107*, 2821–2860.
- 4 J.C. Jansen, Z. Shan, L. Marchese, W. Zhou, N. van der Puil, T. Maschmeyer, *Chem. Commun.*, **2001**, 713–714.
- 5 S. Telalović, A. Ramanathan, G. Mul, U. Hanefeld, *J. Mater. Chem.*, **2010**, *20*, 642-658.
- 6 P. J. Angevine, A. M. Gaffney, Z. Shan, C. Y. Yeh, A.C.S. symposium series, Chapter 9, pp 335–363.
- 7 Z. Shan, J.C. Jansen, W. Zhou, Th. Maschmeyer, *Appl. Catal. A: Gen.*, **2003**, *254*, 339- 343.
- 8 Simons, U. Hanefeld, I.W.C.E. Arends, R.A. Sheldon, Th. Maschmeyer, *Chem. Eur. J.*, **2004**, *10*, 5829-5835.
- 9 (a) J. M. Fraile, J. I. García, C. I. Herrerías, J. A. Mayoral, E. Pires, *Chem. Soc. Rev.*, **2009**, *38*, 695-706.  
 (b) J. M. Fraile, J. I. García, J. A. Mayoral, *Coord. Chem. Rev.*, **2008**, *252*, 624-646.  
 (c) J. I. García, B. López-Sánchez, J. A. Mayoral, E. Pires, I. Villalba, *J. Catal.*, **2008** *258* 378-385.  
 (d) J. M. Fraile, J. I. García, C. I. Herrerías, J. A. Mayoral, M. A. Harmer, *J. Catal.*, **2004**, *221*, 532-540.  
 (e) J. M. Fraile, J. I. García, J. A. Mayoral, M. Roldán, *Org. Lett.*, **2007**, *9*, 731-733.  
 (f) J. M. Fraile, J. I. García, M. A. Harmer, C. I. Herrerías, J. A. Mayoral, *J. Mol. Catal. A: Chem.*, **2001**, *165*, 211-218.  
 (g) J. M. Fraile, J. I. García, M. A. Harmer, C. I. Herrerías, J. A. Mayoral, O. Raiser, H. Werner, *J. Mater. Chem.*, **2002**, *12*, 3290-3295.  
 (h) A. Cornejo, J. M. Fraile, J. I. García, M. J. Gil, C. I. Herrerías, G. Legarreta, V. Martínez-Merino, J. A. Mayoral, *J. Mol. Catal. A: Chem.*, **2003**, *196*, 101-108.  
 (i) A. I. Fernández, J. M. Fraile, J. I. García, C. I. Herrerías, J. A. Mayoral, L. Salvatella, *Catal. Commun.*, **2001**, 165-170.  
 (j) P. J. Alonso, J. M. Fraile, J. García, J. I. García, J. I. Martínez, J. A. Mayoral, M. C. Sánchez, *Langmuir* **2000**, *16*, 5607-5612.  
 (k) J. M. Fraile, J. I. García, J. A. Mayoral, T. Tarnai, M. A. Harmer, *J. Catal.*, **1999**, *186*, 214-221.  
 (l) J. M. Fraile, J. I. García, J. A. Mayoral, T. Tarnai, *Tetrahedron: Asymmetry* **1998**, *9*, 3997-4008.

- (m) J. M. Fraile, J. I. García, J. A. Mayoral, T. Tarnai, *Tetrahedron: Asymmetry* **1997**, *8*, 2089-2092.
- 10 M. T. Janicke, C. C. Landry, S. C. Christiansen, S. Birtalan, G. D. Stucky, B. F. Chmelka, *Chem. Mater.*, **1999**, *11*, 1342-1351.
- 11 A. Corma, V. Fornés, M. T. Navarro, J. Pérez-Pariente, *J. Catal.*, **1994**, *148*, 569-574.
- 12 Z. Luan, C-F. Cheng, H. He, J. Klinowski, *J. Phys. Chem.*, **1995**, *99*, 10590-10593.
- 13 R. Ryoo, C. H. Ko, R. F. Howe, *Chem. Mater.*, **1997**, *9*, 1607-1613.
- 14 Li-Q. Wang, C. L. Aardahl, K. G. Rappé, D. N. Tran, M. A. Delgado, *J. Mater. Res.*, **2002**, *17*, 1843-1848.
- 15 H. Hamdan, S. Endud, H. He, M. N. M. Muhid, J. Klinowski, *J. Chem. Soc. Faraday Trans.*, **1996**, *92*, 2311-2315.
- 16 M. Janicke, D. Kumar, G. D. Stucky, B. F. Chmelka, *Stud. Surf. Sci. Catal.*, **1994**, *84*, 243-250.
- 17 S. Cabrera, J. El Haskouri, S. Mendioroz, C. Guillem, J. Latorre, A. Beltrán-Porter, D. Beltrán-Porter, M. D. Marcos, P. Amorós, *Chem. Commun.*, **1999**, 1679-1680.
- 18 (a) R. E. Lowenthal, S. Masamune, *Tetrahedron Lett.*, **1991**, *32*, 7373-7376.  
(b) R. E. Lowenthal, A. Abuko, S. Masamune, *Tetrahedron Lett.*, **1990**, *31*, 6005-6008.
- 19 (a) A. Crosman, W. F. Hölderich, *J. Catal.*, **2009**, *265*, 229-237.  
(b) A. Crosman, W. F. Hoelderich, *J. Catal.*, **2005**, *232*, 43-50.  
(c) H. H. Wagner, H. Hausmann, W. F. Hölderich, *J. Catal.*, **2001**, *203*, 150-156.
- 20 P. O'Leary, N. P. Krosveld, K. P. De Jong, G. Van Koten, R. J. M. Klein Gebbink, *Tetrahedron Lett.*, **2004**, *45*, 3177-3180.
- 21 C. Reichardt, *Chem. Rev.*, **1994**, *94*, 2319-2358.
- 22 J. Hájek, N. Kumar, P. Mäki-Arvela, T. Salmi, D. Yu. Murzin, *J. Mol. Catal. A: Chem.*, **2004**, *217*, 145-154.
- 23 R. L. Benoit, M. Fréchet, D. Boulet, *Can. J. Chem.*, **1989**, *67*, 2148-2152.
- 24 T. Hayashida, H. Kondo, J. Terasawa, K. Kirchner, Y. Sunada, H. Nagashima, *J. Organomet. Chem.*, **2007**, *692*, 382-394.
- 25 A. Corma, *Catal. Rev. Sci. Eng.*, **2004**, *46*, 369-417.
- 26 B. Scholl, H-J. Hansen, *Helv. Chim. Acta.*, **1986**, *69*, 1936-1958.
- 27 T. Yoshino, S. Imori, H. Togo, *Tetrahedron* **2006**, *62*, 1309-317.

On the Synergistic Catalytic Properties of  
Bimetallic Mesoporous Materials  
Containing Aluminium and Zirconium.  
The Prins Cyclisation of Citronellal

---

Part of this chapter has been published in

S. Telalović, J. F. Ng, R. Maheswari, A. Ramanathan, G. K. Chuah, U. Hanefeld, *Chem. Commun.*, **2008**, 4631-4633.

S. Telalović, A. Ramanathan, J. F. Ng, R. Maheswari, C. Kwakernaak, F. Soulimani, H. C. Brouwer, G. K. Chuah, B. W. Weckhuysen, U. Hanefeld, *Chem. Eur. J.*, **2011**, *17*, 2077-2088. .

## 1. Introduction

Synergy between different types of catalytic sites is a much sought after objective. Synergy might occur between Lewis and Brønsted acid sites in monometallic materials or might be induced by the application of two different active metals. In this respect, the increased activity of hydrothermally treated faujasite-type Y zeolites in catalytic cracking reactions has intrigued scientists for decades. Already very early, the synergy between extra-framework aluminium, Lewis acid sites formed due to partial release of aluminium from the framework upon hydrothermal treatment and Brønsted acid sites was suggested.<sup>1</sup> Enhanced acidity of the catalyst was explained by direct coordination of Lewis acid sites to the Brønsted acid site. Very recently, a different type of mechanism for Brønsted-Lewis acid synergy was proposed based on NMR experiments and DFT calculations: Lewis acid sites in the form of extra-framework aluminium coordinate to the oxygen atom nearest to the Brønsted acid site, though there is no direct interaction between them.<sup>2</sup>

Besides the above mentioned synergy between Brønsted and Lewis acid sites in zeolites there are also other relevant examples found in mesoporous materials. Immobilization of different lanthanide triflates inside the pores of silicious SBA-15 led to different Brønsted/Lewis ratio and corresponding catalytic activity in Friedel-Crafts acylation of naphthalene with *p*-toluoyl chloride.<sup>3</sup> The synergy found for these catalytic systems was explained through the confinement of large molecules such as lanthanide triflates inside the pores of SBA-15 causing significant physical perturbation of the surface hydroxyl groups of the host matrix giving rise to the formation of certain Brønsted type surface acid sites.

Most common and widespread examples of synergy are those found in different bimetallic catalysts used in several important reactions. Synthesis of bimetallic catalysts such as amorphous  $\text{SnO}_2\text{-ZrO}_2$  as to achieve synergistic effect has led to improved catalysts for  $\text{SO}_2$  reduction produced in the Direct Sulfur Recovery Process (DSRP).<sup>4</sup> Steam or autothermal reforming of hydrocarbons is an important source of  $\text{H}_2$  for Proton Exchange Membrane Fuel Cells ( $\text{H}_2\text{-PEMFC}$ ). However, reformed gas contains considerable amounts of CO leading to poisoning of the fuel cell. Pt and Pd mutually immobilized on perovskite oxide showed higher activity and stability in the water gas shift reaction in order to reduce

CO compared to their monometallic counterparts.<sup>5</sup> The same effect was observed by applying CuO-CeO<sub>2</sub> instead of individual oxides (CuO and CeO<sub>2</sub>) or their physical mixtures.<sup>6</sup> The properties of light metal hydrides, which are interesting for their high hydrogen storage capacity, were improved by the addition of Fe and Zr through enhanced H<sub>2</sub> desorption kinetics.<sup>7</sup> An Fe-Ce-ZSM-5 catalyst showed high NO conversion in the selective catalytic reduction of NO by NH<sub>3</sub> in a wide temperature window and even in presence of H<sub>2</sub>O and SO<sub>2</sub> relative to Fe-ZSM-5 or Ce-ZSM-5.<sup>8</sup>

An alternative approach to study the synergy between Brønsted and Lewis acid sites as seen in the industrially important Y zeolites is to synthesize a bimetallic mesoporous catalyst. This approach necessitates the partial replacement of aluminium inside an aluminosilicate material possessing both Brønsted and Lewis acid sites by a transition metal generating exclusively Lewis acid sites. Framework incorporated transition metals having different electronic properties from aluminium would affect the strength of the Brønsted acid sites already present. Three-dimensional mesoporous materials lend themselves particularly for such an approach as diffusion effects are virtually non existent and if synergy between acid sites does exist it would improve the catalytic activity of three-dimensional mesoporous materials to that of zeolites. Thus diffusion limitations would be reduced without loss of acidity based activity, relative to zeolites. This bimetallic approach making use of mesoporous MCM-41 materials has been explored for Zn-Al and Ce-Al combinations and did yield indications for synergy, however conclusive results were not yet obtained and this necessitates the exploration of other suitable mesoporous matrices.<sup>9, 10</sup>

TUD-1 is such a porous solid as it is a well established mesoporous material with a three-dimensional structure, tuneable pore size distribution and surface area reaching values of 900 m<sup>2</sup> g<sup>-1</sup>.<sup>11,12</sup> The main advantage of TUD-1 concerning the study of Brønsted-Lewis acid synergy is that it is excellent for framework incorporation of different metals.<sup>13,14,15</sup> This high degree of framework incorporation is due to the complexing agent used in the synthesis of TUD-1, triethanolamine. It forms atrane complexes with different metals (M), thus ensuring incorporation as isolated metals rather than metal oxide clusters. Employing this approach a wide range of M-TUD-1 with framework incorporated metals can be prepared and Al-TUD-1 materials possessing both Brønsted and Lewis acid sites have been applied in the Lewis acid-catalyzed Friedel-Crafts alkylation of phenol.<sup>16</sup> Zr-TUD-1 on the other hand possesses exclusively Lewis acid sites due to high degree of metal incorporation

inside the TUD-1 matrix.<sup>15</sup> By combining both metals inside the TUD-1 matrix it should become possible to fine-tune the ratio of Lewis and Brønsted acid sites due to the different types of acidity of the metals.<sup>17</sup> Thus Al-Zr-TUD-1 should be a showcase material with adjustable Brønsted and Lewis acidity, ideal to investigate whether synergy between these two types of acidity really exist and can be exploited for fine tuning catalytic activity.

This is the topic of this article. Al-Zr-TUD-1 has been used to investigate the presence of synergy between Brønsted and Lewis acid sites by performing a systematical variation of aluminium and zirconium inside the TUD-1 matrix with constant Si/M ratio instead of increasing the weight percentage of one metal while keeping the weight percentage of the second constant. Bimetallic mesoporous catalysts were compared with their monometallic counterparts Al-TUD-1 and Zr-TUD-1 using both, spectroscopic methods and catalytic conversions. It will be shown that the synergistic effect between different Brønsted and Lewis acid sites in bimetallic mesoporous catalysts is very specific, substrate as well as reaction mechanism dependent.

## **2. Results and Discussion**

### **2.1 Al-Zr-TUD-1 as a novel bimetallic mesoporous material**

The mesoporous nature of Al-Zr-TUD-1 samples is evidenced by the high-resolution transmission electron micrographs (HR-TEM) and representative images are given in Fig. 1 a-c. All samples exhibit a sponge-like structure typical for TUD-1. HR-TEM analysis proves the framework incorporation of Al and Zr in the TUD-1 matrix. No crystalline nanoparticles of  $\text{ZrO}_2$  or  $\text{Al}_2\text{O}_3$  were detected, suggesting that both metals were incorporated into the framework as expected. This is in line with earlier results for monometallic Zr-TUD-1 and Al-TUD-1 with Si/M ratio of 25.<sup>15,16</sup> Accordingly XRD analysis (Fig. 2) further confirmed the mesoporous character of Al-Zr-TUD-1.

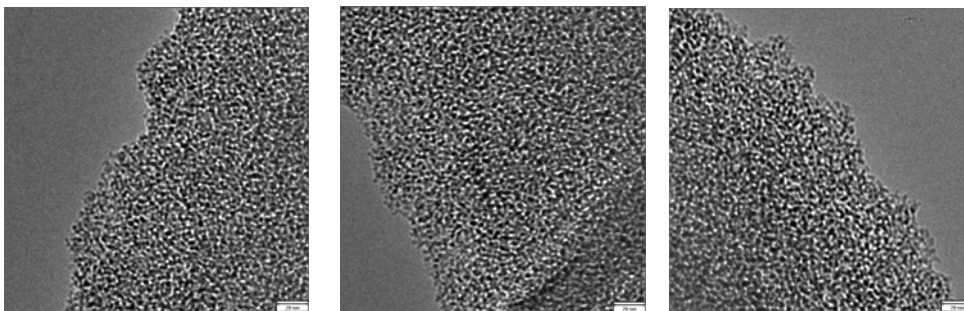


**Figure 1** HR-TEM images of Al-Zr-TUD-1 materials with a Si/M ratio of 25 varying in their Al:Zr ratio: Al-Zr-2:2 (left), Al-Zr-1:3 (center) and Al-Zr-3:1 (right). The bar represents 20 nm.

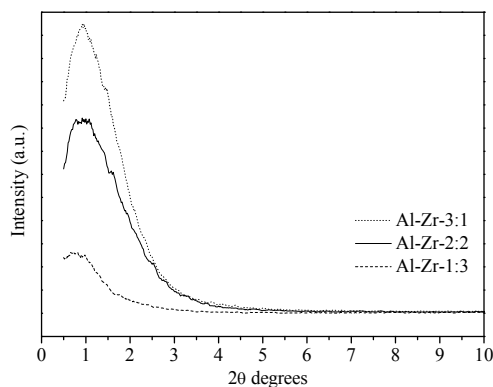


**Figure 2** Al-Zr-TUD-1 catalysts with varying ratios of Al : Zr (3 : 1, 2 : 2 and 1 : 3) but constant Si/M ratio of 25 show an intense peak at low angle (0.8-1  $2\theta$ ) in their X-ray powder diffraction patterns. The higher the percentage zirconium incorporated, the lower the intensity of the peak and therefore the degree of order of the corresponding Al-Zr-TUD-1. No evidence of crystalline  $\text{ZrO}_2$  or  $\text{Al}_2\text{O}_3$  phases was found in the X-ray diffractograms, suggesting that both metals were incorporated into the framework as expected.

$\text{N}_2$ -physisorption measurements obtained at 77 K (Fig. 3) and the results from elemental analysis (ICP-OES) are summarized in Table 1. The surface area of the three samples varies from 689 to 877  $\text{m}^2 \text{g}^{-1}$  and is not correlated with the amount of the different metals present. Pore size ( $d_{\text{p, BJJ}}$ ) and pore volume ( $V_{\text{p, BJJ}}$ ) are also not correlated to the type of metal

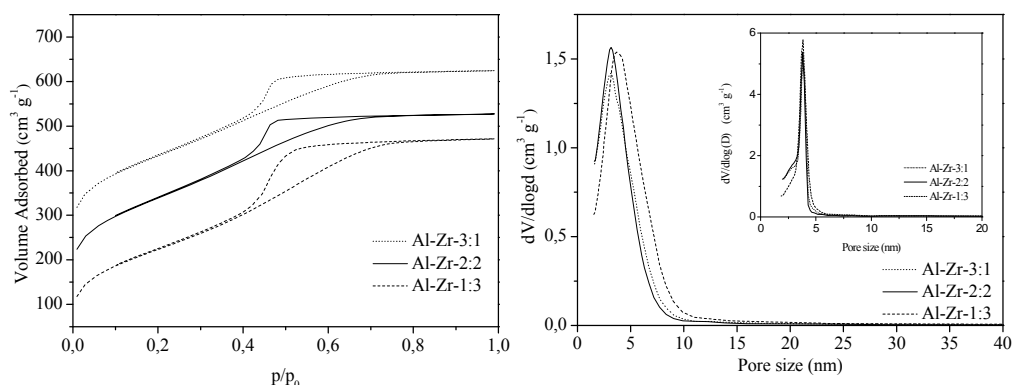


**Figure 3** Isotherms of bimetallic TUD-1 catalysts with Si/M ratio of 25 and Al-Zr-3:1, Al-Zr-2:2 and Al-Zr-1:3 obtained from N<sub>2</sub> physisorption analysis (left figure) and pore size distribution of the same catalysts calculated from adsorption and desorption branch (inset) using the Barret-Joyner-Halenda (BJH) model (right figure).

present in the Al-Zr-TUD-1 samples. The Si/Zr ratios present in calcined samples differ from those in the initial synthesis gel. The more zirconium present in the sample the higher is the deviation from the initial synthesis gel Si/(Al+Zr) ratio of 25, maximum obtained Si/(Al+Zr) ratio of 30 for the Al-Zr-1:3 sample. The same deviations were found during the

**Table 1** Physicochemical and acidic properties of TUD-1 based catalysts.

Catalysts	$n_{\text{Si}}/n_{\text{M}}^a$	$n_{\text{Si}}/n_{\text{Al}}$	$n_{\text{Si}}/n_{\text{Zr}}$	$n_{\text{Si}}/n_{(\text{Al}+\text{Zr})}$	$S_{\text{BET}}$ ( $\text{m}^2 \text{g}^{-1}$ )	$V_{\text{meso}}$ ( $\text{cm}^3 \text{g}^{-1}$ )	$D_{\text{meso}}$ (nm)	Total Acidity ( $\text{mmol NH}_3 \text{g}^{-1}$ )	B/L Ratio <sup>b</sup>
Al-TUD-1	25	26.6	-	26.6	956	0.95	3.7	0.40	2.41
Al-Zr-3:1	25	31	135	25	705	0.70	4.2	0.33	2.15
Al-Zr-2:2	25	47	69	28	686	0.85	4.6	0.32	2.05
Al-Zr-1:3	25	92	45	30	877	0.70	3.3	0.38	3.21
Zr-TUD-1	25	-	25	25	764	1.23	8.8	0.69	-

<sup>a</sup> Synthesis mixture ratio of silica to the total amount of metal incorporated. <sup>b</sup> Determined by dividing the area under the Lewis acid region ( $1460\text{--}1440 \text{ cm}^{-1}$ ) and the Brønsted acid region ( $1557\text{--}1538 \text{ cm}^{-1}$ ) found in spectra recorded at  $200^\circ\text{C}$ .

synthesis of zirconium containing aluminosilicate of BEA structure, Zr-Al- $\beta$ . The Si/Al ratio of calcined Zr-Al- $\beta$  was similar to that of the synthesis gel while the Si/Zr ratio was higher than that of the synthesis gel.<sup>18</sup>

<sup>27</sup>Al-NMR spectra of the three bimetallic catalysts are similar and reveal that around 50% of aluminium is tetrahedrally incorporated, around 30% is hexa-coordinated



aluminium and is assigned to extra framework aluminium responsible for Lewis acidity and finally around 20 % of aluminium is penta-coordinated (Fig. 4). The Al in Al-Zr-TUD-1 induces therefore both Brønsted and Lewis acid sites.

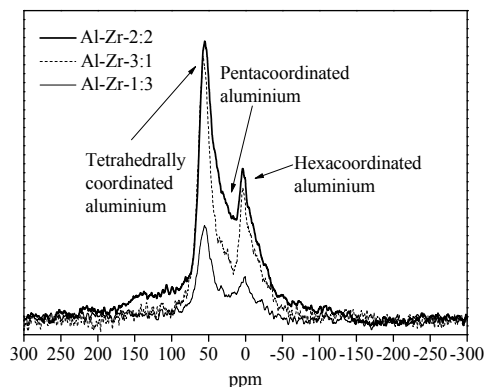


**Figure 4**  $^{27}\text{Al}$  MAS NMR spectrum of Al-Zr-2:2, Al-Zr-3:1 and Al-Zr-1:3 catalyst.

From the XPS measurements, the binding energies for Si  $2p$  and O  $1s$  photoelectron lines resemble those found in silicon dioxide ( $\text{SiO}_2$ ). The spectra of O  $1s$ , however, can be deconvoluted in five species for mono- and bimetallic TUD-1 catalysts (Table 2, Fig. 5). The National Institute of Standards and Technology (NIST) X-ray Photoelectron Spectroscopy Database give a value of the O  $1s$  binding energy of  $532.9 \pm 0.9$  eV for  $\text{SiO}_2$  and  $530.6 \pm 0.7$  eV for both  $\text{Al}_2\text{O}_3$  and  $\text{ZrO}_2$ .<sup>19</sup>

The Si-TUD-1 containing Si-O bonds only, has a O  $1s$  peak with a main peak always present at 533.0 eV. This main peak is flanked by a peak with a binding energy of 531.9 eV and 534.2 eV respectively. (Table 2, Fig. 5 (A)). The binding energy of O  $1s$  around 534 eV is due to the presence of air borne species such as water vapour, carbon dioxide or remaining template. An alternative explanation of the three peaks suggests that in Si-TUD-1, an amorphous mesoporous material, three prominent configurations of Si-atom bonded to O-atom are present.

Monometallic as well as bimetallic TUD-1 catalysts have O  $1s$  binding energies that have a lower value than that of silicon oxide (Table 2). Here, the electronegativity of the Al ( $\chi_{\text{Pauling}} = 1.61$ ) and Zr ( $\chi_{\text{Pauling}} = 1.33$ ), as opposed to Si ( $\chi_{\text{Pauling}} = 1.90$ ), renders

the O-atom to be more ionic.<sup>20</sup> The mutual repulsion of the electrons in the O-ion reduces the O  $1s_{1/2}$  binding energy.

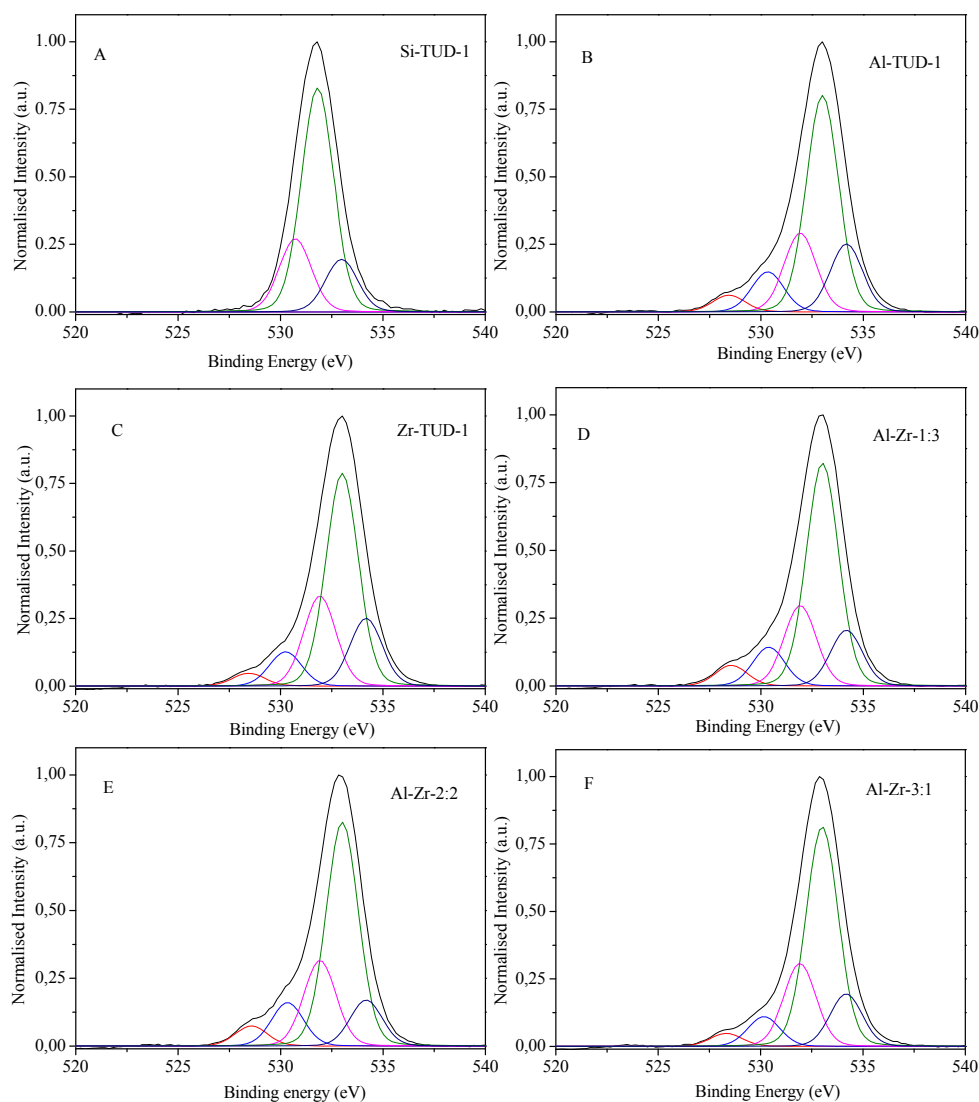


**Figure 5** Deconvoluted O  $1s$  spectra obtained by XPS analysis of (A) Si-TUD-1; (B) Al-TUD-1; (C) Zr-TUD-1; (D) Al-Zr-1:3; (E) Al-Zr-2:2 and (F) Al-Zr-3:1.

The presence of incorporated metal ions in the mesoporous framework apparently induces two spectral features at about 528.5 eV and 530.3 eV respectively. The latter peak

can be ascribed to the ‘normal’ ionic compounds  $\text{Al}_2\text{O}_3$  or  $\text{ZrO}_2$ .<sup>[19]</sup> It is also very clear from the spectra that it does not make a difference whether Al or Zr is involved (Fig. 5).

**Table 2** The XPS binding energy (in eV) of the O *1s*, Al *2p*, Si *2p*, and Zr *3d* photoelectrons and position of the Auger lines for Al, Si and Zr and the Si/Al and Si/Zr ratios obtained from XPS.<sup>a</sup>

Spectral line	Si-TUD-1	Zr-TUD-1	Al-TUD-1	Al-Zr-1:3	Al-Zr-2:2	Al-Zr-3:1
Al <i>2p</i>	-	74.1	75.1	74.9	74.4	74.8
Si <i>2p</i>	103.5	103.5	103.5	103.5	103.5	103.5
Zr <i>3d</i> <sub>5/2</sub>	-	183.7	184.1	183.7	183.6	183.9
Zr <i>3d</i> <sub>3/2</sub>	-	186.2	186.6	186.1	186.0	186.30
O <i>1s</i> (1)	-	528.45	528.45	528.56	528.57	528.33
O <i>1s</i> (2)	-	530.24	530.34	530.39	530.34	530.16
O <i>1s</i> (3)	531.9	531.92	531.92	531.92	531.92	531.92
O <i>1s</i> (4)	533.01	533.01	533.01	533.01	533.01	533.01
O <i>1s</i> (5)	534.18	534.18	534.18	534.18	534.18	534.18
Si/Al	-	-	21	40	31	28
Si/Zr	-	29	-	55	81	69

<sup>a</sup> The composition at the surface (Si/Al and Si/Zr ratios) of the catalysts is determined from the integrated photoelectron intensities using appropriate sensitivity factors for the area of the photoelectron lines.

They produce nearly the same spectra. The nature of the Al and Zr species is only derived from the binding energies of the metallic species. The presence of the ionic species does not affect the fraction of the flanking peaks too much (i.e. O *1s* (3) and O *1s* (5) in Table 3), but reduces the central peak remarkably (i.e. O *1s* (4)). This indicated that Al and Zr are

**Table 3** XPS analysis: The area fraction of the O *1s* in percent of the total area, given for mono- as well as bimetallic TUD-1 catalysts.

Spectral line	Si-TUD-1	Zr-TUD-1	Al-TUD-1	Al-Zr-1:3	Al-Zr-2:2	Al-Zr-3:1	Remark
O <i>1s</i> (1)	-	3.1	4.0	4.9	4.8	3.3	MO <sub>x</sub>
O <i>1s</i> (2)	-	8.2	9.5	9.3	10.4	7.5	MO <sub>x</sub>
O <i>1s</i> (3)	20.9	21.6	18.8	19.2	20.4	20.8	TUD-1
O <i>1s</i> (4)	64.0	50.9	51.5	53.3	53.4	55.2	TUD-1
O <i>1s</i> (5)	15.1	16.2	16.2	13.3	11.0	13.2	TUD-1, CO, H <sub>2</sub> O

incorporated in the zeolite framework at the expense of the Si-O bonds.

The binding energy of about  $183.7 \pm 0.1$  eV of Zr  $3d_{5/2}$  is higher than the values reported for  $\text{ZrO}_2$ <sup>[19]</sup> and corresponds to the values found in complex zirconium oxides as reported for  $\text{ZrSiO}_4$  and zirconium silicate alloy thin films.<sup>[21, 22]</sup> All zirconium found is incorporated into the  $\text{SiO}_2$  framework.

Based on  $\text{NH}_3$ -TPD analysis (Fig. 6) of different Al-Zr-TUD-1 catalysts the acidity is of comparable order in all samples. The monometallic Zr-TUD-1 possesses a larger amount of weak acid sites and Al-TUD-1 has a larger amount of strong acid sites compared to the other catalysts (see Table 1). Mutual incorporation of Al and Zr into TUD-1 leads to both a decrease of weak as well as strong acid sites and thus to a decrease of overall acidity.

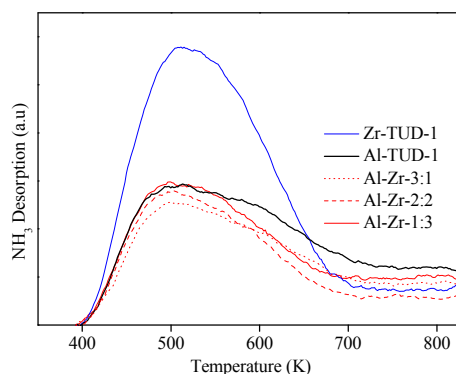


**Figure 6**  $\text{NH}_3$ -TPD profile of different TUD-1 catalysts with Si/M ratio of 25: Zr-TUD-1, Al-TUD-1, Al-Zr-3:1, Al-Zr-2:2 and Al-Zr-1:3.

IR spectra of a KBr pressed disc of three samples in the skeletal region (Fig. 7) show a typical band at  $1093\text{ cm}^{-1}$  together with a shoulder at  $1220\text{ cm}^{-1}$  due to asymmetric stretching vibrations of Si-O-Si bridges. The band at  $798\text{ cm}^{-1}$  is caused by symmetric stretching vibration of Si-O-Si.<sup>23</sup> The signal for Si-OH or Si-O-M at approximately  $970\text{ cm}^{-1}$  is not resolved.<sup>21,24,25</sup>

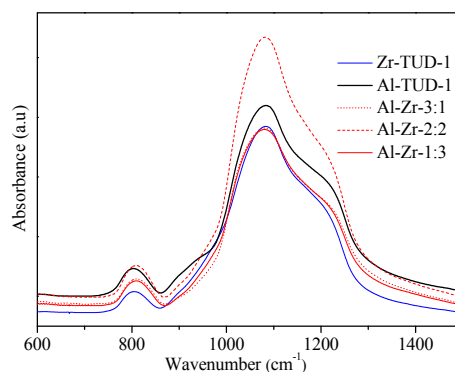


**Figure 7** FT-IR skeletal spectra of different TUD-1 catalysts with Si/M ratio of 25: Zr-TUD-1, Al-TUD-1, Al-Zr-3:1, Al-Zr-2:2 and Al-Zr-1:3.

FT-IR of the OH region of the three bimetallic catalysts and those of Zr-TUD-1 and Al-TUD-1 (Fig. 8) show a band centred around  $3745\text{ cm}^{-1}$ , asymmetric towards lower frequencies, commonly assigned to terminal silanol groups. However, there is a

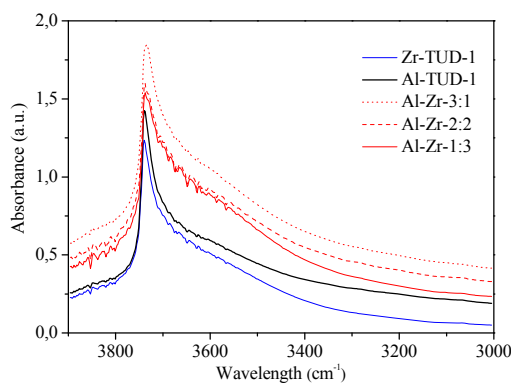


**Figure 8** FT-IR spectra in OH region acquired at  $400\text{ }^{\circ}\text{C}$  of different TUD-1 catalysts with Si/M ratio of 25: Zr-TUD-1, Al-TUD-1, Al-Zr-3:1, Al-Zr-2:2 and Al-Zr-1:3.

distinct difference between monometallic and bimetallic catalysts. Major bands centred at  $3745\text{ cm}^{-1}$  for the bimetallic catalysts have higher values for the full width at half maximum compared to monometallic catalysts. This is an indication of higher degree of heterogeneity of different silanol groups inside Al-Zr-TUD-1 catalysts.

In addition to isolated silanol groups all catalysts display a broad adsorption band in the 3700-3400  $\text{cm}^{-1}$  region. Usually broad absorption in this region is due to the stretching vibrations of H-bonded hydroxyl groups.<sup>26</sup> This underlying broad band in this region is more prominently present in Al-Zr-TUD-1 catalysts than it is in their monometallic counterparts. For Al-Zr-TUD-1 catalysts a shoulder at 3580  $\text{cm}^{-1}$  is clearly distinguishable.

The strong bridged hydroxyl groups (Brønsted acid site) at around 3613  $\text{cm}^{-1}$  as seen in zeolites could not be distinguished in any of the mesoporous TUD-1 samples with incorporated aluminium; which is typical for mesoporous materials as they possess lower Brønsted acidity.<sup>27</sup> Furthermore, due to their amorphous nature the presence of Brønsted acid sites is overshadowed by different H-bonded hydroxyl groups in the 3700-3400  $\text{cm}^{-1}$  region. However, the presence of Brønsted acid sites of zeolitic strength should not be excluded. In addition to catalytical experiments performed with amorphous aluminosilicates proving the existence of Brønsted acid sites of zeolitic strength, further spectroscopic evidence has been provided in a recent publication.<sup>28</sup> However, their density is much lower than that found in zeolites in the H-form.

## **2.2 Differentiation and changes in different Brønsted and Lewis acid sites using different basic probe molecules in FT-IR spectroscopy**

### *2.2.1 Pyridine FT-IR*

In order to differentiate between Brønsted and Lewis acid sites in the Al-Zr-TUD-1 catalysts, pyridine FT-IR was employed (Fig. 9). Pyridine is a more reliable probe molecule than ammonia since the IR absorption bands do not overlap. Moreover, ammonia decomposes even at rather low temperatures, when adsorbed onto catalysts.<sup>29</sup>

For the Al-TUD-1 sample the presence of Lewis acid sites is indicated by bands at 1455  $\text{cm}^{-1}$  (L1) and 1623  $\text{cm}^{-1}$ . However these bands are not symmetrical and show the

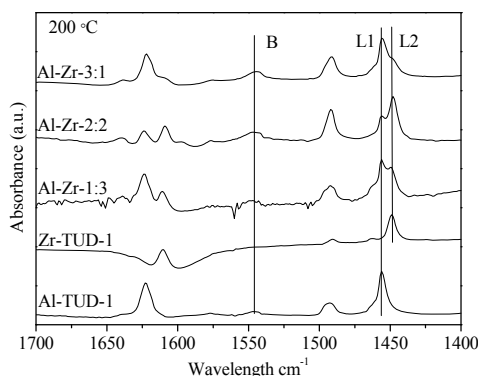


**Figure 9** FT-IR spectra after pyridine desorption at 200 °C of different TUD-1 catalysts with Si/M ratio of 25: Al-Zr-3:1, Al-Zr-2:2 Al-Zr-1:3, Zr-TUD-1 and Al-TUD-1. B stands for Brønsted acid site at 1545  $\text{cm}^{-1}$  and Lewis acid sites L1 (associated with aluminium) and L2 (associated with zirconium) at respectively 1455 and 1448  $\text{cm}^{-1}$ .

presence of other Lewis acid sites at 1460 and 1620  $\text{cm}^{-1}$ . The presence of these bands has already been reported for H-beta, other zeolites and silica-alumina.<sup>30</sup> The IR band at 1460  $\text{cm}^{-1}$  was assigned to iminium ions, formed by attack of protons on the pyridine complex bound to Lewis acid sites. Brønsted acidity is clearly present in Al-TUD-1 as indicated by the band at 1545  $\text{cm}^{-1}$  (B).

For Zr-TUD-1 the strength of the Lewis acid site at 1448  $\text{cm}^{-1}$  (L2) accompanied by a band at 1612  $\text{cm}^{-1}$  seems to be lower than is the case for Al-TUD-1. While for Al-TUD-1 temperatures above 400 °C are needed to desorb pyridine, for Zr-TUD-1 temperatures above 200 °C are already sufficient. Based on this we can conclude that Lewis acidity imparted by partial exchange of aluminium with zirconium generates weaker Lewis acid sites. Brønsted acid sites seem to be absent at outgassing temperatures of 200 °C which is line with earlier reports on the synthesis of Zr-TUD-1 leading to framework incorporation of tetravalent zirconium.<sup>15</sup>

Al-Zr-TUD-1 samples show the presence of all the bands present in Al-TUD-1 and Zr-TUD-1. Varying the Al/Zr ratio but keeping the Si/M ratio constant leads to variation of the ratio of different Lewis acid sites L1/L2. However, the relation between Lewis acid sites L1 and L2 in Al-Zr-TUD-1 samples does not follow the ratio between the different metals incorporated into the TUD-1 matrix.

The Lewis/Brønsted ratio in all three samples varies (Table 1). For the bimetallic samples containing large amounts of aluminium the Lewis/Brønsted ratio is smaller than that found in Al-TUD-1. However, the sample with the highest amount of zirconium incorporated, Al-Zr-1:3, has a larger Lewis/Brønsted ratio than Al-TUD-1, 3.21 compared to 2.41. Overall, five catalysts with varying B/L ratios are thus available.

### 2.2.2 CO FT-IR

CO is a weak base that adsorbs end on through the carbon on polarized sites.<sup>27</sup> In contrast to more basic ammonia and pyridine, CO is capable of differentiating between sites of very similar acid strength. Its small size, weak basicity, low reactivity (at low temperatures) and sensitivity make it ideal for investigation of samples with both Brønsted and Lewis acid sites.<sup>31</sup> Due to the similarities of the shifts of  $\nu_{\text{OH}}$  and  $\nu_{\text{CO}}$  modes of all Al-Zr-TUD-1's and monometallic TUD-1 catalysts only the Al-Zr-2:2 FT-IR spectra are discussed here (Fig. 10 and 11).

In the difference spectra of the  $\nu_{\text{OH}}$  mode of Al-Zr-2:2 at very low pressures of CO a broad band appears at  $3506\text{ cm}^{-1}$ , without development of a clear negative band. At such low pressures, CO will first interact with stronger acid sites as Brønsted acid sites and hydroxyl groups stronger than isolated silanol groups. The broadness of this band suggests heterogeneity of the sample. Even though no clear negative band has developed the red shift of this band ( $\Delta\nu_{\text{OH}}$ ) relative to isolated silanol groups is equal to  $240\text{ cm}^{-1}$ . This value lies between the  $\Delta\nu_{\text{OH}}$  for silanol groups ( $90\text{ cm}^{-1}$ ) and  $\Delta\nu_{\text{OH}}$  values for strong Brønsted acid sites found in zeolites ( $300\text{ cm}^{-1}$ ); implying the presence of medium strong Brønsted acid sites.<sup>32,33</sup> Isolated silanol groups at these low pressures are unperturbed and appear as a sharp peak at  $3750\text{ cm}^{-1}$ . Isolated Si-OH groups usually encountered at  $3746\text{ cm}^{-1}$  display a blue shift upon cooling to  $3750\text{ cm}^{-1}$ , a known temperature effect.<sup>27</sup>

With gradual increase of CO pressure the sharp band at  $3750\text{ cm}^{-1}$  associated with weak silanol groups gradually decreases and is accompanied by the development of a positive band at  $3660\text{ cm}^{-1}$  with a shoulder at  $3598\text{ cm}^{-1}$  once all isolated silanol groups are saturated. At the same time negative bands at  $3746$  and  $3741\text{ cm}^{-1}$  have developed with a shoulder at  $3716\text{ cm}^{-1}$ . The red shift of isolated silanol groups  $\Delta\nu_{\text{OH}}$  is equal to  $87\text{ cm}^{-1}$



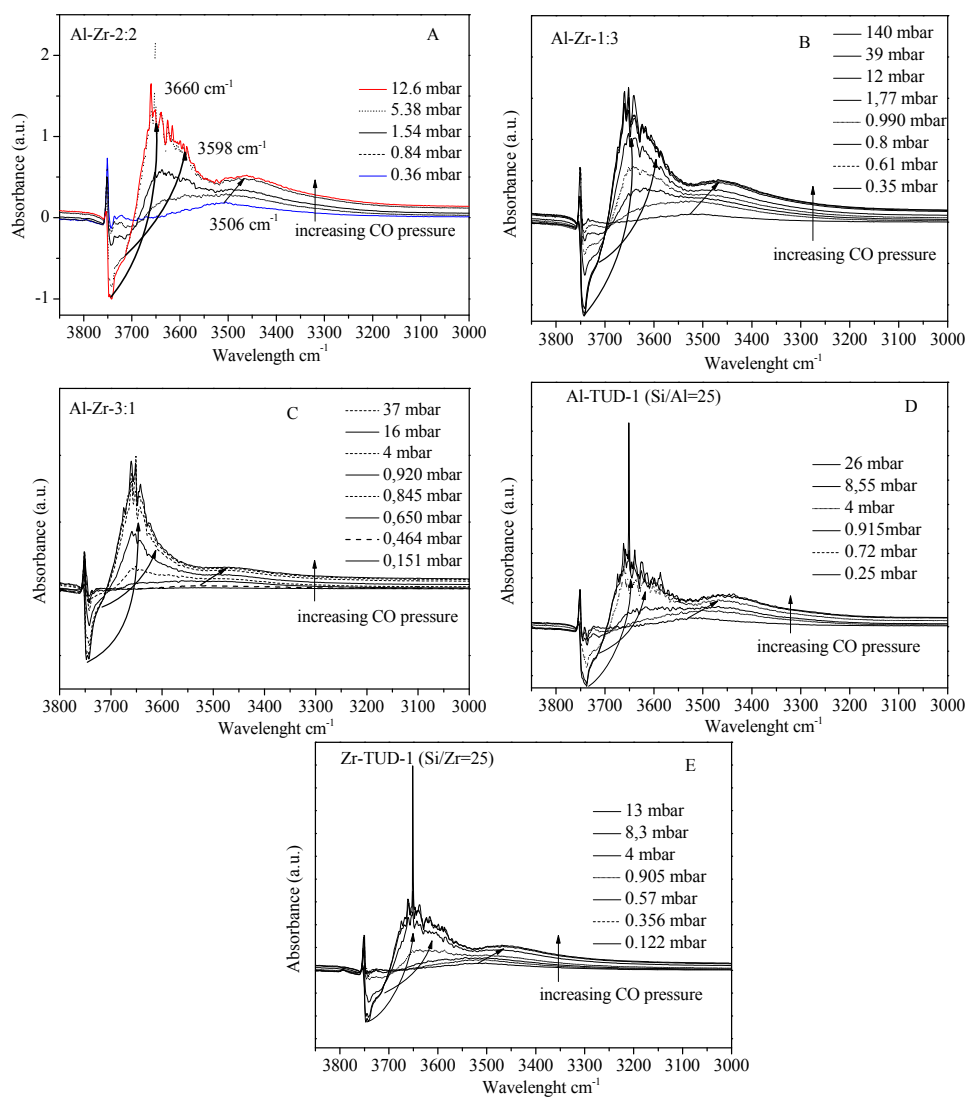


**Figure 10** FT-IR difference spectra of the  $\nu_{\text{OH}}$  region following CO adsorption obtained at 77 K of: (A) Al-Zr-2:2; (B) Al-Zr-1:3; (C) Al-Zr-3:1; (D) Al-TUD-1 and (E) Zr-TUD-1. The spectra are presented as difference plots: from the measured spectra after adsorption of CO, a spectrum of the corresponding pre-treated catalyst has been subtracted. A positive contribution represents peaks that are growing as a result of CO adsorption whereas negative contributions represent peaks that are reduced in intensity upon CO adsorption.

which is common for silanol groups.<sup>31, 32</sup> The broad band at  $3506\text{ cm}^{-1}$  associated with Brønsted acid sites and strong hydroxyl groups have in the mean time undergone a red shift to  $3468\text{ cm}^{-1}$  due to the solvent effect.<sup>34</sup> The very sharp peak developed at  $3650\text{ cm}^{-1}$  at high CO pressure is related to the measuring equipment.

The accompanied  $\nu_{\text{CO}}$  mode at low pressure of CO shows two bands appearing at  $2229\text{ cm}^{-1}$  and  $2196\text{ cm}^{-1}$ , the latter band having much higher intensity. The blue shift of CO ( $\Delta\nu_{\text{CO}}$ ) relative to the free molecule ( $\nu_{\text{CO}}$  liquid is  $2138\text{ cm}^{-1}$ ) is  $91\text{ cm}^{-1}$  for the band at  $2229\text{ cm}^{-1}$  which is usually associated with strong Lewis acid sites related to highly coordinatively unsaturated extra framework  $\text{Al}^{3+}$ .<sup>35,36</sup> The low intensity of this band indicates that the amount of extra framework Al species is quite low. The band at  $2196\text{ cm}^{-1}$  having much higher intensity is associated with CO adsorbed on  $\text{Zr}^{4+}$  Lewis acid sites, based on CO FT-IR measurements on Zr-TUD-1 and literature values.<sup>37,38</sup> Lewis acid sites related to  $\text{Zr}^{4+}$  with a lower frequency shift ( $\Delta\nu_{\text{CO}} = 58\text{ cm}^{-1}$ ) are weaker than Lewis acid sites associated with extra framework  $\text{Al}^{3+}$ . This reconfirms the results of the pyridine FT-IR.

With the increase of CO pressure additional bands become evident. Between the high intensity band at  $2159\text{ cm}^{-1}$  (generally associated to CO adsorbing to silanol groups) and  $2191\text{ cm}^{-1}$  band (shifted due to solvent effect) a new band appears at  $2177\text{ cm}^{-1}$  that can be assigned to Brønsted acid sites according to CO FT-IR measurements performed on Al-TUD-1 and literature values.<sup>39,40</sup>

With further increase of CO pressure, bands associated with liquid like CO at  $2138\text{ cm}^{-1}$  develop. A very weak band at  $2110\text{ cm}^{-1}$  is present as well and has been explained by CO interacting with pairs of ions through oxygen ends.<sup>35</sup>

Substantial shifts in the position of Brønsted acid sites in different Al-Zr-TUD-1 catalysts have not been observed as would be expected if synergistic interaction between Lewis and Brønsted acid sites were present (Table 4).

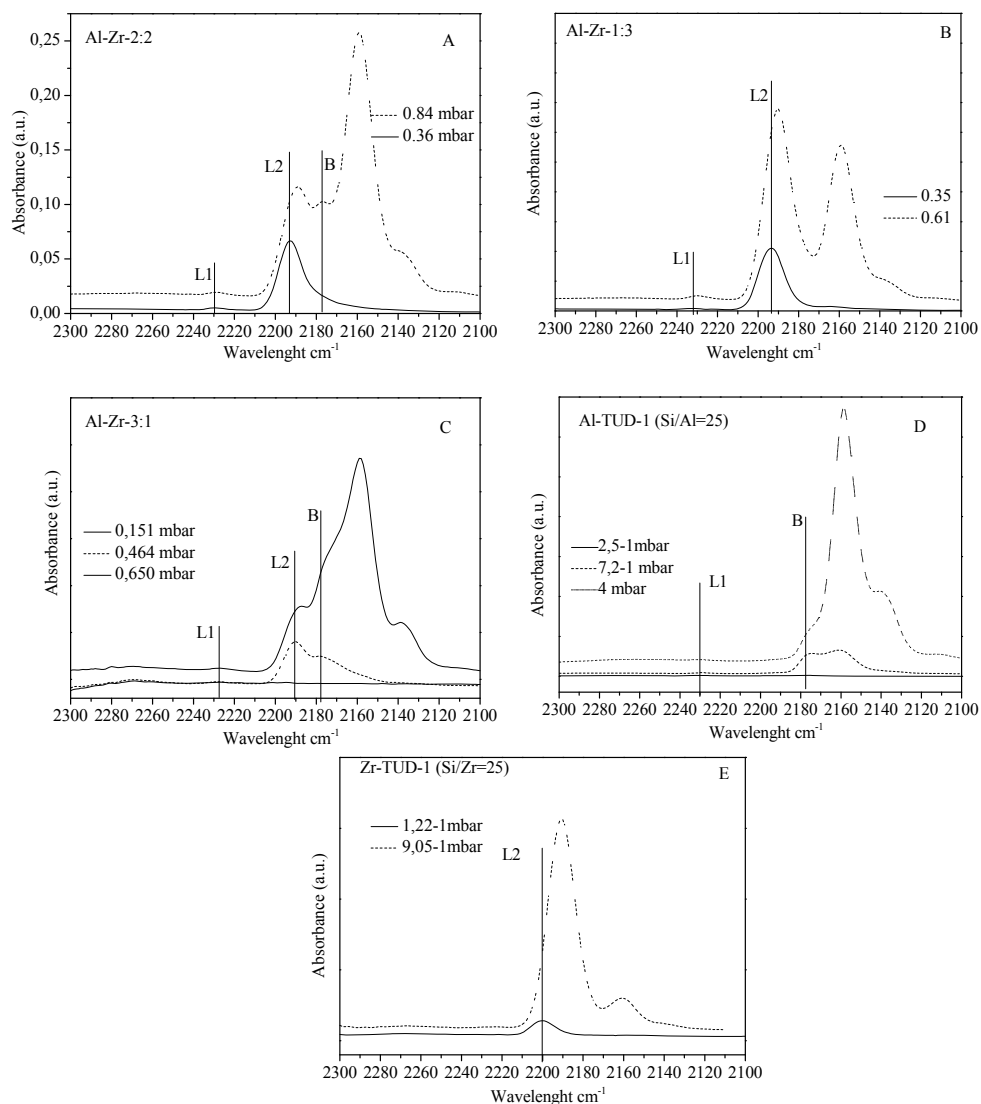


**Figure 11** FT-IR difference spectra of the  $\nu_{(\text{CO})}$  region following CO adsorption obtained at 77 K of: (A) Al-Zr-2:2; (B) Al-Zr-1:3; (C) Al-Zr-3:1; (D) Al-TUD-1 and (E) Zr-TUD-1. The spectra are presented as difference plots: from the measured spectra after adsorption of CO, a spectrum of the corresponding pre-treated catalyst has been subtracted. A positive contribution represents peaks that are growing as a result of CO adsorption whereas negative contributions represent peaks that are reduced in intensity upon CO adsorption. Regions of Brønsted acid sites are marked by capital letter B while Lewis acid sites corresponding to different metals are marked by capital letters L1 for aluminium and L2 for zirconium.

**Table 4** Summary of the FT-IR data on the TUD-1 materials:  $\nu_{\text{OH}}$  and  $\nu_{\text{CO}}$  modes upon CO adsorption at 77 K for Zr-TUD-1, Al-Zr-3:1, Al-Zr-2:2, Al-Zr-1:3 and Al-TUD-1.

	$\nu_{\text{OH}} (\text{cm}^{-1})^a$	$\Delta\nu_{\text{OH}} (\text{cm}^{-1})^a$	$\nu_{\text{CO}} (\text{cm}^{-1})$ Al <sup>3+</sup>	$\nu_{\text{CO}} (\text{cm}^{-1})$ Zr <sup>4+</sup>	$\nu_{\text{CO}} (\text{cm}^{-1})$ Si-OH-Al
Zr-TUD-1	3514	233	-	2200	-
Al-Zr-3:1	3524	223	2227	2190	2177
Al-Zr-2:2	3506	241	2229	2193	2177
Al-Zr-1:3	3525	222	2232	2193	-
Al-TUD-1	3506	241	2230	-	2177

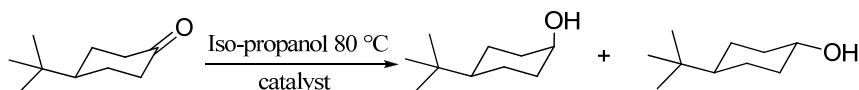
<sup>a</sup>  $\nu_{\text{OH}}$  mode of a broad band appearing at low CO pressure in the difference spectra.

Overall extensive spectroscopic investigation of the surface of different Al-Zr-TUD-1 catalysts based on pyridine FT-IR led to the conclusion that partial exchange of aluminium by zirconium in Al-TUD-1 leads to different proportions of Lewis and Brønsted acid sites but not necessarily to the increase of their strength according to CO FT-IR.

### 2.3 Performance of Al-Zr-TUD-1 as a catalyst

The best way to probe whether synergy between Lewis and Brønsted acid sites in Al-Zr-TUD-1 catalysts exists is to employ them in different Lewis and/or Brønsted acid catalyzed reactions. In that way the presence of different kinds of acid sites or increase in their strength or amount due to mutual incorporation of aluminium and zirconium in the TUD-1 matrix should reflect itself in increased catalytic activity: synergy. For that reason the catalysts were tested in the Lewis acid catalyzed Meerwein-Ponndorf-Verley (MPV) reduction and the C-C bond formation reactions via Prins reaction. This reaction is catalysed both by Lewis and Brønsted acids and it was performed intermolecularly (Nopol synthesis) and intramolecularly (Isopulegol synthesis).

From the study of different Al-Zr-TUD-1 catalysts in the Meerwein-Ponndorf-Verley (MPV) reduction of 4-*tert*-butylcyclohexanone (Scheme 1), it is clear that the

**Scheme 1** Meerwein-Ponndorf-Verley reduction of 4-*tert*-butylcyclohexanone with 2-propanol.

increase in amount of zirconium present in the catalysts leads to an increase of conversion (Fig. 12). Using aluminium rich Al-Zr-3:1 30 % conversion was obtained after 24 h compared to 64 % obtained with the Zr rich catalyst, Al-Zr-1:3. The more zirconium present the more active the catalyst in this Lewis acid catalyzed reaction. Comparison of

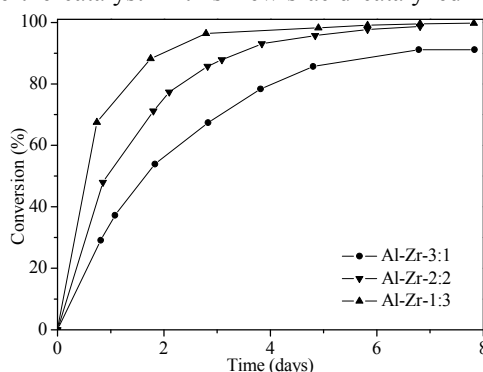


**Figure 12** Reduction of 2 mmol 4-*tert*-butylcyclohexanone in 4 mL 2-propanol at 80 °C in the presence of 0.1 mL 1,3,5-triisopropylbenzene as internal standard, using 50 mg of different bimetallic catalysts with Si/M ratio of 25: Al-Zr-3:1, Al-Zr-2:2 and Al-Zr-1:3.

Al-Zr-2:2 with monometallic Al-TUD-1 and Zr-TUD-1 and their physical mixtures (Fig. 13) however demonstrates absence of synergy between Lewis and Brønsted acid sites in the

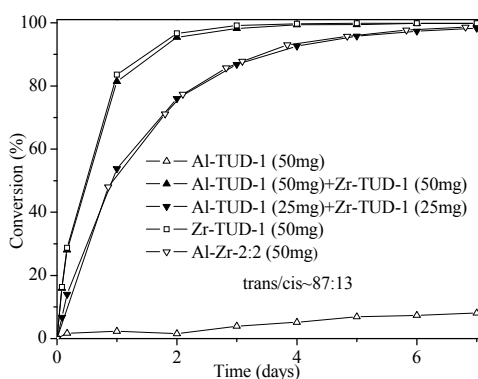
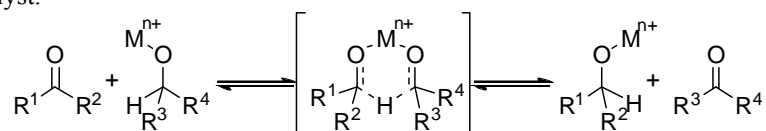


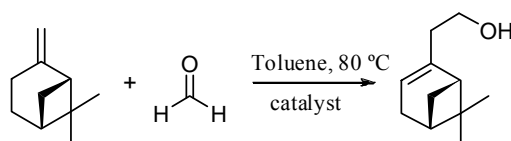
**Figure 13** Comparison of bimetallic Al-Zr-2:2 catalyst with Al-TUD-1 and Zr-TUD-1 and their physical mixture in reduction of 2 mmol 4-*tert*-butylcyclohexanone in 4 mL 2-propanol at 80 °C in the presence of 0.1 mL 1,3,5-triisopropylbenzene as internal standard, using different amounts of activated catalysts. In all reactions the ratio *trans*:*cis* 4-*tert*-butylcyclohexanol was always around 87:13.

Lewis acid catalyzed MPV reduction of 4-*tert*-butylcyclohexanone, the physical mixture showed the same catalytic behaviour as the bimetallic catalyst. Meerwein-Ponndorf-Verley reduction is catalyzed by coordination of an alcohol and ketone or an aldehyde to the Lewis acid site forming a six-membered transition state enabling a carbon-to-carbon hydride transfer (Scheme 2).<sup>15,41,42,43</sup> The more Lewis acid sites a catalyst possesses the more active is the catalyst.



**Scheme 2** Mechanism of the Meerwein-Ponndorf-Verley reduction.

In the nopol synthesis (Scheme 3), a Brønsted and Lewis acid catalyzed Prins reaction, no synergy was observed, either. While all of the catalysts were active in the conversion of  $\beta$ -



**Scheme 3** Intermolecular Prins nopol synthesis from  $\beta$ -pinene and paraformaldehyde in toluene at temperature of 80 °C.

pinene, the yield of nopol was low (Fig. 14). Al-TUD-1 and Al-Zr-3:1-TUD-1 had the highest activity (full conversion of  $\beta$ -pinene within 1 h). The highest selectivity towards nopol was around 30 % obtained after 1 h reaction time with Zr-TUD-1 (Fig. 14). An increase of reaction time led to product degradation. The major side products in nopol synthesis were, according to GC-MS analysis, isomerization products such as limonene, camphene and terpinolene.

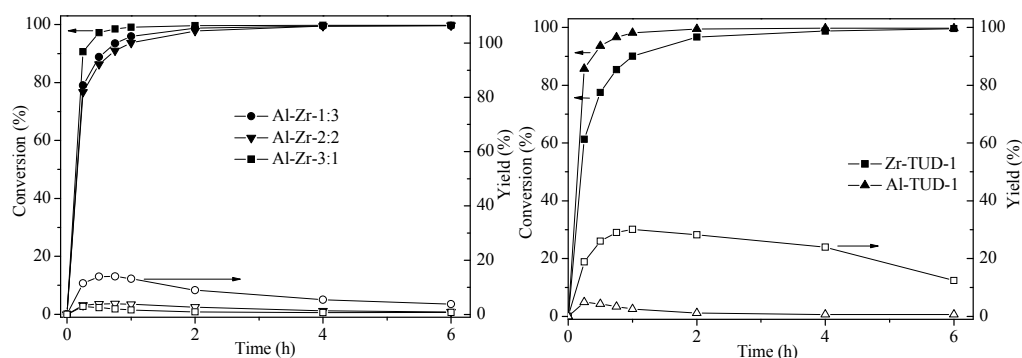
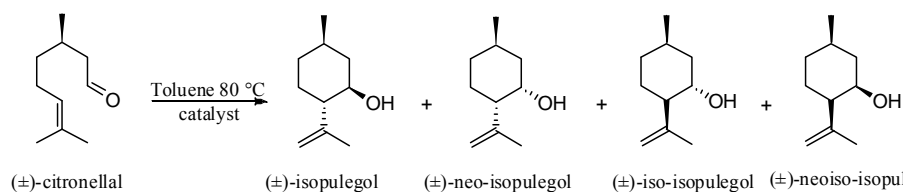


**Figure 14** Nopol Synthesis performed in 4 mL toluene at 80 °C using 2 mmol paraformaldehyde, 1,3,5-triisopropylbenzene as internal standard, 1 mmol  $\beta$ -pinene and 50 mg of activated catalyst. Left figure: results obtained with bimetallic catalysts Al-Zr-1:3, Al-Zr-2:2 and Al-Zr-3:1. Right figure: results obtained with monometallic catalysts Zr-TUD-1 and Al-TUD-1.

However, excellent results were obtained in Prins cyclisation of ( $\pm$ )-citronellal (Scheme 4). All three samples of Al-Zr-TUD-1 catalysts outperformed their monometallic counterparts Al-TUD-1 and Zr-TUD-1 (Fig. 15). This, despite of the fact that both Al-TUD-1 and Zr-TUD-1 possess larger amounts of acid sites according to  $\text{NH}_3$ -TPD. Aluminium rich Al-Zr-TUD-1 catalysts led to high initial rates but full conversions are not



**Scheme 4** Intramolecular Prins cyclisation of citronellal in toluene at 80 °C.

reached, this also holds for the catalyst containing the smallest amount of aluminium, Al-Zr-1:3. Selectivity in all cases was above 95% and major isomers obtained were ( $\pm$ )-isopulegol and ( $\pm$ )-neo-isopulegol.

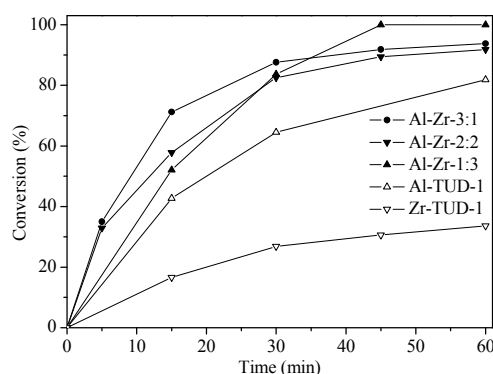
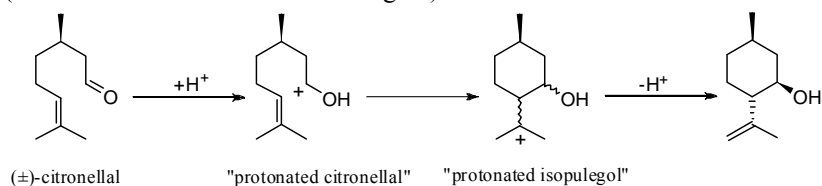


**Figure 15** Intramolecular Prins cyclisation of 4 mmol (±)-citronellal in 5 g of toluene at 80 °C using 50 mg of different TUD-1 catalysts with Si/M ratio of 25: Al-Zr-3:1, Al-Zr-2:2 Al-Zr-1:3, Al-TUD-1 and Zr-TUD-1.

Both types of Prins reactions, intramolecular citronellal cyclisation and intermolecular Nopol synthesis can be catalyzed by Brønsted and/or Lewis acid sites. Exclusively Brønsted acid catalysts catalyze the Prins cyclisation via formation of carbenium ion intermediates (Scheme 5).<sup>44</sup> In the Prins cyclisation of citronellal via intramolecular reaction a more stable tertiary carbocation is formed. Clearly intramolecular reaction will more readily occur than intermolecular reaction as is the case in Nopol synthesis where the availability of the reacting alkene group at the rather hydrophilic surface (based on the FTIR results in Fig. 8) is lower. This difference is even more

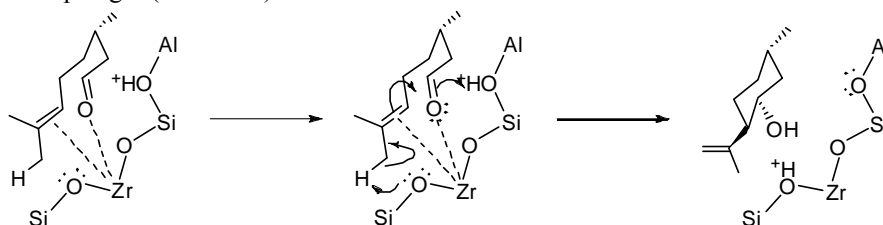


**Scheme 5** The Brønsted acid-catalyzed Prins cyclization of citronellal.

enhanced for catalysts containing both Brønsted and Lewis acid sites. Due to activation of both reacting groups, the alkene and the carbonyl group, by Lewis acid sites and the presence of Brønsted acid sites in close proximity, the rate of the reaction is further enhanced as is the case with bimetallic Al-Zr-TUD-1's in the Prins cyclisation of citronellal. It was already proposed earlier that the desired heterogeneous catalysts for the cyclisation of citronellal should have strong Lewis and weak Brønsted acid sites.<sup>45</sup> It is



believed that citronellal coordinates in an orientation favourable for ring closure where both the oxygen of the aldehyde group as the electron rich double bond are attached to Lewis acid sites in this case zirconium. In the transition state, protonation of the oxygen atom occurs via neighbouring Brønsted hydroxyl group from the surface of the support.<sup>45,46,47</sup> Subsequently, hydrogen is abstracted from the isopropyl group and the ring is closed to form isopulegol (Scheme 6).



**Scheme 6** The Brønsted-Lewis acid-catalyzed Prins cyclization of citronellal, a new carbon-carbon bond is formed between an alkene and an aldehyde.

Based on these results we can conclude that synergy in Al-Zr-TUD-1 obtained in the Prins cyclisation of citronellal is much more complex and more subtle than can be explained by increase of Brønsted acidity due to incorporation of a different Lewis acid. All three samples of Al-Zr-TUD-1 show synergistic properties in the Prins cyclisation of citronellal, even though the proportions of Lewis acid sites to Brønsted acid sites are different according to pyridine FT-IR. The sample Al-Zr-1:3 having predominantly Lewis acidic character has a lower initial rate than more aluminium rich Al-Zr-TUD-1 catalysts, but eventually reaches full conversion first. Demonstration of synergy could not be repeated for other C-C bond formation reactions. A possible explanation could be that in many of the heterogeneously catalyzed reactions, the match between the strength of acid sites and substrates plays an important role. In another study, even though not explicitly mentioned as synergy, a similar observation was made for the same intramolecular Prins reaction. By varying the F : OH ratio during synthesis of nanoscopic magnesium fluorides unexpected catalytic properties were obtained in the Prins cyclisation of citronellal.<sup>48</sup> In that study it was also spectroscopically proven that the different combinations and variable strength of Lewis and Brønsted acid sites are responsible for increased activity.

Another very important difference between Prins cyclisation and nopol synthesis is the difference between intramolecular and intermolecular reaction. Intramolecular

reactions generally proceed much more rapidly and under much milder reaction conditions than their intermolecular counterparts, since the two reacting groups are already in close proximity to one another. Indeed, this is one of the underlying reasons for the great catalytic power of enzymes.<sup>49,50</sup>

### 3. Conclusions

Al-Zr-TUD-1, a three-dimensional mesoporous material containing varying amounts of aluminium and zirconium was synthesized using triethanolamine as complexing agent. Framework incorporation of Al and Zr is evidenced by the absence of  $\text{Al}_2\text{O}_3$  or  $\text{ZrO}_2$  phases, as proven by XRD, HR-TEM and XPS studies. Extensive FT-IR analysis using pyridine and CO as probe molecule did not allow identifying synergistic properties due to incorporation of zirconium as a Lewis acid in addition to aluminium generating both Lewis and Brønsted acidity.

The search for synergistic properties was therefore performed with catalytic experiments. Synergy was not encountered when Al-Zr-TUD-1 catalysts were applied in Lewis acid catalyzed Meerwein-Ponndorf-Verley reduction of 4-*tert*-butylcyclohexanone or the intermolecular Prins nopol synthesis. However, synergistic properties of Al-Zr-TUD-1 catalysts were clearly evidenced in the Prins cyclisation of citronellal due to proximity effects of reacting groups in this intramolecular reaction. Along with the excellent properties of TUD-1 type materials allowing framework incorporation of different metals as well as a systematic variation of two metals rather than merely increasing the weight percentage of one metal while keeping the weight percentage of the second constant. While we do not have yet the right spectroscopic technique in combination with probe molecules to discriminate between the sites so to identify synergistic effects, catalytic reactions can pinpoint to synergistic properties. However, it is only possible for specific reactions, such as the Prins cyclisation of citronellal. In another type of Prins reaction (Nopol synthesis) synergistic effect could not be observed due to the intermolecular nature of the reaction and hydrophilic surface of the catalyst. In other words, synergistic effects seem to be reaction mechanism dependent.

## 4. Experimental Section

### 4.1 Materials synthesis

Monometallic Al-TUD-1 and Zr-TUD-1 were synthesized according to previous reports and were described earlier in full detail.<sup>15,16</sup> Al-Zr-TUD-1's were synthesized using triethanolamine (TEA,  $\geq 99.0\%$ , Fluka) as a complexing agent in a one pot surfactant-free procedure based on the sol-gel technique. Al-Zr-TUD-1's with constant Si/(Al+Zr) molar ratio of 25 with varying Al : Zr ratios were synthesized by adjusting the molar ratio of  $\text{SiO}_2$  :  $x \text{ Al}_2\text{O}_3$  :  $y \text{ ZrO}_2$  : tetraethylammonium hydroxide (TEAOH) : (0.5–1) TEA : (10–20)  $\text{H}_2\text{O}$ . In a typical synthesis (Al : Zr = 1 : 3), 0.51 g of aluminum(III) isopropoxide (98 +%, Aldrich) and 0.32 g zirconium(IV) propoxide solution (70 wt% in 1-propanol, Aldrich) dissolved in a 1:1 mixture of isopropanol (HPLC grade, Fisher Chemicals, 0.013 %  $\text{H}_2\text{O}$ ) and absolute ethanol (J. T. Baker, 0.2 %  $\text{H}_2\text{O}$ ) was added to 17.3 g of tetraethyl orthosilicate (98 %, Aldrich). After stirring for a few minutes, a mixture of 12.5 g of TEA ( $\geq 99.0\%$ , Fluka) and 9.4 g of water was added, followed by addition of 10.2 g of TEAOH (35 wt% in  $\text{H}_2\text{O}$ , Aldrich) under vigorous stirring. The clear gel obtained after these steps was then aged at room temperature for 12–24 h and dried at 98 °C for 12–24 h, followed by hydrothermal treatment in a Teflon-lined autoclave at 180 °C for 4–24 h and final calcination in the presence of air up to 600 °C with a temperature ramp of 1 °C  $\text{min}^{-1}$ . Al-Zr-TUD-1 samples with constant Si/(Al+Zr) ratio of 25 and varying Al : Zr ratio of 3, 1 and 0.33 were prepared and are denoted as Al-Zr-3:1, Al-Zr-2:2 and Al-Zr-1:3, respectively.

### 4.2 Materials Characterization

Chemical analysis of Si, Al and Zr were performed in duplet by dissolving the samples in 1 % HF (48 % in  $\text{H}_2\text{O}$ , 99.99 +% based on metal basis, Aldrich) and 1.25 %  $\text{H}_2\text{SO}_4$  (99.999 %, Aldrich) solution and measuring them with Inductively Coupled Plasma – Optical Emission Spectroscopy (ICP-OES) on a Perkin Elmer Optima 3000DV instrument. The textural properties of the materials were characterized by volumetric  $\text{N}_2$  physisorption at 77 K using Micromeritics ASAP 2010 equipment. Prior to the physisorption experiment, the

samples were dried overnight at 573 K ( $p \leq 10^{-2}$  Pa). From the nitrogen sorption isotherms, the specific surface area  $S_{\text{BET}}$ , the pore diameter  $dP_{\text{BJH}}$  and the pore volume  $VP_{\text{BJH}}$  were calculated.

High-resolution transmission electron microscopy (HR-TEM) was performed on a Philips CM30UT electron microscope with a LaB6 filament as the source of electrons operated at 300 kV. Samples were mounted on Quantifoil® carbon polymer supported on a copper grid by placing a few droplets of a suspension of ground sample in ethanol on the grid, followed by drying at ambient conditions.

Powder X-ray diffraction (XRD) patterns were obtained on a Philips PW 1840 diffractometer equipped with a graphite monochromator using  $\text{Cu}_{K\alpha}$  radiation.

$^{27}\text{Al}$  MAS NMR experiments were performed at 9.4 T on a Varian VXR-400 S spectrometer operating at 104.2 MHz with a pulse width of 1 ms. 4-mm zirconia rotors with a spinning speed set to 6 kHz were used. The chemical shifts are reported with respect to  $\text{Al}(\text{NO}_3)_3$  as external standard at  $\delta = 0$  ppm.

The XPS measurements were performed with a PHI 5400 ESCA provided with a dual Mg/Al anode X-ray source, a hemispherical capacitor analyser and a 5 keV ion-gun. Powdered catalyst samples were pressed into clean indium foil (Alfa Products, purity 99,9975%) with a thickness of 0.5 mm and subsequently placed on a flat specimen holder. The input lens optical axis to the analyser was at a take off angle of  $15^\circ$  with respect to the sample surface normal. The input lens aperture used was  $3.5 \times 1.0$  mm. All spectra were recorded with non-monochromated magnesium radiation. The X-ray source was operated at an acceleration voltage of 13 keV and a power of 200 W. A survey spectrum was recorded between 0 and 1000 eV binding energy using pass energy of 71.95 eV and step size of 0.25 eV. The spectra of the separate photoelectron and Si-Auger lines were recorded with pass energy of 35.75 eV and step size of 0.2 eV. The Zr-Auger electron line was recorded with pass energy of 89.45 eV and step size of 0.5 eV. The spectra were evaluated with Multipak 8.0 software (Physical electronics). Firstly, the satellite photoelectron lines were subtracted from the spectrum. Next the energy scale was aligned adopting a value of  $103.5 \pm 0.2$  eV for the binding energy of the Si  $2p$  photoelectron line present in the Si-TUD-1 carrier implying a binding energy of  $532.9 \pm 0.2$  eV for the O  $1s$  line.<sup>19</sup> Then, the background intensity was subtracted from the spectra using a Shirley method.<sup>51</sup> Afterwards, the spectra were fitted with (symmetrical) mixed Gauss-Lorentz functions using the linear least square

method to resolve the chemical states of the constituting components. The peaks describing sample Si-TUD-1 were kept fixed during the deconvolution of the Al and Zr loaded catalysts.

Temperature-programmed desorption (TPD) of ammonia was carried out on a Micromeritics TPR/TPD 2900 equipped with a Thermal Conductivity Detector (TCD). The sample (30 mg) was pre-treated at 823 K to remove volatile components. Prior to the TPD measurements the samples were saturated with ammonia gas at 393 K. This procedure was repeated three times. The measurements were only started when as much as possible physisorbed  $\text{NH}_3$  was removed. Desorption of  $\text{NH}_3$  was monitored in the range between 393 and 823 K at a ramp rate of  $10 \text{ K min}^{-1}$ .

Skeletal FTIR spectra were measured in the  $1500 - 600 \text{ cm}^{-1}$  region. FTIR spectra of KBr diluted wafers of samples were recorded using a Perkin Elmer Spectrum One instrument. In total 19 scans were taken with a resolution of  $4 \text{ cm}^{-1}$ .

FT-IR spectra of the OH region were measured in the  $3900\text{-}3000 \text{ cm}^{-1}$  region. FTIR spectra of self-supported wafers were recorded with a Thermo Nicolet FT-IR Nexus instrument. Self-supported wafers were pre-treated at  $500^\circ\text{C}$  in three-window cells ( $\text{CaF}_2$ ) under a flow of He. In total 128 scans were taken with resolution of  $4 \text{ cm}^{-1}$ .

A Perkin Elmer 2000 FT-IR instrument was used to record FT-IR spectra after pyridine desorption at various temperatures. Self supported catalyst wafers ( $18\text{-}25 \text{ mg}/16 \text{ mm}$ ) were pressed at 3 bar pressure applied for 10 s. The wafer was placed inside a glass cell with KBr windows and subsequently evacuated to  $10^{-6}$  bar followed by drying at  $300^\circ\text{C}$  ( $3^\circ\text{C min}^{-1}$ ) for 1 h. The cell was cooled down to room temperature and the IR spectrum was collected. Then the temperature of the cell was raised to  $50^\circ\text{C}$  and the sample was brought into contact with pyridine vapour (3.1 mbar) for 10 min. Afterwards by applying vacuum for 30 min physisorbed and loosely bound pyridine was removed. FT-IR spectra were recorded under vacuum under various conditions by increasing the temperature ( $3^\circ\text{C min}^{-1}$ ) from  $50$  to  $450^\circ\text{C}$ . For each spectrum 25 scans were recorded with resolution of  $4 \text{ cm}^{-1}$ .

$\text{CO}$  adsorption experiments were performed with Perkin Elmer 2000 FTIR instrument. Self supporting wafers were prepared by applying 3 bar pressure for 10 s. The wafers were placed in a stainless steel IR transmission cell ( $12\text{-}17 \text{ mg}/13 \text{ mm}$ ) equipped with  $\text{CaF}_2$  windows. The cell was evacuated at  $10^{-8}$  bar followed by drying at  $300^\circ\text{C}$  (ramp

rate  $3\text{ }^{\circ}\text{C min}^{-1}$ ) for 1 h. Subsequently the wafers were cooled down to 77 K with liquid  $\text{N}_2$ . A background spectrum was taken prior to CO exposure. CO was introduced as 10% CO in He (Linde gas) (0.1 mbar to 30 mbar) at 77 K. For each spectrum 25 scans were recorded with a resolution of  $4\text{ cm}^{-1}$ .

### 4.3 Materials testing

#### 4.3.1 Meerwein-Ponndorf-Verley reduction of 4-tert-butylcyclohexanone

The catalytic experiments were performed in dried glassware using Schlenk techniques. The anhydrous solvents were used as received.

For the Meerwein-Ponndorf-Verley reductions 2 mmol of 4-tert-butylcyclohexanone (99 %, Aldrich), 4 mL of 2-propanol (99.5 %, Aldrich) and 0.1 mL of 1,3,5-triisopropylbenzene (96 %, Aldrich, internal standard) were loaded in the Schlenk flask containing 50 mg of activated Al-Zr-TUD-1 catalyst ( $600\text{ }^{\circ}\text{C}$ , 10 h,  $1\text{ }^{\circ}\text{C min}^{-1}$ ). The reaction flask was immersed into a preheated oil bath at  $80\text{ }^{\circ}\text{C}$ . Periodically samples were withdrawn (20  $\mu\text{L}$ ) and analyzed on a GC (Shimadzu GC-17A gas chromatograph) equipped with a 25 m x 0.32 mm x 0.25  $\mu\text{m}$  chiral column Chrompack<sup>TM</sup> Chirasil-Dex CB and a FID detector. The reactants and products were identified by comparison with the retention times of authentic samples and additionally by NMR as described earlier.<sup>15</sup> Employing an isotherm ( $120\text{ }^{\circ}\text{C}$ ) following retention times were recorded: 1,3,5-triisopropylbenzene (3.86 min), 4-tert-butylcyclohexanone (4.86 min), cis-4-tert-butylcyclohexanol (5.4 min) and trans-4-tert-butylcyclohexanol (5.8 min).

#### 4.3.2 Intermolecular Nopol synthesis employing paraformaldehyde and $\beta$ -pinene

In the intermolecular Nopol synthesis catalysts (50 mg) were dried at  $120\text{ }^{\circ}\text{C}$  under vacuum for 1 h. To the dried catalyst materials paraformaldehyde (2 mmol, 0.07 g, 95 %, Merck) was added followed by dry toluene (4 mL, 99.8 %, Aldrich) and 1,3,5-triisopropylbenzene (0.5 mmol, 0.10 g, 96 %, Aldrich) as internal standard. Finally,  $\beta$ -pinene (1 mmol, 0.14 g, 99 %, Aldrich) was added. The reaction was started by submerging the reaction mixture into a preheated oil bath at  $80\text{ }^{\circ}\text{C}$ . Samples (20  $\mu\text{L}$ ) were analyzed by GC (Shimadzu GC-

2014 gas chromatograph) equipped with a 50 m x 0.53 mm x 1.0  $\mu$ m CP-Sil 5CB column and using a FID detector. Employing an isotherm (110 °C) following retention times were recorded:  $\beta$ -pinene (2.01 min), nopol (7.24 min) and 1,3,5-triisopropylbenzene (10.40 min).

#### *4.3.3 The intramolecular Prins cyclisation of ( $\pm$ )-citronellal*

The intramolecular Prins reaction was performed as reported earlier. [46] The catalysts were dried at 100 °C overnight. To 50 mg of catalyst 4 mmol ( $\pm$ )-citronellal ( $\geq$  95.0 %, Aldrich) and 5 g of solvent, toluene (99.8 %, Aldrich) or *tert*-butanol ( $\geq$ 99.5 %, Aldrich), were added. The reactions were performed at 80 °C or at room temperature. Samples were withdrawn periodically and analyzed by GC (Agilent's HP5 column). The different isomers were identified by  $^1\text{H}$  NMR.

#### **Acknowledgements**

We thank A. Ramanathan for providing samples of Al-Zr-TUD-1.

## 5. References

- 1 C. Mirodatos, D. Barthomeuf, *J. Chem. Soc. Chem. Commun.* **1981**, 2, 39-40.
- 2 S. Li, A. Zheng, Y. Su, H. Zhang, L. Chen, J. Yang, C. Ye, F. Deng, *J. Am. Chem. Soc.* **2007**, 129, 11161-11171.
- 3 S. Selvakumar, N. M. Gupta, A. P. Singh, *Appl. Catal. A: Gen.* **2010**, 372, 130-137.
- 4 G. B. Han, N-K. Park, S. H. Yoon, T. J. Lee, K. L. Yoon, *Appl. Catal. A: Gen.* **2008**, 337, 29-38.
- 5 Y. Sekine, H. Takamatsu, S. Aramaki, K. Ichishima, M. Takada, M. Matsukata; E. Kikuchi, *Appl. Catal. A: Gen.* **2009**, 352, 214-222.
- 6 F. Mariño, G. Baronetti, M. Laborde, N. Bion, A. Le Valant, F. Epron, D. Duprez, *Int. J. Hydrogen Energy* **2008**, 33, 1345-1353.
- 7 A. Kale, N. Bazzanella, R. Checchetto, A. Miotello, *Appl. Phys. Lett.* **2009**, 94, 204103-1-3.
- 8 G. Carja, G. Delahay, C. Signorile, B. Coq, *Chem. Commun.* **2004**, 1404-1405.
- 9 M. Selvaraj, A. Pandurangan, K. S. Seshadri, P. K. Sinha, K. B. Lal, *Appl. Catal. A: Gen.* **2003**, 242, 347-364.
- 10 P. Kalita, N. M. Gupta, R. Kumar, *J. Catal.* **2007**, 245, 338-347.
- 11 J. C. Jansen, Z. Shan, L. Marchese, W. Zhou, N. v. d. Puil, T. Maschmeyer, *Chem. Commun.* **2001**, 713-714.
- 12 S. Telalović, A. Ramanathan, G. Mul, U. Hanefeld, *J. Mater. Chem.* **2010**, 20, 642-658.
- 13 Z. Shan, E. Gianotti, J. C. Jansen, J. A. Peters, L. Marchese, T. Maschmeyer, *Chem. Eur. J.* **2001**, 7, 1437-1443.
- 14 R. Anand, M. S. Hamdy, U. Hanefeld, T. Maschmeyer, *Catal. Lett.* **2004**, 95, 113-117.
- 15 A. Ramanathan, M. C. C. Villalobos, C. Kwakernaak, S. Telalović, U. Hanefeld, *Chem. Eur. J.* **2008**, 14, 961-972.
- 16 R. Anand, R. Maheswari, U. Hanefeld, *J. Catal.* **2006**, 242, 82-91.
- 17 S. Telalović, J. F. Ng, R. Maheswari, A. Ramanathan, G. K. Chuah, U. Hanefeld, *Chem. Commun.* **2008**, 38, 4631-4633.
- 18 B. Rakshe, V. Ramaswamy, A.V. Ramaswamy, *J. Catal.* **1999**, 188, 252-260.
- 19 C. D. Wagner, A. V. Naumkin, A. Kraut-Vass, J. W. Allison, C. J. Powell, J. R. Jr. Rumble, NIST X-ray Photoelectron Spectroscopy Database, Version 3.5 (Web Version, 2007) (<http://srdata.nist.gov/xps/>)
- 21 A. Infantes-Molina, J. Mérida-Robles, P. Mairales-Torres, E. Finocchio, G. Busca, E. Rodríguez-Castellón, J. L. G. Fierro, A. Jiménez-López, *Microporous Mesoporous Mater.* **2004**, 75, 23-32.



- 22 G. B. Rayner, D. Kang, Y. Zhang, G. Lucovsky, *J. Vac. Sci. Technol. B* **2002**, 20, 1748-1758.
- 23 M. S. Morey, G. D. Stucky, S. Schwarz, M. Fröba, *J. Phys. Chem. B* **1999**, 103, 2037-2041.
- 24 M. A. Cambor, A. Corma, J. Perez-Pariente, *J. Chem. Soc. Chem. Commun.* **1993**, 557-559.
- 25 J. El Haskouri, S. Cabrera, C. Guillem, J. Latorre, A. Beltran, D. Beltran, M. Dolores Marcos, P. Amoros, *Chem. Mater.* **2002**, 14, 5015-5022.
- 26 B. Bonelli, M. F. Ribeiro, A. P. Antunes, S. Valange, Z. Gabelica, E. Garrone, *Microporous Mesoporous Mater.* **2002**, 54, 305-317.
- 27 M. S. Holm, S. Svelle, F. Joensen, P. Beato, C. H. Christensen, S. Bordiga, M. Bjørgen, *Appl. Catal. A: General* **2009**, 356, 23-30.
- 28 D. G. Poduval, J. A. R. van Veen, M. S. Rigutto, E. J. M. Hensen, *Chem. Commun.* **2010**, 46, 3466-3468.
- 29 T. Barzetti, E. Selli, D. Moschetti, L. Forni, *J. Chem. Soc. Faraday Trans.* **1996**, 92, 1401-1407.
- 30 M. Guisnet, P. Ayrault, C. Coutanceau, M. F. Alvarez, J. Datka, *J. Chem. Soc. Faraday Trans.* **1997**, 93, 1661-1665.
- 31 W. Daniell, U. Schubert, R. Glöckler, A. Meyer, K. Noweck, H. Knözinger, *Appl. Catal. A: Gen.* **2000**, 196, 247-260.
- 32 I. Mirsojew, S. Ernst, J. Weitkamp, H. Knözinger, *Catal. Lett.* **1994**, 24, 235-248.
- 33 B. Bonelli, I. Bottero, N. Ballarini, S. Passeri, F. Cavani, E. Garrone, *J. Catal.* **2009**, 264, 15-30.
- 34 H. Knözinger, S. Huber, *J. Chem. Soc. Faraday Trans.* **1998**, 94, 2047-2059.
- 35 A. Zecchina, S. Bordiga, C. Lamberti, G. Spoto, L. Carnelli, C. Otero Arian, *J. Phys. Chem.* **1994**, 98, 9577-9582.
- 36 B. Onida, L. Borello, B. Bonelli, F. Geobaldo, E. Garrone, *J. Catal.* **2003**, 214, 191-199.
- 37 A. V. Kucherov, A. N. Shigapov, A. V. Ivanov, T. N. Kuchero, L. M. Kustov, *Catal. Today* **2005**, 110, 330-338.
- 38 T. N. Vu, J. v. van Gestel, J. P. Gilson, C. Collet, J. P. Dath, J. C. Duchet, *J. Catal.* **2005**, 231, 453-467.
- 39 F. Wakabayashi, J. N. Kondo, K. Domen, C. Hirose, *J. Phys. Chem.* **1995**, 99, 10573-10580.
- 40 C. Paz,; S. Bordiga, C. Lamberti, M. Salvalaggio, A. Zecchina, G. Bellussi, *J. Phys. Chem. B* **1997**, 101, 4740-4751.
- 41 D. Klomp, T. Maschmeyer, U. Hanefeld, J. A. Peters, *Chem. Eur. J.* **2004**, 10, 2088-2093.
- 42 C. R. Graves, H. Zhou, C. L. Stern, S. T. Nguyen, *J. Org. Chem.* **2007**, 72, 9121-9133.

- 43 R. Mello, J. Martínez-Ferrer, G. Asensio, M. A. González-Núñez, *J. Org. Chem.* **2007**, *72*, 9376-9378.
- 44 P. Mäki-Arvela, N. Kumar, V. Nieminen, R. Sjöholm, T. Salmi, D. Y. Murzin, *J. Catal.* **2004**, *225*, 155-169.
- 45 G. K. Chuah, S. H. Liu, S. Jaenicke, L. J. Harrison, *J. Catal.* **2001**, *200*, 352-359.
- 46 F. Neatu, S. Coman, V. I. Pârvulescu, G. Poncelet, D. De Vos, P. Jacobs, *Top. Catal.* **2009**, *52*, 1292-1300.
- 47 Z. Yongzhong, N. Yuntong, S. Jaenicke, G-K. Chuah, *J. Catal.* **2005**, *229*, 404-413.
- 48 S. M. Coman, P. Patil, S. Wuttke, E. Kemnitz, *Chem. Commun.* **2009**, 460-462.
- 49 T. D. H. Bugg, *Introduction to Enzyme and Coenzyme Chemistry*, 2<sup>nd</sup> Ed. Blackwell Publishing, Oxford, **2004**, pages 33-35.
- 50 S. Chandrasekhar, *Res. Chem. Intermed.* **2003**, *29*, 107-123.
- 51 D. A. Shirley, *Phys. Rev. B.* **1972**, 4709-4714

# Investigation of the Cyanosilylation Catalysed by Metal–Silicious Catalysts



## 1. Introduction

The cyanosilylation of carbonyl compounds to form new C-C bonds and to protect alcohol functions is an important reaction as the *O*-protected cyanohydrins can be transformed into a wide range of important intermediates such as  $\alpha$ -hydroxy acids,  $\alpha$ -amino acids and  $\beta$ -amino alcohols.<sup>1</sup> The reaction is mostly catalyzed by homogeneous Lewis acids or base catalysts. However in the last two decades heterogeneous catalysis has gained considerable ground.<sup>2,3</sup> One of the successful heterogeneous catalysts used in cyanosilylation reaction is Al-MCM-41.<sup>4</sup> In cyanosilylation of different aldehydes as well as ketones Al-MCM-41 was not only very active (only 5 mg catalyst was needed to convert 1 mmol benzaldehyde within 1 min) but also recyclable. In contrast, amorphous aluminosilicates showed almost no activity regardless of the Si/Al ratio. The high activity of Al-MCM-41 was explained by the possible cooperation between acid sites and basic sites originating from the presence of a minor amount of sodium.<sup>4</sup>

MCM-41 with its honeycomb structure has one-dimensional pores, which might lead to diffusion limitations. Furthermore its synthesis requires large amounts of surfactants. In contrast the well-established, amorphous three-dimensional TUD-1 with a high surface area and pore size can be synthesized without surfactants.<sup>5,6</sup> Due to these advantages we investigated how amorphous TUD-1 catalysts, containing Al and/or Zr behave in this reaction.<sup>7,8</sup> Both sodium containing and sodium free TUD-1 catalysts were employed and compared with Al-MCM-41 containing different amounts of sodium. In this manner insight into the catalytic mechanism should be obtained. In addition to well-established Al-TUD-1, Na-Al-TUD-1 was synthesized for the first time to test the proposed interaction between Brønsted acid sites and basic sites originating from the presence of sodium as counter cation.

## 2. Results and Discussion

### 2.1 Na-AlTUD-1

Na-Al-TUD-1 (Table 1 entry 2) exhibits an intense peak at  $0.5^\circ$  ( $2\theta$ ) in the X-ray diffractogram like all mesostructured TUD-1 materials (Fig. 1).<sup>5,6</sup> In addition Na-Al-TUD-1

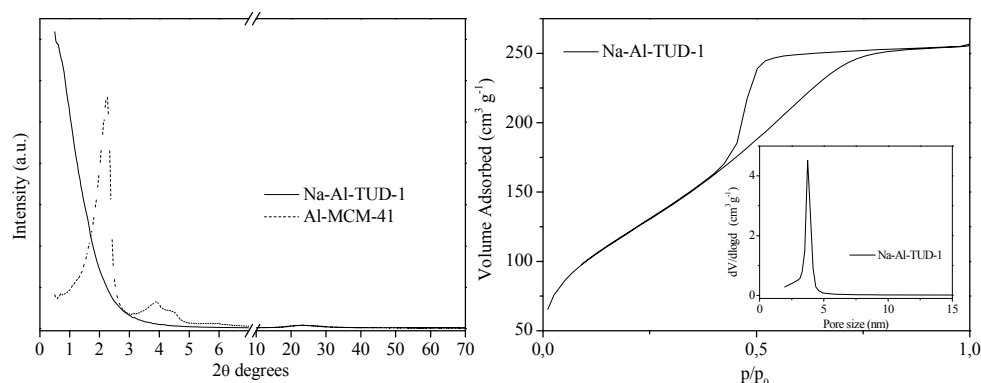


**Figure 1** XRD measurements of Na-Al-TUD-1 and Al-MCM-41 (left) and N<sub>2</sub> physisorption analysis results of Na-Al-TUD-1 sample (right).

displays a peak around  $25^\circ$  ( $2\theta$ ) indicating its amorphous nature. No evidence of crystalline Al<sub>2</sub>O<sub>3</sub> phases was found in the X-ray diffractograms, suggesting that the aluminium was incorporated into the framework. The Na-Al-TUD-1 shows also a typical Type IV isotherm with a type H1 hysteresis loop characteristic for mesoporous materials (Fig. 1). This is pointed out by large uptake of N<sub>2</sub> at relative pressures between 0.4 and 0.8  $p/p_0$  due to capillary condensation in the mesopores. Pore size distribution deduced from desorption gives a narrow pore size distribution with a maximum at 3 nm (Fig. 1, inset). The surface area and pore volume are lower than in the Al-TUD-1 sample (Table 1). Around 50 % of

**Table 1** ICP and N<sub>2</sub>-Physisorption results of TUD-1 and MCM-41 based catalysts.

Catalysts	$n_{\text{Si}}/n_{(\text{Al}+\text{Zr})}^a$	$n_{\text{Si}}/n_{\text{Al}}^a$	$n_{\text{Si}}/n_{\text{Zr}}^a$	$n_{\text{Al}}/n_{\text{Na}}^a$	$S_{\text{BET}}$ ( $\text{m}^2 \text{g}^{-1}$ )	$V_{\text{meso}}$ ( $\text{cm}^3 \text{g}^{-1}$ )	$D_{\text{meso}}$ (nm)
Al-TUD-1 <sup>b</sup>	-	26.6	-	-	760	0.75	3
Na-Al-TUD-1 <sup>c</sup>	-	4.1	-	3.5	441	0.40	3
Al-MCM-41	-	26.0	-	5.5	1052	0.95	3
Al-MCM-41-P	-	29.8	-	12.1	863	0.73	2.7
Al-Zr-3:1-TUD-1 <sup>d</sup>	28	34	142	-	685	0.57	3.3
Al-Zr-2:2-TUD-1 <sup>d</sup>	31	53	73	-	735	0.61	3.3
Al-Zr-1:3-TUD-1 <sup>d</sup>	33	103	48	-	667	0.65	4.4
Zr-TUD-1 <sup>e</sup>	-	-	24.7	-	792	0.76	4

<sup>a</sup> After calcination. <sup>b</sup> Synthesized according to Reference 7. <sup>c</sup> Na-Al-TUD-1 has a ratio of Al/Na of 3.3 or 2 wt % Na. Synthesized according to Reference 10. <sup>e</sup> Synthesized according to Reference 8.

aluminium is tetrahedrally coordinated (Fig. 2), while the rest of the aluminium is penta- and hexacoordinated.

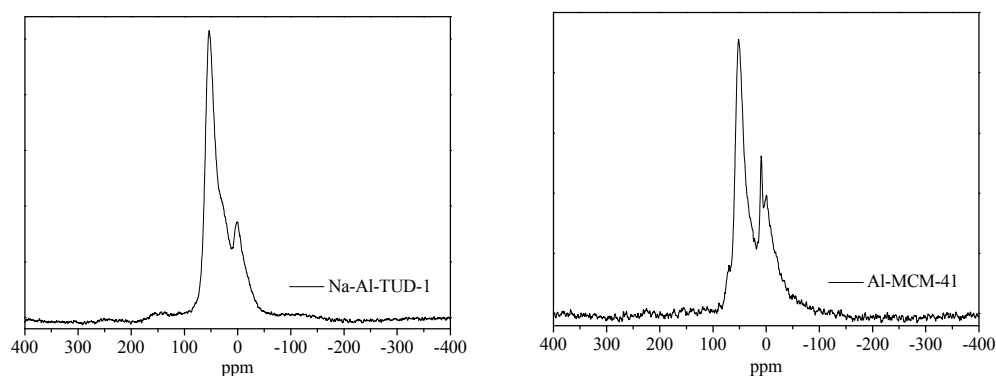


**Figure 2**  $^{27}\text{Al}$ -MAS-NMR of Na-Al-TUD-1(left) and Al-MCM-41 (right).

## 2.2 Al-MCM-41

Al-MCM-41 and an additional sample of Al-MCM-41 with a lower amount of sodium (obtained by treatment of calcined Al-MCM-41 with 1 M  $\text{NH}_4\text{NO}_3$ ) denoted as Al-MCM-41-P were prepared accordingly to the literature.<sup>9</sup> The Al-MCM-41-P sample has a lower amount of sodium and also a reduced surface area, pore size as pore volume (Table 1, entries 3 and 4, Fig. 3).  $^{27}\text{Al}$ -NMR analysis revealed that Al-MCM-41 sample contained 58 % tetrahedrally coordinated aluminium (Fig. 2).

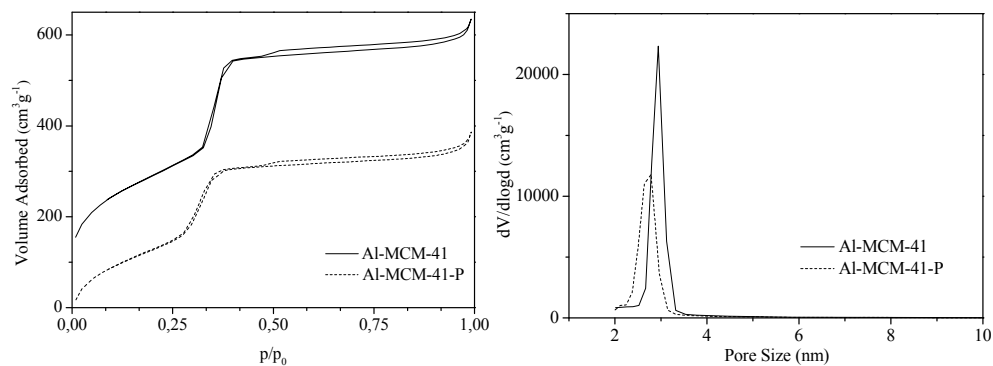
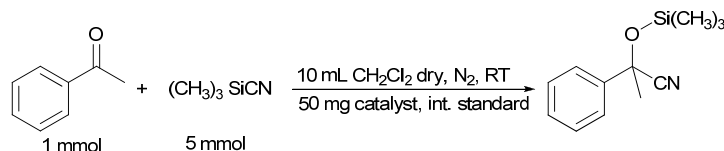


**Figure 3** Isotherms obtained from  $\text{N}_2$  Physisorption results of Al-MCM-41 and treated Al-MCM-41 (Al-MCM-41-P).

## 2.3 Catalysis

To probe the catalysts to the full the ketone acetophenone was chosen as a model compound for the cyanosilylation as it is more difficult to convert than aldehydes (Scheme 1).<sup>1</sup> The catalysts tested also included Zr-TUD-1 and bimetallic Al-Zr-TUD-1 catalysts with different Al/Zr ratios; synthesized according to previous reports.<sup>8,10</sup>



**Scheme 1** Cyanosilylation of acetophenone with trimethylsilyl cyanide (TMSCN).

Al-TUD-1 was the most active catalyst (Fig. 4) of the TUD-1 type. In case of bimetallic Al-Zr-TUD-1 catalysts the more Al was present the more active the catalyst was.

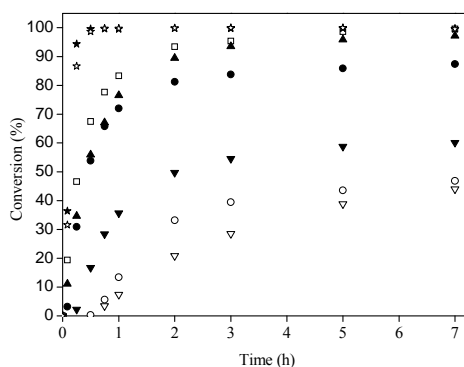


**Figure 4** The activity of TUD-1 and MCM-41 catalysts in the cyanosilylation of acetophenone with TMSCN. Reaction conditions: acetophenone (1 mmol), TMSCN (5 mmol), catalyst (50 mg), CH<sub>2</sub>Cl<sub>2</sub> (10 mL), N<sub>2</sub>, RT. (★) Al-MCM-41, (☆) Al-MCM-41-P, (□) Al-TUD-1, (▲) Al-Zr-3:1, (●) Al-Zr-2:2, (▼) Al-Zr-1:3, (○) Zr-TUD-1, (▽) Na-Al-TUD-1.

Synergistic interaction between Lewis acid sites imparted due to the presence of different metals and Brønsted acid sites originating from the presence of Al could not be observed. Introduction of sodium into Al-TUD-1 considerably reduced its activity. This is in

contradiction with the hypothesis that sodium plays an activating role in this reaction. The same was the case if Al was replaced by Zr (Zr-TUD-1). Both Zr-TUD-1 and Na-Al-TUD-1 display a lag during the first half an hour, obviously the active catalytic species first needs to be released. Acetophenone was added first in the catalytic experiments. It coordinates to Lewis acid sites, Zr or Al, making the surface hydrophobic and inhibiting the catalytic species originating from interaction between trimethylsilyl cyanide and Lewis acid sites.

The best results were obtained with Al-MCM-41 catalysts (Fig. 4), whether or not pre-treated in order to remove sodium. Within half an hour complete conversion was attained. This again indicates that Na does not play an important role in the catalysis. It also demonstrates that diffusion is a parameter of no importance in this reaction, given the fact that the difference in surface area between the two MCM-41 based catalysts is around  $200 \text{ m}^2 \text{ g}^{-1}$  (Table 1). Catalysts containing aluminium, i.e. Brønsted acid sites and Lewis acid sites, were the most active.

As the results obtained with all catalysts could not be reproduced when TMSCN was added prior to acetophenone, we suspected that silylation of surface OH groups was the source of this discrepancy. In Figure 5 catalysts pre-treated with TMSCN prior to

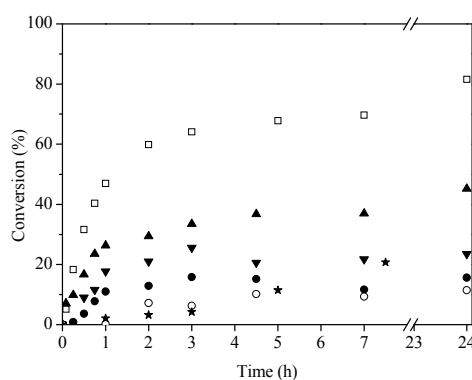


**Figure 5** The activity of TUD-1 and MCM-41 catalysts in cyanosilylation of acetophenone after TMSCN pre-treatment. Reaction conditions same as in Figure 2. (★) Al-MCM-41, (□) Al-TUD-1, (▲) Al-Zr-3:1, (●) Al-Zr-2:2, (▼) Al-Zr-1:3, (○) Zr-TUD-1.

cyanosilylation of acetophenone showed greatly decreased reactivity. The loss of activity was most pronounced for TMSCN pre-treated Al-MCM-41. While Al-TUD-1 with its three



dimensional pore structure in this case was the best catalyst, Al-MCM-41 displayed very little activity. Only Zr-TUD-1 and the Al-Zr-TUD-1's with a large Zr to Al ratio performed worse than Al-MCM-41.

The silylation of surface OH groups was proven by FT-IR. In the pre-treated sample of Al-MCM-41, the characteristic OH signal in the range  $3800\text{--}3000\text{ cm}^{-1}$  has largely disappeared (Fig. 6 (A)). The same observation was made with the other catalysts. In addition we also performed  $^{29}\text{Si}$  MAS NMR cross polarization measurements. In all samples we could clearly distinguish  $\text{OSiMe}_3$  groups formed on the surface of the catalyst

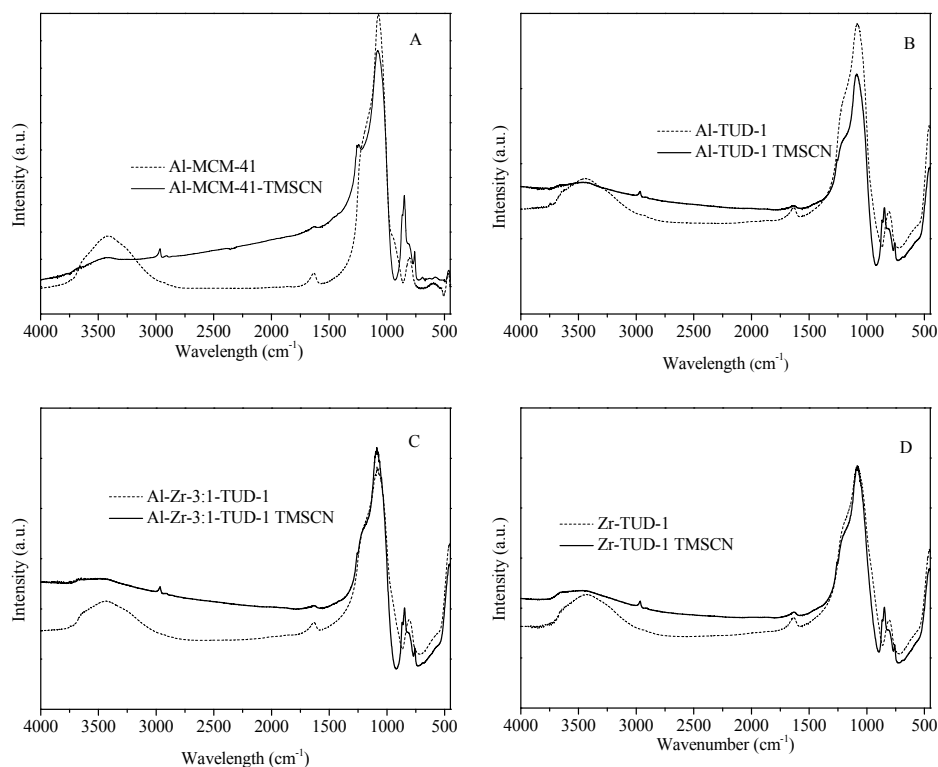


**Figure 6** FT-IR measurements of different mono- and bimetallic catalysts before and after treatment with TMSCN: (A) Al-MCM-41; (B) Al-TUD-1; (C) Al-Zr-3:1 and (D) Zr-TUD-1.

at 14 ppm (Fig. 7).<sup>11</sup> This rigorously proves that TMSCN protects the silanol groups. Since CN is known to be a pseudo halogen, TMSCN obviously acts just like  $\text{TMSCl}$  on siliceous materials.

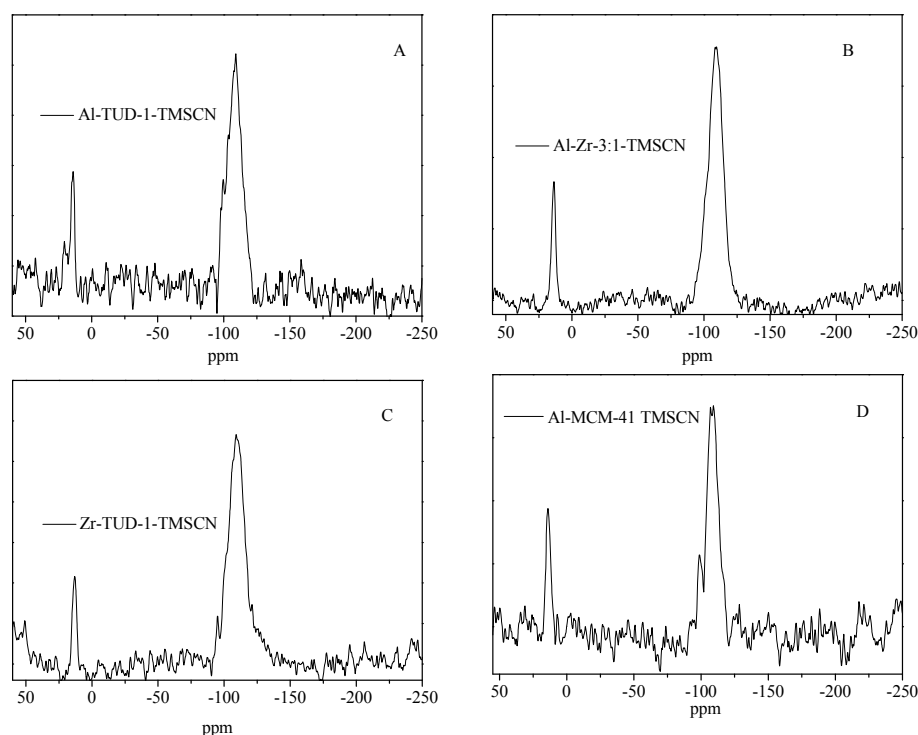


**Figure 7** Cross-polarization  $^{29}\text{Si}$  MAS NMR of different mono- and bimetallic catalysts after treatment with TMSCN: (A) Al-TUD-1; (B) Al-Zr-3:1; (C) Zr-TUD-1 and (D) Al-MCM-41.

It has previously been shown that hetero-polyacids such as dodecatungstophosphoric acid ( $\text{H}_3\text{PW}_{12}\text{O}_{40}$ ) employed as solid Brønsted acid or protic  $\text{CF}_3\text{SO}_3\text{H}$  can catalyse the cyanosilylation.<sup>12,3</sup> Moreover also the Lewis acidic silylated triflic acid,  $\text{CF}_3\text{SO}_3\text{SiMe}_3$  is able to catalyse the reaction; which led to a proposal of a mechanism in which TMSCN reacts with Brønsted acid sites to generate a trimethylsilyl cation like Lewis acid site.<sup>3</sup> As both Al-TUD-1 and Al-MCM-41 according to  $^{27}\text{Al}$ -NMR analysis contain similar amount of tetrahedrally coordinated aluminium (Si/Al ratio being in both cases 26) and therefore similar amount of Brønsted acid sites, the exceptionally high activity of Al-MCM-41 can only be explained by its ordered structure. The influence of the order in a heterogeneous catalyst has recently also been shown for Al-MCM-41 applied in Mukaiyama aldol reaction.<sup>13</sup> Al-MCM-41 submitted to mechanical compression lost its intrinsic order and was therefore much less active.<sup>13</sup>

While amorphous  $\text{SiO}_2\text{-Al}_2\text{O}_3$  with Si/Al ratios of 2, 5 or 20 were not active at all, the activity of aluminium increased with increase of order of the material from Al-TUD-1 to Al-MCM-41.<sup>4</sup> Al-TUD-1, even though amorphous is however also mesoporous and three-dimensional and therefore more structured and active than amorphous  $\text{SiO}_2\text{-Al}_2\text{O}_3$ . Ordered or not, all catalysts are silylated by TMSCN, strongly influencing their reactivity. The presence of both Lewis acid sites and Brønsted acid sites as is the case in Al-TUD-1 and Al-MCM-41 is essential for their high activity compared to other catalysts.

### **3. Conclusion**

In conclusion, the reagent TMSCN reacts with silanol groups of the siliceous material. Silylation of the surface leads to greater inhibition in case of two-dimensional Al-MCM-41 than three-dimensional Al-TUD-1. Sodium does not have a positive effect on the catalysis. The presence of both Lewis and Brønsted acid sites as is the case in the monometallic aluminium based catalysts gives best catalytic results. In addition, the most important parameter for activity is the degree of order of the material, the higher the order the more active the catalyst.

## 4. Experimental

Dry solvents were purchased from Aldrich, all other reagents were purchased from Aldrich, Across or Fluka.

### 4.1 Catalyst Preparation

Zr-TUD-1, Al-TUD-1 and bimetallic Al-Zr-TUD-1 catalysts were synthesized according to previous reports.<sup>7,8,10</sup>

#### 4.1.1 Al-MCM-41<sup>9</sup>

A clear solution of sodium silicate with Si/Na ratio of 2 was prepared by combining NaOH (1 M, 37.13 g) with colloidal silica (30 wt% in water, 14.33 g) by vigorous stirring at 80 °C for 2 h (mixture A). In the mean time sodium aluminate (54% Na<sub>2</sub>O · Al<sub>2</sub>O<sub>3</sub>, 0.27 g) was dissolved in 5 g H<sub>2</sub>O and added to the stirred solution of cetyltrimethylammonium bromide (CTABr, 4.33g), 25 wt% NH<sub>3</sub> (0.25 g) and 13.37 g H<sub>2</sub>O at room temperature (mixture B). A cooled solution of sodium silicate was added dropwise to mixture B under vigorous stirring. After the addition of sodium silicate the entire mixture was vigorously stirred at 90 °C for 1 h. The resulting gel mixture had a molar composition of: 6 SiO<sub>2</sub> : 1 CTABr : 0.24 Al<sub>2</sub>O<sub>3</sub> : 1.5 Na<sub>2</sub>O : 0.15 NH<sub>4</sub>OH : 300 H<sub>2</sub>O.

The gel mixture inside a polypropylene bottle (lid was loose to allow for pressure change) was transferred to an oven at 97 °C for 1 day. The mixture was cooled to room temperature and subsequently the pH of the mixture was adjusted to pH = 11 by dropwise addition of 25 wt% acetic acid under vigorous stirring. After the pH adjustment the reaction mixture was heated again to 97 °C for 1 day. The pH adjustment and subsequent heating were repeated twice. The precipitated product was filtered off, washed with distilled water and dried in an oven at 97 °C. The following day the solids were calcined at 550 °C for 5 h at ramp rate of 1 °C min<sup>-1</sup>.

#### 4.1.2 Al-MCM-41-P (NH<sub>4</sub>NO<sub>3</sub> pretreated Al-MCM-41)

Al-MCM-41 (1 g) was stirred with 50 mL 1 M  $\text{NH}_4\text{NO}_3$  solution at 90 °C overnight. The solid was filtered off and washed with approx. 450 mL demineralised water followed by drying at 97 °C overnight. Finally the solid was calcined at 500 °C for 5 h at a ramp rate of 1 °C  $\text{min}^{-1}$ .

#### 4.1.3 Na-Al-TUD-1

Dry 2-propanol (45 g) was added to aluminium(III) isopropoxide (0.02 mol, 4.24 g) and the mixture was stirred for 2 h. As silica source tetraethyl orthosilicate (0.08 mol, 17.30 g) was added followed by a mixture of triethanolamine (0.08 mol, 12.50 g) and water (0.28 mol, 5 g). After vigorous stirring for 30 min, tetraethylammonium hydroxide (0.02 mol, 7.86 g) was added followed by NaOH (6.23 mmol, 0.25 g) dissolved in water (0.35 mol, 6.34 g). The mixture had the following molar ratio: TEOS : 0.25  $\text{Al}(\text{iPrO})_3$  : 1 TEA : 0.225 TEAOH : 11  $\text{H}_2\text{O}$  : 0.075 NaOH.

The clear gel obtained after these steps was then aged at room temperature for 24 h and dried at 98 °C for 24 h, followed by hydrothermal treatment in a Teflon-lined autoclave at 180 °C for 21 h and finally calcination in the presence of air up to 600 °C at a temperature ramp of 1 °C  $\text{min}^{-1}$ . The colour of the catalyst was yellowish even though it was calcined twice under the same conditions.

## 4.2 Catalyst Characterization

Powder X-ray diffraction (XRD) patterns were obtained on a Philips PW 1840 diffractometer equipped with a graphite monochromator using  $\text{Cu}_{\text{K}\alpha}$  radiation.

The textural properties of the materials were characterized by volumetric  $\text{N}_2$  physisorption at 77 K using Micromeritics ASAP 2010 equipment. Prior to the physisorption experiment, the samples were dried overnight at 573 K ( $p \leq 10^{-2}$  Pa). From the nitrogen sorption isotherms, the specific surface area  $S_{\text{BET}}$ , the pore diameter  $dP_{\text{BJH}}$  and the pore volume  $VP_{\text{BJH}}$  were calculated. The latter two were determined from the adsorption branch of the nitrogen sorption isotherms as typically applied for TUD-1-type materials.<sup>5,6</sup>

Chemical analysis of Si, Al, Zr and Na were performed in duplet by dissolving the samples in 1 % HF and 1.25%  $\text{H}_2\text{SO}_4$  solution and measuring them with Inductively

Coupled Plasma – Optical Emission Spectroscopy (ICP-OES) on a Perkin Elmer Optima 3000DV instrument.

FTIR spectra were carried out in the 450 - 4000  $\text{cm}^{-1}$  region. FTIR spectra of KBr diluted wafers of samples were recorded using a Perkin Elmer Spectrum One instrument. In total 19 scans were taken with resolution of 4  $\text{cm}^{-1}$ .

Solid state  $^{27}\text{Al}$  MAS NMR experiments were performed at 9.4 T on a Bruker Avance-400 MHz spectrometer operating at 104.2 MHz with a pulse width of 1 ms. 4-mm zirconia rotors with a spinning speed set at 11 kHz were used. The chemical shifts are reported with respect to  $\text{Al}(\text{NO}_3)_3$  as external standard at  $\delta = 0$  ppm.

Solid state cross polarization  $^{29}\text{Si}$  MAS NMR analysis was recorded on a Bruker Avance-400 MHz instrument operating at 79.4 MHz with a spectral width of 25062 Hz and pulse width of 3s. Chemical shifts were reported with respect to TMS ( $\delta = 0$  ppm).

#### *Catalytic tests*

### **4.3 Catalytic reactions**

#### *4.3.1 Cyanosilylation reaction*

TUD-1 catalysts were calcined at 600  $^{\circ}\text{C}$  for 10 h with a ramp rate of 1  $^{\circ}\text{C min}^{-1}$ .<sup>7</sup> MCM-41 catalysts were dried at 120  $^{\circ}\text{C}$  for 1 h under vacuum. Dry  $\text{CH}_2\text{Cl}_2$  (10 mL) was added to calcined or dried catalysts (50 mg) followed by acetophenone (1 mmol, 0.12 g) and the internal standard dodecane (1 mmol, 0.17 g). The reaction was started by addition of trimethylsilyl cyanide (5 mmol, 0.49 g) at room temperature and under  $\text{N}_2$  atmosphere. The reaction was followed by taking aliquotes (20  $\mu\text{L}$ ) every 5, 15, 30, 45 min and then every 1, 2, 3, 5 and 7 h. Samples were analyzed by GC, a Shimadzu GC-17A gas chromatograph, equipped with a 25 m x 0.32 mm x 0.25  $\mu\text{m}$  column Chrompack Chirasil-Dex CB, He was used as carrier gas. Employing an isotherm (130  $^{\circ}\text{C}$ ) following retention times were recorded: acetophenone (1.75 min), dodecane (3.03 min) and 2-trimethylsilyloxy-2-phenylpropanenitrile (4.55 min). For all of the reactions the selectivity was more than 99 %.

#### *4.3.2 Cyanosilylation reaction with TMSCN treated catalysts*

To calcined TUD-1 catalysts (50 mg, 600 °C, 10 h, 1 °C min<sup>-1</sup>) 10 mL dry CH<sub>2</sub>Cl<sub>2</sub> and 5 mmol trimethylsilyl cyanide (TMSCN) was added. The entire mixture was left stirring for 30 min. Subsequently the liquid layer was removed with a syringe equipped with a cotton plug and the catalyst was washed with 10 mL dry CH<sub>2</sub>Cl<sub>2</sub>. Directly after the TMSCN pretreatment catalysts were employed in cyanosilylation reaction as described above.

Al-MCM-41 catalysts were dried at 120 °C for 1 h at vacuum conditions. To the dried catalysts (150 mg) 30 mL dry CH<sub>2</sub>Cl<sub>2</sub> was added at room temperature under N<sub>2</sub> atmosphere. Silylation was started by addition of trimethylsilylcyanide (2 mL). After 30 min reaction was filtered and extensively washed with dry CH<sub>2</sub>Cl<sub>2</sub> (5x, in total 50 mL). Finally the catalysts were dried at 100 °C for 1 h under vacuum and stored under N<sub>2</sub> to be used later in cyanosilylation under conditions as described above.

### **Acknowledgements**

We thank S. Ajaikumar for his help with the synthesis of Al-MCM-41.

## 5. References

- 1 (a) M. North, D. L. Usanov, C. Young, *Chem. Rev.*, **2008**, *108*, 5146-5226.  
(b) F. L. Cabirol, A. E. C. Lim, U. Hanefeld, R. A. Sheldon, I. M. Lyapkalo, *J. Org. Chem.*, **2008**, *73*, 2446-2449.  
(c) J. Holt, U. Hanefeld, *Curr. Org. Synth.*, **2009**, *6*, 15-37.
- 2 (a) K. Sukata, *Bull. Chem. Soc. Jpn.*, **1987**, *60*, 3820-3822.  
(b) M. Onaka, K. Higuchi, K. Sugita, Y. Izumi, *Chem. Lett.*, **1989**, 1393-1396.  
(c) K. Higuchi, M. Onaka, Y. Izumi, *J. Chem. Soc., Chem. Commun.*, **1991**, 1035-1036.  
(d) Y. Izumi, M. Onaka, *J. Mol. Catal.*, **1992**, *74*, 35-42.  
(e) B. M. Choudary, N. Narender, V. Bhuma, *Synth. Commun.*, **1995**, *25*, 2829-2836.  
(f) M. Curini, F. Epifano, M. C. Marcotullio, O. Rosati, M. Rossi, *Synlett* **1999**, 315-316.  
(g) B. He, Y. Li, X. Feng, G. Zhang, *Synlett* **2004**, 1776-1778.  
(h) M. L. Kantam, P. Sreekanth, P. L. Santhi, *Green Chem.*, **2000**, 47-48.  
(i) C. Beleizão, B. Gigante, D. Das, M. Alvaro, H. Garcia A. Corma, *Chem. Commun.*, **2003**, 1860-1861.  
(j) A. Procopio, G. Das, M. Nardi, M. Oliverio L. Pasqua, *ChemSusChem*, **2008**, *1*, 916-919.  
(k) B. Karimi, L. Ma'Mani, *Org. Lett.*, **2004**, *6*, 4813-4815.  
(l) S. Huh, H.-T. Chen, J. W. Wiench, M. Pruski, V. S. Y. Lin, *Angew. Chem. Int. Ed.*, **2005**, *44*, 1826-1830.  
(m) C. Beleizão, B. Gigante, D. Das, H. Garcia, A. Corma, *J. Catal.*, **2004**, *221*, 77-84.
- 3 K. Higuchi, M. Onaka, Y. Izumi, *Bull. Chem. Soc. Jpn.*, **1993**, *66*, 2016-2032.
- 4 K. Iwanami, J.-C. Choi, B. Lu, T. Sakakura, H. Yasuda, *Chem. Commun.*, **2008**, 1002-1004.
- 5 J. C. Jansen, Z. Shan, L. Marchese, W. Zhou, N. v. d. Puil, T. Maschmeyer, *Chem. Commun.*, **2001**, 713-714.
- 6 S. Telalović, A. Ramanathan, G. Mul, U. Hanefeld, *J. Mater. Chem.*, **2010**, *20*, 642-658.
- 7 R. Anand, R. Maheswari, U. Hanefeld, *J. Catal.*, **2006**, *242*, 82-91.
- 8 A. Ramanathan, M. C. C. Villalobos, C. Kwakernaak, S. Telalović, U. Hanefeld, *Chem. Eur. J.*, **2008**, *14*, 961-972.
- 9 H. Nur, H. Hamid, S. Endud, H. Hamdan, Z. Ramli, *Mater. Chem. Phys.*, **2006**, *96*, 337-342.
- 10 S. Telalović, J. F. Ng, R. Maheswari, A. Ramanathan, G. K. Chuah, U. Hanefeld, *Chem. Commun.*, **2008**, 4631-4633.



- 11 J. K. F. Buijink, J. J. M. van Vlaanderen, M. Crocker, F. G. M. Niele, *Catal. Today* **2004**, 93-95, 199-204.
- 12 H. Firouzabadi, N. Iranpoor, A. A. Jafari, *J. Organomet. Chem.*, **2005**, 690, 1556-1559.
- 13 K. Iwanami, T. Sakakura, H. Yasuda, *Catal. Commun.*, **2009**, 10, 1990-1994.



Conducting chemistry in a sustainable way is a necessity due to growing population and depletion of resources but also from an economic point of view. One, if not the most important approach to reduce the number of steps, solvents and energy used during the chemical synthesis is to use catalysts: enzymes, homogeneous or heterogeneous catalysts.

Heterogeneous catalysts, namely zeolites (crystalline aluminosilicates with pore size up to 1.2 nm) are successfully used in petroleum industry already for many decades. However, due to their narrow pore size, their applicability is limited to the production of mostly small sized, bulk chemicals. Due to the application of heterogeneous catalysis the E-factor (Introduced by R. A. Sheldon and defined as kg waste/kg product) in the petroleum industry is less than 1 while for production of Fine Chemicals and especially Pharmaceuticals it can reach values of up to 100. And this is exactly the focus of this thesis, to extend the use of heterogeneous catalysts for the production of fine chemicals by applying mesoporous materials that can accomodate much larger molecules than traditional zeolites can accommodate.

Starting point is a mesoporous material, TUD-1 (having pore size larger than 2 nm), developed at the Technical University Delft. It can be compared with more famous mesoporous materials as MCM-41 (Mobile Crystalline Material) and SBA-15 (Santa-Barbara Amorphous Material). TUD-1 has an amorphous, three-dimensional open structure with large pores that can accommodate various chemicals.

Chapter 1 gives an overview of the synthesis and application of TUD-1 as a catalyst and/or carrier in various reactions since its introduction in 2001. Silicious TUD-1 has been used for framework incorporation of different metals or for generating metal-oxide nanoparticles upon increase of metal content. As such they have been used as acidic, oxidation or photocatalyst. In addition Al-TUD-1 possessing Brønsted acid sites has been successfully used as carrier for a homogeneous chiral hydrogenation catalyst, namely  $[\text{Rh}(\text{MonoPhos})_2\text{cod}]$  with retention of yield, enantioselectivity and selectivity upon immobilization.

Chapter 2 extends the use of TUD-1 based materials as carriers, this time for successful chiral cyclopropanation catalysts. Highly strained cyclopropanes are found in many natural products e.g. in insecticides such as pyrethrins. TUD-1 has been used as

Brønsted acidic mesoporous support. Brønsted acid sites were introduced by supporting phosphotungstic acid on an all alumina TUD-1 matrix (PW-TUD- $\text{Al}_2\text{O}_3$ ) or by substitution of Si by Al in an all silica TUD-1 matrix (Al-TUD-1). The chiral cyclopropanation catalyst Cu(I)- 2,2-methylene [(4R,5S)-4,5-diphenyl-2-oxazoline] was immobilized by different non-covalent immobilization techniques; ion-exchange in solution and solid-gas ion-exchange. The chiral cyclopropanation catalyst was adsorbed on PW-TUD- $\text{Al}_2\text{O}_3$  during ion-exchange in solution. This catalyst system displayed high leaching of copper reaching values of 21 %. When using Al-TUD-1 as support copper was introduced as CuCl via gas-phase ion-exchange at temperatures from 550 °C to 850 °C followed by introduction of the ligand. Non-covalent immobilization by solid-gas ion-exchange of CuCl on Al-TUD-1 resulted in a heterogeneous catalyst with only 1% leaching of copper but also moderate results in the cyclopropanation of styrene in terms of yield (33%) and enantioselectivities.

In Chapter 3 we look more in detail to different parameters governing the successful noncovalent immobilization of chiral cyclopropanation catalysts. Different parameters such as solvent used during immobilization, impact of side products on the leaching of the metal, choice of the ligand or metal to be immobilized are taken into account. Mesoporous amorphous aluminosilicates of TUD-1 structure have been used as supports for chiral cyclopropanation catalysts, Cu (I)-bis(oxazoline) and Ru(II)-Pybox. Two different supports have been synthesized: Brønsted acidic H-Al-TUD-1 and Na-Al-TUD-1. Non-covalent methods, adsorption and liquid ion-exchange were used to immobilise the cyclopropanation catalysts. During immobilisation of the Cu (I)-bis(dsiphenyl oxazoline) complex on H-Al-TUD-1, solvents of different polarity were used. The polar methanol proved to be the most suitable solvent leading to non-detectable leaching of Cu (I) in the benchmark cyclopropanation reaction of styrene with ethyl diazoacetate. However, low yields and absence of enantioselectivity were observed. Changing the cation on the support to be exchanged for the cyclopropanation catalyst to Na-Al-TUD-1, did increase the yield and enantioselectivity in the cyclopropanation but also induced leaching of Cu (I) of up to 4%. Immobilising Ru (II)-Pybox on H-Al-TUD-1 also led to increase in yield and enantioselectivities with modest leaching of Ru of 2.88 %.

In Chapter 4 we focused on increase of acidity of mesoporous TUD-1 based catalysts. It is generally known that mesoporous aluminosilicates are much weaker acids than crystalline aluminosilicates such as zeolites. To achieve this goal we synthesized bimetallic

Al-Zr-TUD-1 catalysts. Al-Zr-TUD-1's were synthesized with variable amounts of aluminium and zirconium to study the effect on the Brønsted and Lewis acidity as well as on the resulting catalytic activity. The materials were characterized by various spectroscopic techniques using  $\text{NH}_3$ , pyridine and CO as probe molecules. In addition the synthesized Al-Zr-TUD-1 materials were tested as catalyst materials in the Lewis acid-catalyzed Meerwein-Ponndorf-Verley reduction of 4-*tert*-butylcyclohexanone, the intermolecular Prins synthesis of nopol and in the intramolecular Prins cyclisation of citronellal. Al-Zr-TUD-1 catalysts outperformed monometallic Al-TUD-1 as well as Zr-TUD-1 in the Prins cyclisation of citronellal. This proves the existence of the synergistic properties of Al-Zr-TUD-1. Combination of the intramolecular nature of the Prins cyclisation of citronellal, hydrophilic surface of the catalyst as well as the presence of both Brønsted as Lewis acid sites synergy could be obtained.

Finally in chapter 5 we were interested whether amorphous Al-TUD-1 catalyst would be as active as Al-MCM-41 in cyanosilylation of acetophenone as it has been shown that amorphous aluminosilicates are not active in this reaction. Different amorphous mesoporous TUD-1 catalysts were employed in the cyanosilylation of acetophenone with trimethylsilyl cyanide in dichloromethane at room temperature. Catalysts were monometallic Al-TUD-1, Zr-TUD-1 and bimetallic Na-Al-TUD-1 and Al-Zr-TUD-1's with constant Si/Metal ratio but different Al/Zr ratios. Al-TUD-1 proved to be the most active TUD-1 catalyst. Introduction of sodium or Lewis acidic Zr into Al-TUD-1 to achieve synergistic properties did not lead to increased activity. During the reaction we observed silylation of the catalysts, as proven by FT-IR and cross-polarization analysis. The best results were achieved using Al-MCM-41 catalysts due to their higher degree of ordering and well defined pore size. However, this catalyst was silylated, too.



Het duurzaam toepassen van chemie is niet alleen een noodzaak geworden door de toegenomen bevolking en schaarste van grondstoffen maar ook vanuit een economisch perspectief. De belangrijkste manier om het aantal stappen, de hoeveelheid oplosmiddel en de energieconsumptie tijdens chemische syntheses te verminderen is de toepassing van katalysatoren: enzymen, homogene- of heterogene katalysatoren.

Zeolieten (kristallijne aluminosilicaten met porie grootte tot 1.2 nm) zijn een voorbeeld van heterogene katalysatoren. Ze worden al decennia lang succesvol toegepast in de petroleumindustrie. Echter, door hun gelimiteerde porie grootte is hun toepasbaarheid beperkt tot de productie van kleine bulkchemicaliën. Door de toepassing van onder andere heterogene katalysatoren is de E-factor (geïntroduceerd door R. A. Sheldon en gedefinieerd als kg afval/kg product) in de petroleum industrie minder dan 1, terwijl de E-factor voor productie van fijn chemicaliën en geneesmiddelen waarden tot 100 kan bereiken. Dit is precies de focus van dit proefschrift: uitbreiding van de toepasbaarheid van heterogene katalysatoren voor de synthese van moleculen groter dan die welke traditionele zeolieten kunnen accommoderen.

Uitgangspunt is het mesoporeuze materiaal TUD-1 (porie-grootte 2-50 nm), ontwikkeld aan de Technische Universiteit Delft. Vergelijkbare en bekendere mesoporeuze materialen zijn MCM-41 (Mobile Crystalline Materials) en SBA-15 (Santa-Barbara Amorphous Material). TUD-1 heeft een amorf drie-dimensionale open structuur met grote poriën waardoor het grote moleculen kan accommoderen.

Hoofdstuk 1 geeft een overzicht van de synthese en toepassing van TUD-1 als katalysator of drager in verschillende reacties sinds zijn introductie in 2001. Si-TUD-1 werd gebruikt voor framework incorporatie van verschillende metalen of voor het genereren van metaal oxide nanodeeltjes door toename van het gewichtspercentage metaal. Deze M-TUD-1s zijn gebruikt als zure-, oxidatie- of foto katalysatoren. Daarnaast is Al-TUD-1 dat Brønsted zure “active sites” bevat succesvol gebruikt als drager voor een homogene chirale hydrogenerings katalysator. De katalysator  $[\text{Rh}(\text{MonoPhos})_2\text{cod}]$  behield activiteit, enantioselectiviteit en selectiviteit na immobilisatie op Al-TUD-1.

Hoofdstuk 2 verbreedt de toepassing van TUD-1 materialen als dragers, dit keer voor succesvolle chirale cyclopropaneringskatalysatoren. Cyclopropaneringen worden

gevonden in veel natuurlijke producten zoals de pyrethrine insecticiden. TUD-1 is gebruikt als Brønsted zure mesoporeuze drager. Brønsted zure “sites” zijn geïntroduceerd door immobilisatie van fosforwolframaam zuur op alumina van TUD-1 structuur (PW-TUD- $\text{Al}_2\text{O}_3$ ) of door substitutie van Si door Al in silica TUD-1 structuur (Al-TUD-1). De chirale cyclopropanerings katalysator Cu(I)- 2,2-methylene bis[(4R,5S)-4,5-diphenyl-2-oxazoline] werd geïmmobiliseerd met behulp van verschillende immobilisatie technieken: ion-uitwisseling in oplossing en vaste stof-gas ion-uitwisseling. De chirale cyclopropanerings katalysator was geabsorbeerd op PW-TUD- $\text{Al}_2\text{O}_3$  tijdens ion-uitwisseling in oplossing. Dit katalytische systeem vertoont hoge “leaching” van koper (21%). Koper werd geïntroduceerd op Al-TUD-1 als CuCl op temperaturen van 550 °C tot 850 °C gevolgd door de introductie van de ligand. Non-covalente immobilisatie via vaste stof-gas ion-uitwisseling van CuCl op Al-TUD-1 resulteerde in een katalysator met maar 1% “leaching” van koper maar ook in een lagere opbrengst (33%) en enantioselectiviteit bij de cyclopropanering van styreen.

In Hoofdstuk 3 kijken we naar verschillende parameters die invloed uitoefenen op succesvolle non-covalente immobilisatie van chirale cyclopropaneringskatalysatoren. Mesoporeuze amorfe aluminosilicaten van TUD-1 structuur zijn gebruikt als dragers voor chirale cyclopropaneringskatalysatoren, Cu (I)-bis(oxazoline) en Ru(II)-Pybox. Twee verschillende dragers zijn gesynthetiseerd: Na-Al-TUD-1 en Brønsted zure H-Al-TUD-1. Non-covalente methoden, adsorptie en vloeistof ion-uitwisseling zijn toegepast tijdens de immobilisatie. Verschillende oplosmiddelen zijn gebruikt tijdens de immobilisatie van Cu (I)-bis(diphenyl oxazoline) op H-Al-TUD-1. Het meest polaire oplosmiddel, methanol, bleek het meest geschikt. Er werd geen “leaching” van koper waargenomen tijdens cyclopropanering van styreen met ethyldiazoacetaat. Echter, de opbrengst en enantioselectiviteit waren laag. Toepassing van Na-Al-TUD-1 leidt tot een toename van de opbrengst en de enantioselectiviteit, maar ook tot een verhoging van “leaching” tot 4%. Immobilisatie van Ru(II)-Pybox op H-Al-TUD-1 geeft ook een hogere opbrengst en enantioselectiviteit met redelijk lage “leaching” van Ru (2.88%)

In Hoofdstuk 4 zijn we geïnteresseerd in de introductie van zowel Brønsted als Lewis aciditeit in mesoporeuze TUD-1 gebaseerde katalysatoren. Het is algemeen bekend dat mesoporeuze aluminosilicaten zwakkere zuren zijn dan kristallijne aluminosilicaten zoals zeolieten. Om dit doel te bereiken hebben we verschillende bimetallische Al-Zr-TUD-



Is gesynthetiseerd. Al-Zr-TUD-1s met variabele verhoudingen Al tot Zr werden gesynthetiseerd, om het effect van de Al tot Zr verhouding op de Brønsted en Lewis zuurgraad en de katalytische activiteit te testen. De materialen zijn gekarakteriseerd met verschillende spectroscopische technieken, gebruikmakend van  $\text{NH}_3$ , pyridine en CO als “probe” moleculen. Al-Zr-TUD-1s zijn ook getest in verschillende reacties: Lewis zuur gekatalyseerde Meerwein-Ponndorf-Verley reductie van 4-tert-butylcyclohexanon, intermoleculaire Prins-synthese van nopol en in de intramoleculaire Prins-cyclisatie van citronellal. Bimetallische Al-Zr-TUD-1 katalysatoren bleken actiever te zijn dan Al-TUD-1 of Zr-TUD-1 in de Prins cyclisatie van citronellal. Dit was een duidelijk bewijs voor het bestaan van synergie door toepassing van bimetallische Al-Zr-TUD-1 katalysatoren. De combinatie van de intramoleculaire aard van de Prins-cyclisatie van citronellal, het hydrofiele oppervlakte van de katalysatoren en de aanwezigheid van zowel Brønsted als Lewis zure “sites” resulteren in de waargenomen synergie.

Tenslotte, in Hoofdstuk 5 zijn we geïnteresseerd of amorfe Al-TUD-1 net zo actief zal zijn als Al-MCM-41 in cyanosilylering van acetofenon sinds is aangetoond dat amorfe aluminosilicaten niet actief zijn in deze reactie. Verschillende amorfe mesoporeuze TUD-1 katalysatoren zijn toegepast in cyanosilylering van acetofenon met trimethylsilylcyanide in dichloormethaan als oplosmiddel bij kamertemperatuur. De gebruikte katalysatoren zijn monometallisch Al-TUD-1 en Zr-TUD-1 en bimetallisch Na-Al-TUD-1 en Al-Zr-TUD-1 met constante Si/metaal molaire verhouding, maar met verschillende Al/Zr ratios. Al-TUD-1 bleek de meest actieve TUD-1 katalysator. Introductie van natrium of Lewis zuur Zr in Al-TUD-1 leidt tot verminderde activiteit. Silylering van katalysatoren treedt op tijdens de reactie, zoals werd aangetoond met FT-IR en “cross-polarization” studies. Echter, Al-MCM-41 is de beste katalysator mogelijk door de hogere mate van orde in de structuur van MCM-41 materialen en goed gedefinieerde smalle porie grootte. Desondanks wordt ook deze katalysator gesilyleerd.



Publications

1. *Enantioselective Synthesis of Protected Cyanohydrins*  
L. Veum, M. Kuster, S. Telalović, U. Hanefeld, T. Maschmeyer, *Eur. J. Org. Chem.*, **2002**, 9, 1516-1522.
2. *Zr-TUD-1: A Lewis Acidic, Three-Dimensional, Mesoporous, Zirconium-Containing Catalyst*  
A. Ramanathan, M. C. Castro Villalobos, C. Kwakernaak, S. Telalović, U. Hanefeld, *Chem. Eur. J.*, **2008**, 14, 961-972.
3. *Synergy between Brønsted Acid Sites and Lewis Acid Sites*  
S. Telalović, J. F. Ng, R. Maheswari, A. Ramanathan, G. K. Chuah, U. Hanefeld, *Chem. Commun.*, **2008**, 4631-4633.
4. *TUD-1: Synthesis and Application of a Versatile Catalyst, Carrier, Material...*  
S. Telalović, A. Ramanathan, G. Mul, U. Hanefeld, *J. Mater. Chem.*, **2010**, 20, 642-658.
5. *Noncovalent Immobilization of Chiral Cyclopropanation Catalysts on Mesoporous TUD-1: Comparison of Liquid-phase and Gas-phase Ion-exchange*  
S. Telalović, U. Hanefeld, *Appl. Catal. A: Gen.*, **2010**, 372, 217-223.
6. *On the Synergistic Catalytic Properties of Bimetallic Mesoporous Materials Containing Aluminium and Zirconium: The Prins Cyclisation of Citronellal*  
S. Telalović, A. Ramanathan, J. F. Ng, R. Maheswari, C. Kwakernaak, F. Soulimani, H. C. Brouwer, G. K. Chuah, B. M. Weckhuysen, U. Hanefeld, *Chem. Eur. J.*, **2011**, 17, 2077-2088.
7. *Investigation of the Cyanosilylation Catalysed by Metal-silicious Catalysts*  
S. Telalović, U. Hanefeld, *Catal. Commun.*, **2011**, 12, 493-496.

### Oral presentations

1. “*Noncovalent Immobilization of Cyclopropanation Catalysts on Mesoporous Material*”  
KNCV section Organic Chemistry ,Groningen, The Netherlands, 6 June **2008**.
2. “Synergy in Mesoporous Al-Zr-TUD-1”  
21<sup>st</sup> North American Catalysis Society Meeting, San Francisco, California, USA, 8 June **2009**.

### Posters

1. “*Multifunctional Catalyst for Sustainable Chemistry*”  
S. Telalović, U. Hanefeld, Design & Synthesis, Structure & Reactivity and Biomolecular Chemistry, Lunteren, The Netherlands, 23-25 October **2006**.
2. “*Bifunctional Carrier Materials for Sustainable Chemistry*”  
XIII<sup>th</sup> Netherlands Catalysis and Chemistry Conference, Noordwijkerhout, The Netherlands, 5-7 March **2007**.
3. “*Al-Zr-TUD-1 a Novel Bimetallic Heterogeneous Catalyst for Meerwein-Ponndorf-Veiley and Prins reaction*”  
A. Ramanathan, S. Telalović, G. K. Chuah, U. Hanefeld, Design & Synthesis, Structure & Reactivity and Biomolecular Chemistry, Lunteren, The Netherlands, 29-31 October **2007**.
4. “*Al-Zr-TUD-1 a Novel Bimetallic Heterogeneous Catalyst for Meerwein-Ponndorf-Verley and Prins reaction*”  
IX<sup>th</sup> Netherlands Catalysis and Chemistry Conference, Noordwijkerhout, The Netherlands, 3-5 March **2008**.
5. “*Bifunctional Heterogeneous Acid-chiral Cu(I) Cyclopropanation Catalyst*”  
S. Telalović, U. Hanefeld, Annual Meeting of NWO Mozaïk laureates Den Haag, 13 November **2008**.
6. “*Synergy in Bimetallic Al-Zr-TUD-1*”  
S. Telalović, A. Ramanathan, R. Maheswari, G. K. Chuah, U. Hanefeld, X<sup>th</sup> Netherlands Catalysis and Chemistry Conference, Noordwijkerhout, The Netherlands, 2-4 March **2009**.

## Acknowledgments

---

All the thanks and gratitude belongs to Most Merciful, Most Gracious, Allah dž.š. (the exalted).

At last, after four years of PhD I have come to the point to write these last pages of my thesis and thank all those that directly or indirectly contributed to this book either by scientific discussions during work meetings or small talk during coffee break or in the corridor or otherways.

I would like to thank my promoter Prof. Roger Sheldon for the opportunity to join his group, at that time TOCK (Toegepaste Organische Chemie en Katalyse) where I had the chance to do my master research and later at the newly formed department BOC (Biocatalysis and Organic Chemistry) to start my PhD. For his inspiring lessons in organic chemistry I followed during my time as student of Chemical Engineering and many of his enjoyable presentations I had the chance to attend.

Also thanks to Prof. Isabel Arends as the new head of department of BOC were I finalised my PhD, for her lessons in organic chemistry and the freedom to do this research.

A very special thank to my daily supervisor Ulf Hanefeld. Thank you for introducing me to the wonderfull subject of catalysis, for the lessons in Organic Synthesis, The Disconnection Approach. For many incentives and hints during writing of the proposal for Mozaik fellowship from NWO, the articles and finally the thesis. For always having time for me when I was questioning my approach en results. Thank you.

I want to take the opportunity and thank Mieke van der Kooij for the always precise and quick help concerning many of the forms and arrangements around the conferences, posters, this thesis or other things besides. Thank you for your time and your kindness.

Much of this work would not be possible without the help of Dr. Anand Ramanathan and Chretien Simons. Thank you for teaching me the synthesis of TUD-1 and many discussions.

Many of the analysis would not be possible without the help of Delia van Rij for INAA, Joop Padmos and Olav Steinberger concerning ICP, Patricia Kooymans for HR-TEM. Thanks to Remco for keeping the GCs running and Maarten for the introduction to HPLC. Thanks to Sander Brower for teaching me N<sub>2</sub>-physisorption and NH<sub>3</sub>-TPD analysis. Kristina thank you for many NMRs you measured.

I would also like to thank Prof. B. Weckhuysen for allowing me to analyse the samples at University of Utrecht and the discussions. Fouad Soulimani, thank you for measuring the CO and Pyridine FT-IR.

My stay in Delft as a PhD would not be the same without my colleagues I had the chance to meet and work side by side. Thanks to many colleagues who made my PhD in Delft a memorable and enjoyable time. Thanks to Lars Veum to have the chance to do my research practical under your guidance and have the first paper with my name on it, for teaching me how to do proper research. Sanjib thank you for your sense of humor and “philosophical discussions”. Tobias thank you for allowing me to use your Baan Code in the after days of my PhD and many laughs. I hope as ChatchBio participants we will have the chance to meet occasionally. My thanks also to Jarle, Sander van Pelt, Heidi, John, Andrzej, Aleksandra, Goska, Inga, Daniel, Aida, Mieke Jacobs, Linda, Jeroen, Monika, Florian, Jin, Maria, Frank. I wish you all the best in your lives and careers.

Bez neupitne ljubavi, podrške i vjere u mene od strane mojih roditelja, moje majke (rahmet tvojoj duši i da ti Allah dž. š. podari Džennetske bašće) i moga oca, ja ne bi bio ovdje gdje se sada nalazim. Želim ti mnogo zdravlja i dug život.

Moj život postao je tek potpun kada si ti Sedina došla u moj život. Sa tvojim doćecima, nasmijanosti i radosti učinila si moj život ljepšim i dala si mi motivaciju da što prije završim PhD.

Thanks to all!

Idereen bedankt!

Hvala svima!

Selvedin

## Curriculum Vitae

---

Selvedin Telalović was born on July 1, 1977 in Rotterdam, The Netherlands. After a short stay in the Netherlands he moved with his parents to Bosnia and Hercegovina, at that time Yugoslavia, where he was raised and finished the elementary school. With the outbreak of the war in 1992 he moved once again to his birth place Rotterdam, The Netherlands at the age of 14 years. In 1997 he obtained his secondary school diploma (VWO, Atheneum) at the “Openbare Scholengemeenschap Wolfert van Borselen” in Rotterdam. In September 1997 he started as student of Chemical Engineering at the Technical University of Delft. In 2005 he graduated with the Master thesis entitled “Immobilization of asymmetric cyclopropanation catalyst on Al-TUD-1”. In the same year he applied for and obtained a Mozaïek fellowship from NWO (Netherlands Organisation for Scientific Research) entitled “Multifunctional Catalysts for Sustainable Chemistry”. He started his PhD work in Januari 2006 at Technical University Delft in the Biocatalysis and Organic Chemistry group under supervision of Dr. U. Hanefeld. Currently he obtained a PostDoc position at the University Utrecht in the Inorganic Chemistry and Catalysis group to conduct research on heterogeneous catalysis of the Guerbet reaction under supervision of Dr. J. H. Bitter.

